GENERIC MINERAL TECHNOLOGY CENTER FOR RESPIRABLE DUST

Edited by
Robert L. Frantz
Raja V. Ramani

PUBLICATIONS

1984

PUBLICATIONS

PRODUCED IN

THE GENERIC MINERAL TECHNOLOGY CENTER FOR RESPIRABLE DUST

IN THE YEAR

1984

PENNSTATE

1855

WEST VIRGINIA UNIVERSITY

Published Volumes of the Respirable Dust Center

VOLUME 1	Status Report, 1984-1988
VOLUME 2	Report to the Committee on Mining and Mineral Resources Research,1987
VOLUME 3	Publications, I984
VOLUME 4	Publications, 1985
VOLUME 5	Publications, 1986
VOLUME 6	Publications, 1987
CONFERENCE PROCEEDINGS	Coal Mine Dust Conference West Virginia University Morgantown, West Virginia October I984
CONFERENCE PROCEEDINGS	Respirable Dust in the Mineral Industries: Health Effects, Characterization and Control The Pennsylvania State University University Park, Pennsylvania October I986

GENERIC MINERAL TECHNOLOGY CENTER FOR RESPIRABLE DUST

The Pennsylvania State University
West Virginia University
University of Minnesota
Massachusetts Institute of Technology

PUBLICATIONS 1984

Submitted To
Office of Mineral Institutes
U.S. Bureau of Mines
Washington, D.C.

June 30, 1988

CONTENTS

Page

Foreword vii

National Plan viii

Advisory Council Members ix

I. Control of Dust Generation 1

1. **Design and Fabrication of a Rotary Cutting Simulator** 3
   A. Wahab Khair, Department of Mining Engineering, College of Mineral and Energy Resources, West Virginia University, Morgantown, WV 26506. *S. Peng*, Ed., Proc. Coal Mine Dust Conference, Morgantown, WV, October 8-10, 1984, pp. 190-197. (WV-1)

2. **Study of Fracture Mechanisms in Coal Subjected to Various Types of Surface Tractions Using Holographic Interferometry** 11
   A. Wahab Khair, Department of Mining Engineering, College of Mineral and Energy Resources, West Virginia University, Morgantown, WV 26506. Presented at the 25th U.S. Symposium on Rock Mechanics, Northwestern University, Evanston, IL, June 25-27, 1984, pp. 1-12. (WV-2)

II. Dilution, Dispersion, and Collection of Dust 23

3. **Dust Transport in Mine Airways** 25
   R. V. Ramani and R. Bhaskar, Department of Mineral Engineering, The Pennsylvania State University, University Park, PA 16802. *S. Peng*, Ed., Proc. Coal Mine Dust Conference, Morgantown, WV, October 8-10, 1984, pp. 198-204. (PS-2)

4. **Some Factors Influencing the Airborne Dust Distribution in Longwall Face Area** 32
   H. S. Chiang, S. S. Peng, G. C. Sun, and Y. F. Zhao, Department of Mining Engineering, College of Mineral and Energy Resources, West Virginia University, Morgantown, WV 26506. *S. Peng*, Ed., Proc. Coal Mine Dust Conference, Morgantown, WV, October 8-10, 1984, pp. 206-213. (WV-3)

5. **Analysis of an Airborne Dust Study Made for a Southwestern Pennsylvania Underground Bituminous Coal Mines** 35
   Robert L. Grayson and Syd S. Peng, Department of Mining Engineering, College of Mineral and Energy Resources, West Virginia University, Morgantown, WV 26506. *S. Peng*, Ed., Proc. Coal Mine Dust Conference, Morgantown, WV, October 8-10, 1984, pp. 13-15. (WV-6A)

Page

III. Dust Characterization 43

6 **Instrumentation for the Measurement of Respirable Coal Mine Dust** 45
Virgil A. Marple and Kenneth L. Rubow, Department of Mechanical Engineering, University of Minnesota, Minneapolis, MN 55455. *S. Peng*, Ed., Proc. Coal Mine Dust Conference, Morgantown, WV, October 8-10, 1984, pp. 214-221. (MN-1)

7. **Pulmonary Surfactant Interaction with Respirable Dust** 53
W. E. Wallace, Jr., M. J. Keane, V. Vallyathan, T. M. Ong, V. Castranova, National Institute for Occupational Safety and Health, 944 Chestnut Ridge Road, Morgantown, WV 26506. *S. Peng*, Ed., Proc. Coal Mine Dust Conference, Morgantown, WV, October 8-10, 1984, pp. 180-187. National Technical Information Service Resport PB86 169380/AS, Springfield, VA:NTIS. (WV-12)

IV. Dust Lung Interaction 61

8. **The Development of an Electro-Optical Technique to Measure Superoxide Release from Pulmonary Alveolar Macrophages Exposed to Coal Dusts** 63
Kevin A. DiGregorio, Eugene V. Cilento, and R. Clark Lantz, Departments of Chemical Engineering and Anatomy, West Virginia University, Morgantown, WV 26506. *S. Peng*, Ed., Proc. Coal Mine Dust Conference, Morgantown, WV, 1984, pp. 222-226. (WV-9)

V. Relationship of Mine Environment, Geology and Seam Characteristics to Dust Generation and Mobility 69

9. **An Analysis of Coal and Geologic Variables Related to Coal Workers' Pneumoconiosis** 71
Jan M. Mutmansky and Changwoo Lee, Department of Mineral Engineering, The Pennsylvania State University, University Park, PA 16802. *S. Peng*, Ed., Proc. Coal Mine Dust Conference, Morgantown, WV, October 8-10, 1984, pp. 236-249. (PS-5)

10. **The Relationship Between the Hardgrove Grindability Index and the Potential for Respirable Dust Generation** 85
Michael P. Moore and Christopher J. Bise, Department of Mineral Engineering, The Pennsylvania State University, University Park, PA 16802. *S. Peng*, Ed., Proc. Coal Mine Dust Conference, Morgantown, WV, October 8-10, 1984, pp. 250-255. (PS-5)

CONTENTS

		Page
11.	**Correlation of Respirable Dust Mass Concentration with Worker Positions** *R. L. Grayson and S. S. Peng*, Department of Mining Engineering, College of Mineral and Energy Resources, West Virginia University, Morgantown, WV 26506. *S. Peng*, Ed., Proc. Coal Mine Dust Conference, Morgantown, WV, October 8-10, 1984, pp. 256-260. (WV-6A)	91
	INDEX	97
	Cumulative Author Index	99
	Cumulative Subject Index	100

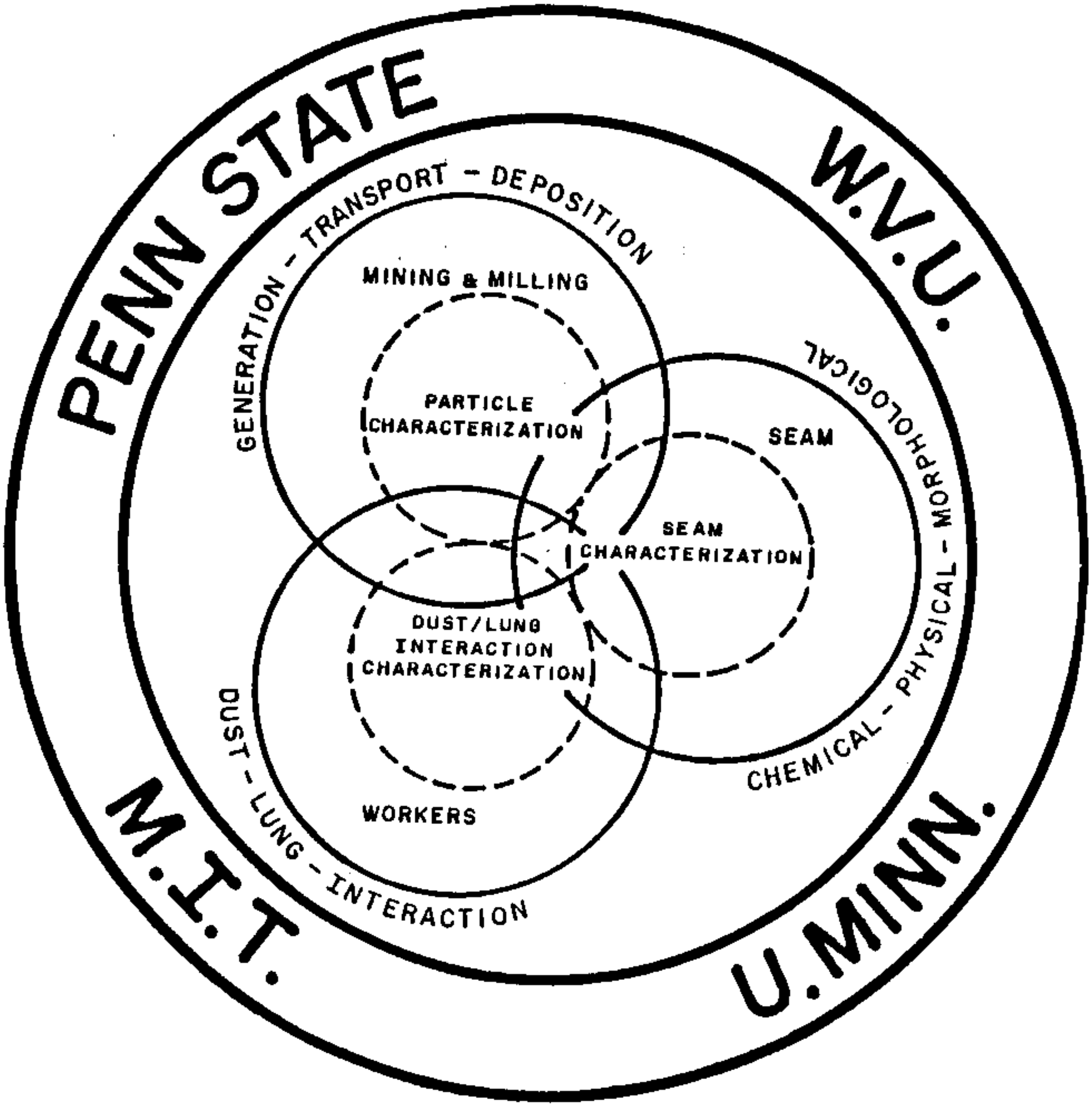

The Respirable Dust Center

FOREWORD

This volume contains publications resulting from respirable dust research performed in the Generic Mineral Technology Center for Respirable Dust by faculty, staff and graduate students at The Pennsylvania State University, West Virginia University, University of Minnesota, and Massachusetts Institute of Technology. These publications have appeared in scientific journals, proceedings of the national and international symposiums and meetings. Complete citations of the publications can be found in the text. The Generic Mineral Technology Center for Respirable Dust is funded by the U.S. Bureau of Mines through the Mining and Mineral Resources Research Institute Program. The opinions and conclusions expressed in the papers are those of the authors alone and do not represent the opinions of the Generic Mineral Technology Center for Respirable Dust, the Mining and Mineral Resources Research Institute Program or the U.S. Bureau of Mines. Citation of manufacturers' names in the papers were made for general information purposes, and do not imply endorsement of the products by the authors.

All of the publications in this volume are on research that has been supported by the Department of the Interior's Mineral Institute program administered by the Bureau of Mines through the Generic Mineral Technology Center for Respirable Dust under allotment grant number G1135142 or G1175142.

In addition to these papers, a dust conference was organized by the Center and held at West Virginia University in October 1984. The conference was co-sponsored by ACGIH, MSHA, NIOSH and USBM. Proceedings from this conference are available in the publication, Coal Mine Dust Conference, 1984. The generic center maintains a reference center that serves as a clearinghouse for technical information for the generic area and supplies reports on generic center accomplishments.

The support from the United States Congress for the Generic Mineral Technology Center for Respirable Dust is gratefully acknowledged. We also acknowledge and appreciate the support and inputs from USBM, NIOSH, MSHA, the Research Advisory Council, and the Committee on Mining and Mineral Resources Research which have significantly contributed to the activities of the Generic Mineral Technology Center for Respirable Dust.

Respectfully submitted,

Robert L. Frantz
Co-Director, Generic Mineral
Technology Center for Respirable Dust
Co-Editor

R. V. Ramani
Co-Director, Generic Mineral
Technology Center for Respirable Dust
Co-Editor

THE RESPIRABLE DUST CENTER

Excerpted From The

1988 UPDATE TO THE NATIONAL PLAN FOR RESEARCH IN MINING AND MINERAL RESEARCH

Report to:

December 15, 1987

The Secretary of the Interior
The President of the United States
The President of the Senate
The Speaker of the House of Representatives

Section 9(e) of Public Law 98-409 of August 29, 1984, (98 Stat. 1536 et seq.) mandates that the Committee on Mining and Mineral Resources Research submit an annual update to the National Plan for Research in Mining and Mineral Resources: "Improving Research and Education in Mineral Science and Technology through Government-(Federal, State and Local), Industry, and University Cooperation."

....

Respirable Dust (centered at Pennsylvania State U. and West Virginia U., with affiliates at U. of Minnesota and Massachusetts Institute of Technology): brings together experts concerned with particles causing potentially disabling or fatal diseases, including pneumoconiosis ("black lung"), silicosis, and asbestosis, the latter of deep concern not just to workers in the mineral sector of the economy but also to the general populace.

....

SIGNED:

Carl W. Randolph
Mining Industry

Win Aung
National Science Foundation

Don L. Warner
University Administrator

Walter R. Hibbard, Jr.
National Academy of Sciences

John H. DeYoung, Jr.
U.S. Geological Survey

Joseph N. Crowley
University Administrator

John C. Calhoun, Jr.
National Academy of Engineering

John D. Morgan
Bureau of Mines

Edward S. Frohling
Mining Industry

Orme Lewis, Jr.
Conservation Community
COCHAIR

James W. Ziglar
Asst. Secretary-Water & Science
U.S. Department of the Interior
COCHAIR

Generic Mineral Technology Center For Respirable Dust

RESEARCH ADVISORY COUNCIL MEMBERS

Dr. John A. Breslin
Senior Staff Physical Scientist
U.S. Bureau of Mines
2401 E Street, N.W.
Columbia Plaza
Washington, D.C. 20241
(202) 634-1220

Dr. Ronald Munson
Director, Office of Mineral
Institutes - MS 1020
U.S. Department of the Interior
2401 E Street, N.W.
Washington, D.C. 20241
(202) 634-1328

Dr. Lewis Wade
Research Director
Twin Cities Research Center
U.S. Bureau of Mines
5629 Minnehaha Avenue, S.
Minneapolis, MN 55417
(612-725-4610

Dr. John A. Campbell
Director, Engineering and
Technology Support
Kerr-McGee Corporation
P.O. Box 25861
Oklahoma City, OK 73125
(405) 270-3778

Mr. John Murphy
Research Director
Pittsburgh Research Center
U.S. Bureau of Mines
P.O. Box 18070
Pittsburgh, PA 15236
(412-675-6601

Dr. James L. Weeks, C.I.H.
Deputy Administrator for
Occupational Health
United Mine Workers of
America
900 15th Street, N.W.
Washington, D.C. 20005
(202) 842-7300

Mr. Robert E. Glenn
Director, Division of Respiratory
Disease Studies - NIOSH
944 Chestnut Ridge Road
Morgantown, WV 26505
(304) 459-5978

Dr. Kandiah Sivarajah
State Toxicologist
Room 825--Health and Welfare
Building
Harrisburg, PA 17108
(717) 787-1708

Dr. Jerome Kleinerman
Department of Pathology
Cleveland Met. General Hospital
3395 Scranton Road
Cleveland, OH 44109
(216) 459-5978

Dr. Pramod Thakur
Research Group Leader
CONOCO, Inc.
R & D Division
Route #1, Box 119
Morgantown, WV 26505
(304) 983-2251

PAST RESEARCH ADVISORY COUNCIL MEMBERS

Mr. Darrel Auch
Senior Vice President
Northern West Virginia Region
Consolidation Coal Company
P.O. Box 1314
Morgantown, WV 26507
(304) 296-3461

Dr. Thomas Falkie
President
Berwind Natural Resources
Company
Centre Square West
1500 Market Street
Philadelphia, PA 19102
(215) 563-2800

Mr. C. Wesley McDonald
Senior Vice President
(Mining)
Northern West Virginia
Region
Consolidation Coal Company
P.O. Box 1314
Morgantown, WV 26505
(304) 296-3461

Dr. J. Harrison Daniel
Program Manager, Mining
Research
Health and Safety
2401 E Street, N.W.
Washington, D.C. 20241
(202) 634-1253

Dr. Fred Kissell
Research Supervisor
Pittsburgh Safety Research Center
U.S. Bureau of Mines
4800 Forbes Avenue
Pittsburgh, PA 15213
(412) 675-6679

Dr. Donald Reid
Deputy Secretary for Public
Health Programs
Department of Health
Health and Welfare Building
P.O. Box 90
Harrisburg, PA 17108
(717) 783-8804

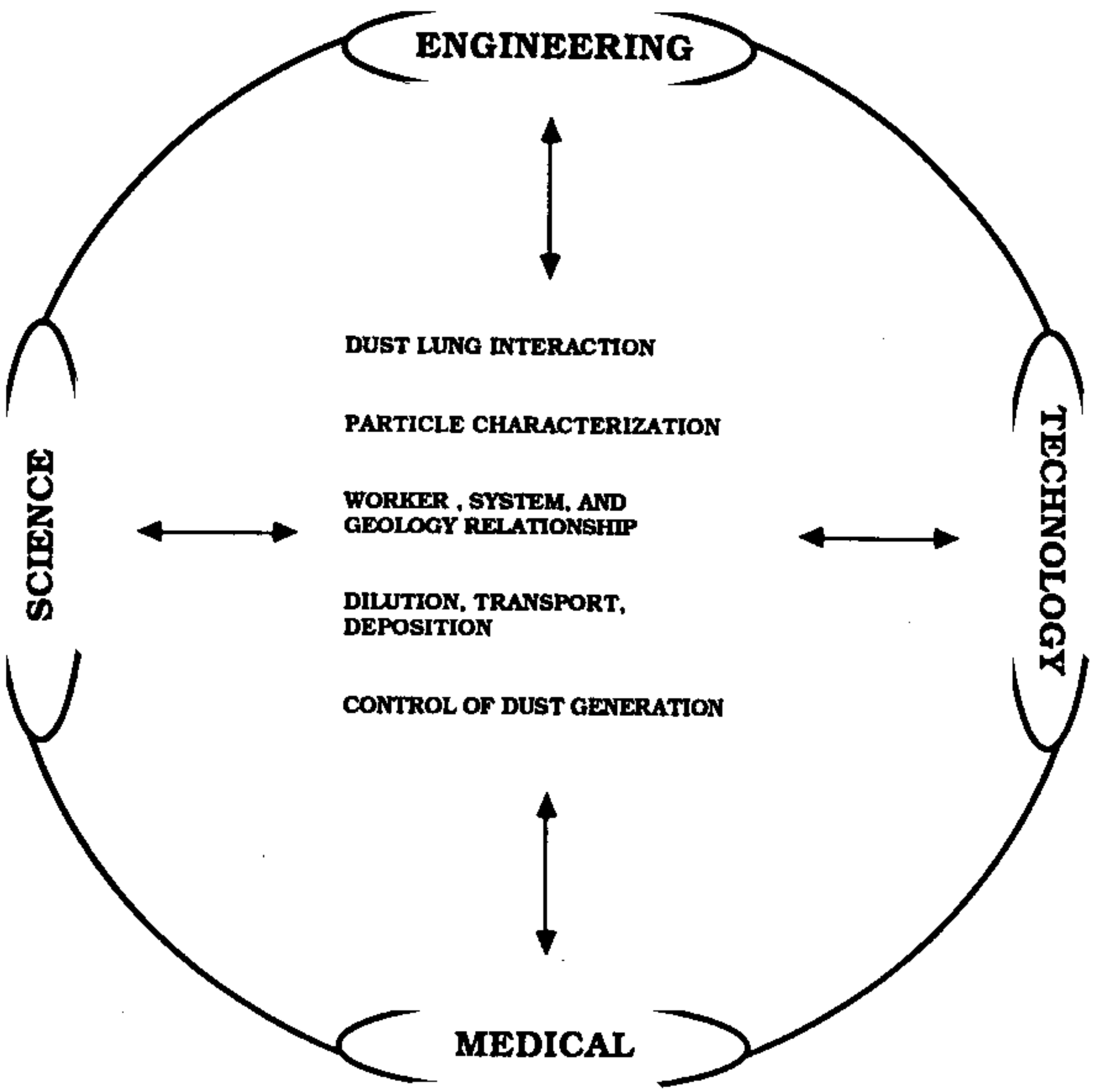
ENGINEERING
SCIENCE
TECHOLOGY
MEDICAL
DUST LUNG INTERACTION
PARTICLE CHARACTERIZATION
WORKER , SYSTEM, AND
GEOLOGY RELATIONSHIP
DILUTION, TRANSPORT,
DEPOSITION
CONTROL OF DUST GENERATION

RESEARCH

CONTROL OF GENERATION

- Amount
- Fracture

DILUTION, TRANSPORT AND DEPOSITION

- Concentration
- Size Consist
- Modeling

MINE WORKER, MINING SYSTEM, SEAM GEOLOGY

- Seam Sections
- Silica
- Trace Elements
- System Configuration
- Worker Location

- Coal Data Bank
- Mine Samples

SUITE OF GENERATED RESPIRABLE DUSTS

- Anthracite
- Medium Volatile Bituminous
- High Volatile Bituminous
- Silica
- Fireclay
- Rock Dust

CHARACTERIZATION

- Size/Shape/ Composition
- Surface/Functional Groups
- Particle Interaction

DUST LUNG INTERACTION

- Medical/Cellular
- Medical/Animal
- Medical/Human
- Medical/Engineering

TRAINING

1984

SAMPLING AND DUST GENERATION METHODS

Gravimetric Personal Sampler	Mini-Ram	Ram	Multi-Stage Impactors	Elpram Chamber	Planetary Ball Mill	Mini-Jet Mill	Fresh Dust Generator	Donaldson Jet Mill and Classifier

SUITE OF CHARACTERIZED DUST SAMPLES

1. Anthracite (Low Volatile)
2. Bituminous (Medium Volatile)
3. Bituminous (High Volatile)
4. Fireclay
5. Silica
6. Rockdust

SUITE OF MEDICAL TESTS

1. Rats
2. Guinea Pigs
3. Dogs
4. Non-Human Primates
5. Black Lung Patients
6. Healthy People

Dust Lung Interaction

- PS4 Lung Injury
- PS10 Immunology
- WV5 Inhalation Toxicity
- WV9 Superoxides
- WV8 Airway Reactivity

Medical/Cellular — Medical/Animal — Medical/Human — Medical/Engineering

Particle Characterization

- PS8 Wetting Characteristics
- MIT1 Aerosol Testing
- WV10 Free Radicals
- WV12 Surface Characteristics
- PS3 Dust Particles
- MN1 Mine Dust
- PS9 One-By-One Analysis

Size/Shape/Composition — Surface Functional Group — Particle Interaction

WV4 General Support Characterization

Mine Workers Mining System Seam Geology Dust Relationship

- PS5 Dust Potential
- WV3 Longwall Dust
- WV6A Dust Correlation

Respirable Dust Dilution, Transport, and Deposition

- PS2 Ambient Dust
- WV2 Experimental Dispersion
- MN2 Aerodynamic Diameter
- PS7 Longwall Modeling
- WV11 Mathematical Models
- WV3 Measurements of Dust

Control of Dust Generation

- PS1 Fracture Mechanics
- WV1 Dust Generation

SIZE, CHEMICAL AND MINEROLOGICAL ANALYSIS

Microtrac Particle Size Analysis	Laser Velocimetry Particle Size	Image Analysis	Pixie Analysis	P-7	X-Ray Diffraction	Particle By Particle Microprobe	Laser Raman Spectroscopy	Particle Acoustic Spectroscopy

The Generic Mineral Technology Center for Respirable Dust

SUITE OF CHARACTERIZED DUST SAMPLES	SAMPLING AND DUST GENERATION METHODS	SUITE OF MEDICAL TESTS
1. Anthracite (Low Volatile)	Dust/Lung Interaction	1. Rats
2. Bituminous (Medium Volatile)	Particle Characterization	2. Guinea Pigs
3. Bituminous (High Volitile)	Mine Workers. Mining System. Seam Geology Dust Relationship	3. Dogs
4. Fireclay	Respirable Dust Dilution. Transport and Deposition	4. Non-Human Primates
5. Silica	Control of Dust Generation	5. Black Lung Patients
6. Rockdust		6. Healthy People

SIZE, CHEMICAL AND MINEROLOGICAL ANALYSIS

Statement of Goal

The primary goal of the Generic Mineral Technology Center for Respirable Dust is to reduce the incidence and severity of respirable dust disease through advancing the fundamental understanding of all aspects of respirable dust associated with mining and milling and the interaction of dust and lungs.

I

Control of Dust Generation

DESIGN AND FABRICATION OF A ROTARY COAL CUTTING SIMULATOR

A. Wahab Khair, Ph.D.
Department of Mining Engineering
College of Mineral and Energy Resources
West Virginia University
Morgantown, WV 26506

ABSTRACT

This paper deals with the description of the capabilities of a unique rotary coal cutting simulator which has been designed and fabricated at West Virginia University. It operates under the simulated mining conditions with in-situ stresses (horizontal and vertical stresses) being applied to a coal block of 18 in. x 15 in. x 6 in. located in a suitably designed confining chamber. Cutting drum rotation can be varied from 1 to 40 rpm with the capability of stopping the drum after a predetermined number of rotations. Tests can be performed with four different bit angles, 15, 30, 45 and 60 degrees. A maximum of seven bits could be used in seven different orbits. Various cutting depths up to a maximum of 4 in. is possible.

Monitoring devices constitute, Linear Variable Differential Transformers (LVDTs), pressure transducers, cascade impactors, flow meters, flow controls and drum cutting speed. LVDTs are used to monitor the displacement of the coal block as well as the depth of cut. Pressure transducers are used to monitor the changes in pressure, both due to the thrust and due to the intermittent cutting nature of the rotary cutting. Flow controls will be used to run the drum at a set rpm between 1 and 40 and to provide a different rate of advance. All the above mentioned devices can be operated and monitored by a fully automated control system. Six-stage cascade impactors are used to determine the mass distribution of dust along the rotation path of the drum. The fracture size, shape and intensity can be studied by optical microscopy and the dust entrainment by using high speed photography.

This equipment will basically be used to study the fracture mechanism in coal, associated with operating and in-situ parameters and further relate it to dust generation and entrainment in underground coal mines.

INTRODUCTION

The Federal Coal Mine Health and Safety Act of 1969 was enacted to enforce on the coal operators that the airborne respirable dust not exceed 2 mg/m^3, intended to reduce the incidence of coal workers pneumoconiosis. This, including the other aspects of the legislation and the subsequent monitoring and enforcement by MSHA made it very imperative on the coal operators to provide a relatively healthier and safer working environment to the coal miners. Yet, it has been accounted that since 1970, the Federal government has paid over 11.7 billion dollars to over 470,000 miners with coal workers pneumoconiosis and their survivors (4). These regulations coupled with the assessment of the continuing burden on the miners, the mining industry and taxpayers appears to have provided an impetus for the mining community towards comprehending the different parameters that influence the dust generation and entrainment.

Dust control techniques such as conventional water sprays and dust collectors are only partially effective and require additional equipment expenditures. A more authentic approach would be to reduce the respirable dust at the source, the continuous mining machine cutting head. Improving the fragmentation process will not only reduce the respirable dust at the face, but it will also decrease the amount of respirable dust that can be liberated during secondary handling. As a result a number of research projects were initiated in the area of understanding the generation of primary dust and its control to improve the existing coal cutting technology or to develop a new one.

DESIGN PHILOSOPHY

Because of the complex nature of dust generation and the uniquely varying mining conditions under which it is generated, it is essential to develop basic solutions to problems that are more generic, which will be of a greater benefit to a larger segment of the mining industry than those resulting from previous research. Review of literature on the coal cutting technology revealed that most of the existing coal cutting machinery is of the rotary type and hence any research on dust control and entrainment should be based on the rotary coal cutting concepts and its parameters. Design and fabrication of the unique automated rotary coal cutting simulator (Fig. 1) at West Virginia

Presented at the Proc. Coal Mine Dust Conference, Morgantown, W. Va., October 8-10, 1984.

University was based on this premise. Furthermore, the design was done with an idea of incorporating the capability to study the different machine and in-situ parameters that influence the fragmentation of coal and the resulting dust generation and entrainment.

Fragmentation of coal which is very closely related to the generation and entrainment of dust particles into air can be expressed as a function of three major groups of parameters, namely: (1) coal properties, (2) in-situ conditions, and (3) operating parameters.

Furthermore, the operating factor consists of parameters such as velocity of the cutting drum, rate of advance, angle of attack, bit configuration, and bit lacing (spacing and pattern).

The unique automated rotary coal cutting simulator (Fig. 1) has the capability to study all these above mentioned parameters.

DESCRIPTION OF THE SIMULATOR

The description of the simulator can be subdivided into the following:

1. Main Frame
2. Confining Chamber
3. Cutting Drum
4. Bit Blocks
5. Hydraulic Unit

Main Frame

The machine is mounted on a rectangular frame of 5 ft. x 3.5 ft. side dimensions with four legs which are further mounted on wheels for easy maneuvering capability (Fig. 1). The legs are 37 inches in height and are made of hollow pipe material into which one end of a screw type bolt of 1 in. in diameter is screwed in. A flat plate of 0.5 in. x 4 in. x 4 in. in dimension is welded on to the other end of this bolt. When the machine is in position for tests the screw bolt can be screwed down from the hollow pipe of the leg so that the wheels are clearly off the ground and the legs stand on the flat plate end of the screw bolt.

Confining Chamber

The confining chamber is made of 1 inch thick steel. Its inside dimensions are 24 in. x 20 in. x 6 in. The base plate of the confining chamber is extended by 6 inches on either side of the confining chamber (Fig. 2). A slot is made in the middle of this extended base plate on either side of the confining chamber in order to facilitate the mounting of the confining chamber on the main frame. Four corners of this extended base plate are bolted to the four L-shaped structures which are further bolted to the main frame (Fig. 3). This type of mounting was designed to limit the tilting of the confining chamber. Between the four L-shaped structures and the extended base plate of the confining chamber there are 4 columns and 6 rows of springs (Fig. 3). These springs absorb the sudden impact of the cutting drum on the coal block. The stiffness of these springs can be adjusted as and when needed. The L-shaped structures are reinforced by welding angled plates between the vertical and the horizontal plates. To further limit the rotation of the confining chamber which consequently limits the bending of the frame, two plates of about 1 in. x 5 in. x 10 in. in size are welded to the middle of the vertical plates that make up the confining chamber. These plates are then bolted to the main frame with rubber washers in between. The extended slots in these plates enables the operator to adjust the springs stiffness between the L-shaped structures and the confining chamber (Fig. 2). Angled plates are welded between these horizontal plates and the vertical confining chamber plates in order to provide adequate requirements (Fig. 4).

Confining pressure in the confining chamber is accomplished by 4 hydraulic lifting cylinders. Two of these are of 10 ton capacity each with 1.5 inches stroke and the other two are of 20 ton capacity each with 1.75 inches stroke. The 10 ton capacity cylinders are used for horizontal pressure and the 20 ton capacity cylinders are used for vertical pressure. Hydraulic pressure is accomplished by two manually operated hydraulic pumps, one connected to the two 10 ton cylinders while the other is connected to the two 20 ton capacity cylinders. Hydraulic cylinders are placed in the slots of the wooden blocks which are made to conform to the dimensions of the hydraulic cylinders. These cylinders apply pressure on the steel plates of 1 in. x 6 in. x 18 in. size at the side and ' in. x 6 in. x 14 in. size at the bottom which ensures the application of uniform pressure on the coal block. After allowing room for the hydraulic cylinders on the right and bottom sides of the confining chamber, coal blocks of up to a maximum of 18 in. x 14 in. x 6 in. size can be confined. For this maximum size of the specimen, confining pressure equivalent to that which exists at 1000 ft. depth of mining can be applied.

Cutting Drum

The cutting drum (Fig. 5) is 8 inches in diameter and 12 inches in width. Depending on the height of the bit blocks which are made to conform to certain predetermined bit attack angles, the tip to tip diameter varies virtually with every single kind of cutting bit. The metered hydraulic fluid flow controls give the operator enough flexibility to virtually rotate the drum at any rpm from 1 to 40 and to advance the drum into coal at any rate of 0 to 4 inches per minute.

Power for the rotation of the drum is provided by a gerotor type hydraulic motor which has a speed reducer of 20:1. The motor has a continuous torque of 867 in-lbs and a peak torque of 1350 in-lbs. With a 20:1 speed reduction ratio, the drum shaft attains a peak torque of 27,000 in-lbs. The unique feature of this gerotor type motor is that it multiplies the actual displacement of the gerotor and provides the mechanical advantage of 6:1 gear reduction. This accounts for the high fluid displacement and low speed characteristics with 95% volumetric efficiency (1).

Advancing and retreating of the cutting drum is accomplished by four hydraulic cylinders, two for advancing and two for retreating. These cylinders have a piston diameter of 1 in. and a stroke of 6 inches. The pistons of the two hydraulic cylinders which are located at the operator end, one each on either side of the main frame push the movable frame on which the drum and the motor is mounted. The retreating of the drum is accomplished by the two cylinders located at the confining chamber end, one on either side of the main frame. The advance and retreat cylinders can be seen in Figs. 6 and 7.

The drum has the provision to mount a maximum of seven bits in an echelon pattern or two or three bits straight across the width of the drum (Fig. 5). It can also accommodate 4 different bit blocks (Fig. 8), which are fabricated to conform to 4 different predetermined bit attack angles, 15, 30, 45, and 60 degrees (measured with respect to the drum axis).

Bit Blocks

Four types of bit blocks (7 each type) are fabricated to conform to 4 different predetermined bit attack angles, 15, 30, 45, and 60 degrees (measured with respect to the drum axis (Fig. 8). The bit block is made of steel which is welded to a base plate of 0.5 in. x 3.5 in. x 3.5 in. size that is curved to conform to the curvature of the drum. Four holes are drilled at the four corners of this plate. These holes are machined in such a way, so as to conform to the holes machined on the drum. Then a block of 1.5 in. x 2.5 in. x 4 in. size is taken and cut in such a way so as to conform to the curvature of the base plate (base plate conforms to the curvature of drum) and the necessary angle at which the bit is supposed to be with the axis of the drum. Then a one inch hole is drilled in this block into which the different cutting bits will be inserted. The block is then welded on to the base plate in between the four corner holes of the base plate. A one fourth inch hole is also made on the bit block which goes through the top end of the one inch bit hole. Then an allen screw is screwed in this hole which holds the bit in place. This allen screw is adjustable to facilitate the rotation of the bit in the bit block. This results in the symmetric wear of the bit. Four notches are made in the bit block, two in the front and two at the back in order to provide enough room to run the bolts through the base plate on to the drum.

Moveable Frame Arrangement

The movement of the movable frame is guided by 8 rollers, 4 on each side of the main frame. Two of these rollers movement is horizontal (Fig. 9) while the movement of the other two is vertical (Fig. 9).

Two steel plates which are bolted to each other in an L-shape are bolted to the main frame. In between these L-shaped plates two rollers move in a horizontal direction. These rollers held another plate to which two small plates of 0.5 in. x 2 in. x 5.5 in. size are welded. These small plates are bolted with two more rollers which move vertically and are guided by the horizontal plate of the L-shaped plates (Fig. 7). The same arrangement is there on the other side of the main frame. This special arrangement guides the movement of the cutting drum in a straight line along the main frame.

Two small plates of 1 in. x 5 in. x 9 in. are welded (one on each side of the main frame) to the steel plates that are held by the rollers. On these small plates the speed reducer with motor is mounted on the right side of the main frame and the drum shaft assembly on the left side of the main frame.

A horizontal bar of 1 in. x 2 in. x 35 in. which extends from one end of the main frame to the other is welded to the steel plates that are held by the rollers on either side of the main frame (Fig. 6). The two hydraulic cylinders one on each side of the main frame which are mounted on the operator end push the horizontal bar which in turn pushes the steel plates that are held by the rollers.

The movable frame can be dismantled, completely to mount the optical microscope with a camera in order to photograph the fracture surface.

Dust Collection

Collection of dust particles is accomplished by a vacuum pump through an aluminum hood (Fig. 10) and the three cascade impactors (Fig. 11). Coal fragments are collected by using a canvas which is hooked to the main frame (Fig. 12).

An aluminum hood of 40 in. x 45 in. side dimensions up to a height of 12 inches in height and tapered from thereon is used. A two way coupling connects the tapered end of the hold and the hose which is connected to the vacuum pump. A horizontal pipe connects the hood and the sliding pipe (Fig. 10). The sliding pipe slides on a vertical pipe which is fitted to the right corner of the main frame behind the confining chamber. Two springs are hooked between the plate on top of the vertical steel pipe and the sliding pipe (Fig. 10). The sliding pipe has a handle and a locking screw which facilitates the operator to fix the hood at any desired position over a vertical distance of 19 inches. The hood can also be rotated over 360 degrees. The left side of the tapered part of this hood has a plexiglass viewing window (Fig. 10). An aluminum plate can be slid beneath this plexiglass so as to keep the plexiglass clean when not in use.

Hydraulic Unit

The rotary coal cutting simulator is powered by a hydraulic unit (Fig. 13) through a solenoid controlled actuator assembly (Fig. 1). The hydraulic system is powered by a 25 hp electric motor which runs at 1800 rpm. The motor is powered by 230/460 volts at 64/32 ampherage rating. The hydraulic reservoir has a capacity to hold 25 gallons. The headline flow meter monitors the flow from the hydraulic unit reservoir to the directional controlled solenoid valve (Fig. 13). The solenoid valve has a pressure rating of 3500 psi with a flow capacity of 20 gpm (75 ℓpm). Its operating oil temperature is 180° F (82° C). The solenoid controlled actuator assembly is powered by 12 V DC. The solenoid controlled actuator assembly can be actuated manually (Fig. 1) and automatically.

INSTRUMENTATION

Instrumentation involves devices such as acoustic emission transducer (AET), linear variable differential transformers (LVDT)(2), pressure transducers, cascade impactors (3), flow meters and flow control valves.

It also involves other instrumentation such as signal conditioning unit, 10 channel analog data acquisition recorders, optical microscope with a camera fitted to it, high speed photography unit, hydraulic cylinders and hydraulic pumps.

Under a particular set of in-situ and operating conditions a number of parameters will be monitored using the above mentioned instrumentation. The parameters that will be measured are: (1) acoustic emission activity to characterize the fragmentation process, (2) penetration of bit into coal and displacement of confining chamber using linear variable differential transformers, (3) penetration resistance (thrust and cutting) using pressure transducers, (4) collection of the respirable dust particles by cascade impactors for respirable dust characterization, (5) study the aerodynamic characteristics of the fragmented dust particles by high speed photography, and finally (6) the fracture surface will be photographed with a camera fitted on the optical microscope, to characterize the fracture size, shape, and intensity for different bit configurations.

AUTOMATED CONTROL AND MONITORING SYSTEM (ACMS)

Apart from being able to operate manually the rotary cutting simulator can also be operated by a fully automated control and monitoring system (Fig. 14).

The ACMS controls and monitors a number of preset series of functions depending on the signals which it receives from the program that has been incorporated into the system.

The ACMS has switches to operate in a programmed or manual run mode and continuous or counter run mode. The first switch is self explanatory while the second switch runs the drum continuously or stops it after a predetermined number of revolutions. There are switches to rotate the drum clockwise and counter clockwise, while the thrust is always in the forward direction.

The system has a cutter drum rpm sensor which gives a digital readout of the drum while it is recording on the recorder in analog form. It has a thrust cylinder pressure sensor and a cutter drum motor pressure sensor which give an analog output of the pressures on the thrust cylinders and the cutter drum motor.

The system operates in two modes. In the first mode, the rotation of the drum, the advancement of the drum into coal, the number of rotations of the drum and the retreating of the drum is all automatic. In the other mode, the rotation of the drum, the advancement of the drum into coal, the number of rotations of the drum is automatic while the retreating of the drum is manual.

The system also has a limit switch which stops the drum advancement after a predetermined depth of cut (Fig. 6). One other feature of the system is to advance the drum to a predetermined depth of cut and then start cutting. The counting of the number of revolutions of the drum is accomplished by mounting a disc on the drum shaft. This disc has a number of teeth on it. The program incorporates the conversion factor to change these number of teeth into the number of revolutions (Fig. 15).

ACKNOWLEDGMENTS

The author acknowledges the assistance of N. P. Reddy, a graduate student in the Mining Engineering Department, in the design of the rotary coal cutting simulator. The author also acknowledges the assistance of the American Quality Equipment for implementing the design with necessary modifications during fabrication. This project was funded by the Generic Center for Respirable Dust Research sponsored by the United States Bureau of Mines under Grant Number G1135142.

REFERENCES

1. Allen, J., "Personal Communication," American Quality Equipment.

2. Anon, "LVDT and RVDT Linear and Angular Displacement Transducers," Schaevitz Technical Bulletin 1002C, pp. 20-21.

3. Hinds, C. W., 1982, "Acceleration and Particle Motion," Aerosol Technology, Chapter 5, pp. 119-124.

4. Newmeyer, G. E., 1981, "Cost of the Black Lung Program," Mining Congress Journal, V. 67, No. 11, November, pp. 74-75.

Fig. 1. The overall setup (a) rotary coal cutting simulator, (b) hydraulic unit, (c) ACMS control panel, (d) data acquisition system, (e) handles to actuate the solenoid valves manually, (f) solenoid valves.

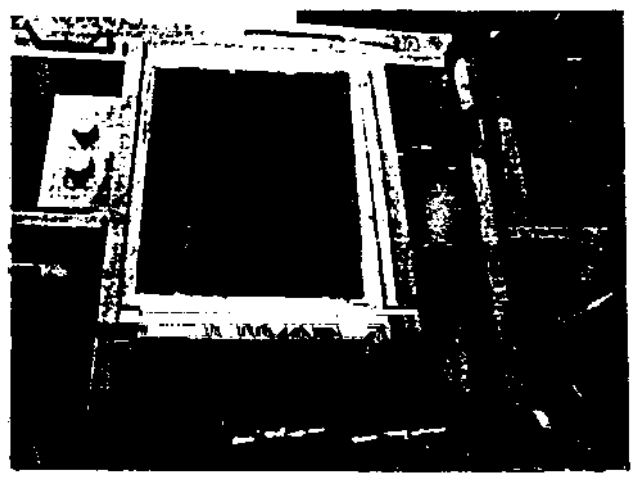

Fig. 2. Confining chamber with coal block.

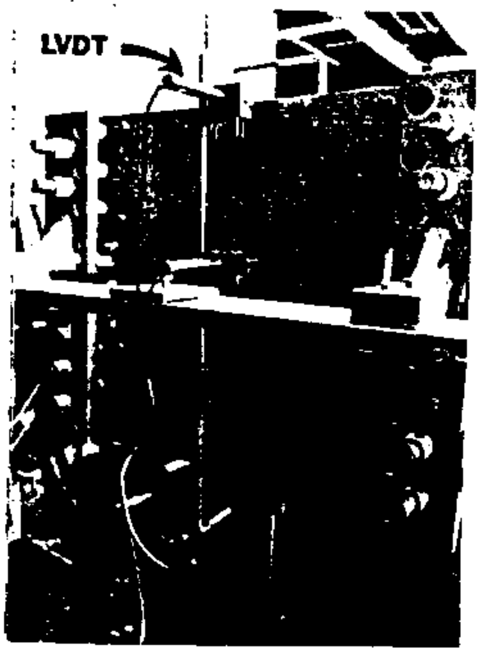

Fig. 3. Four L-shaped structures for mounting confining chamber to the main frame, shock absorbing elements and the LVDTs arrangement.

Fig. 4. Horizontal plates to limit the rotation of the confining chamber and shock absorbing arrangement.

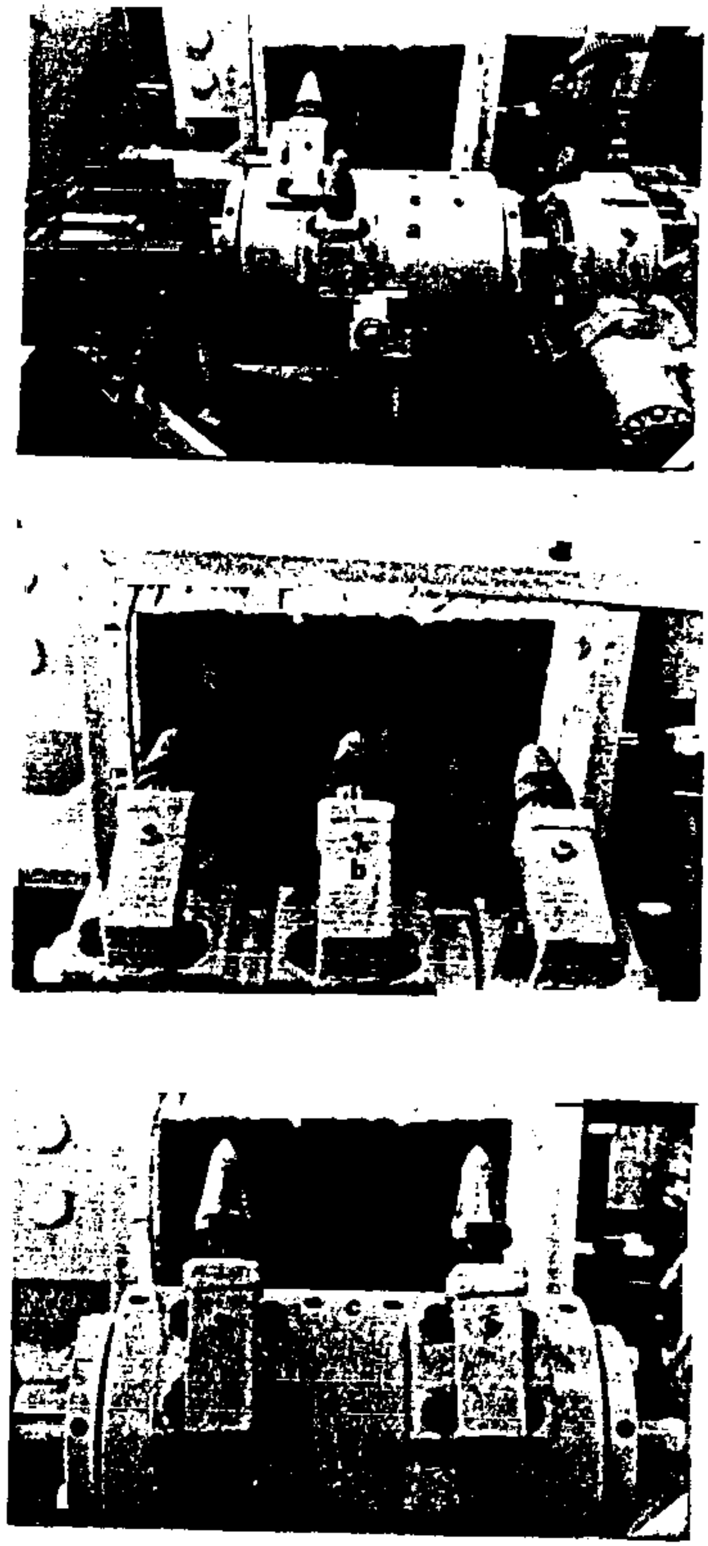

Fig. 5. Cutting drum and bit arrangement (a) 7 bits, (b) 3 bits, (c) 2 bits.

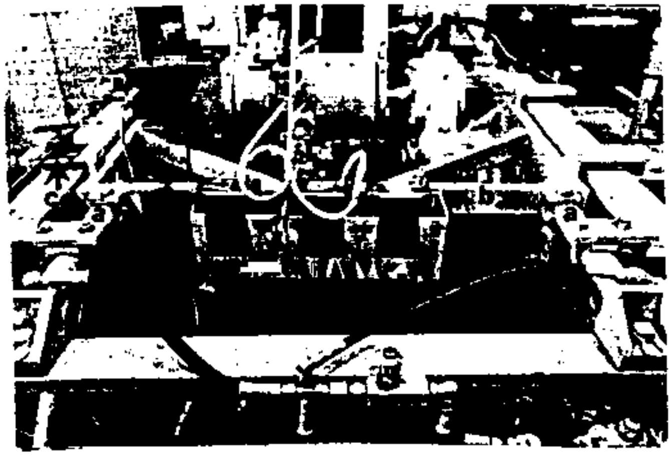

Fig. 6. (a) Advancing cylinders, (b) Horizontal bar, (c) Horizontal distance limit arrangement.

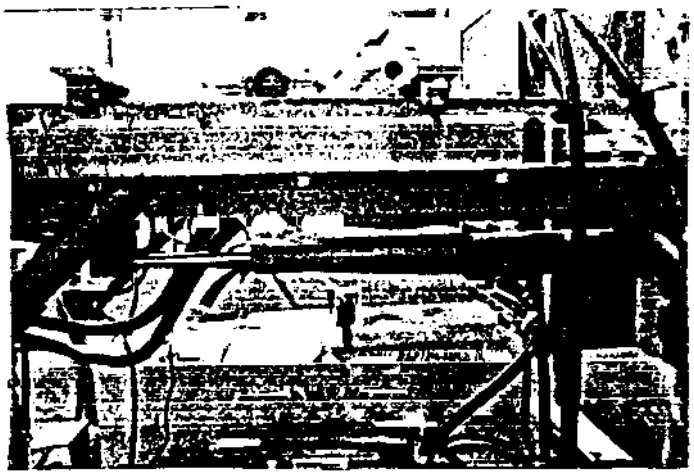

Fig. 7. Retreating cylinder.

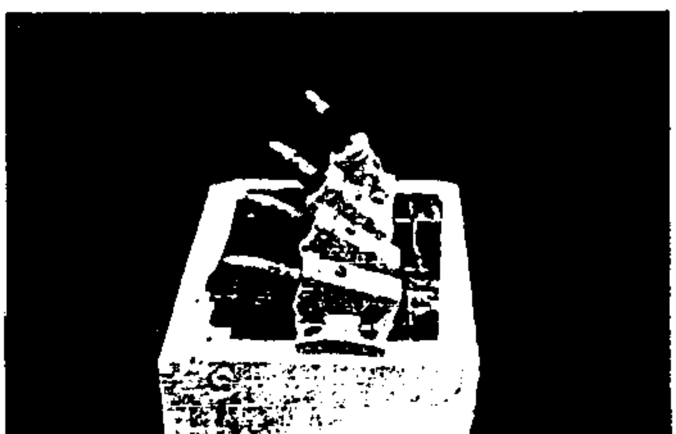

Fig. 8. Bit blocks depict four different attack angles, 15, 30, 45, and 60 degrees with respect to the drum axis.

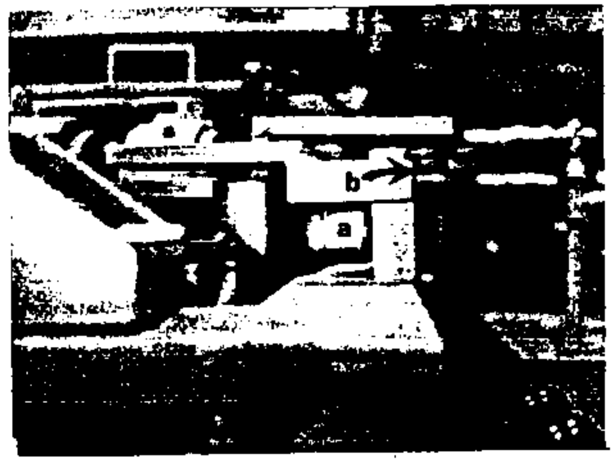

Fig. 9. Cutting head guiding arrangment (a) along horizontal plane, (b) along vertical plane.

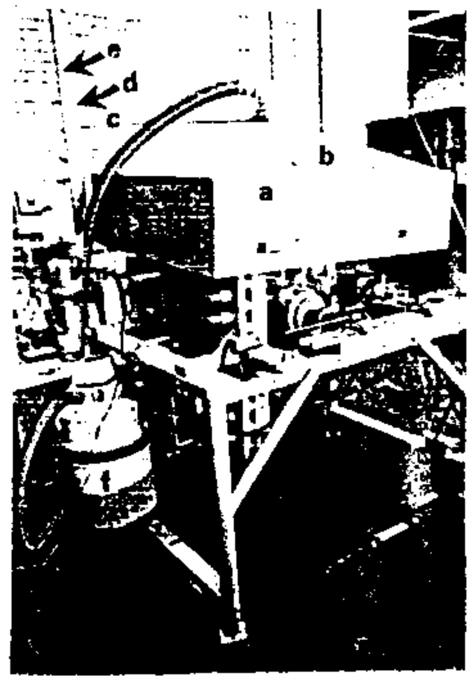

Fig. 10. Illustrates the dust collecting arrangement. (a) Aluminum hood, (b) Plexiglass viewing window, (c) Horizontal pipe, (d) Vertical pipe, (e) Lifting spring, (f) Vacuum pump.

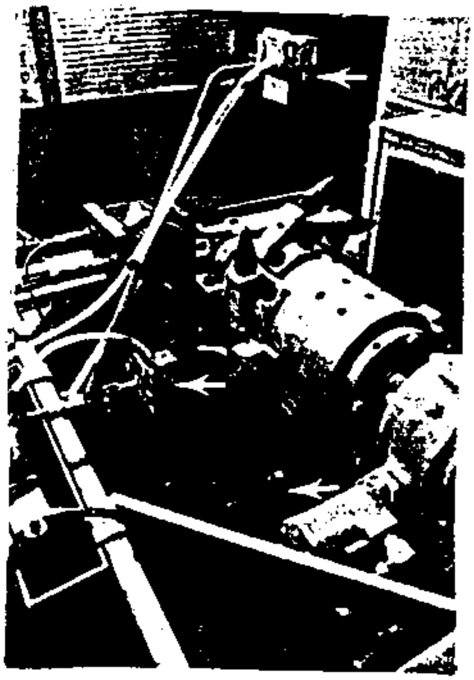

Fig. 11. Dust sampling arrangment with three cascade impactors.

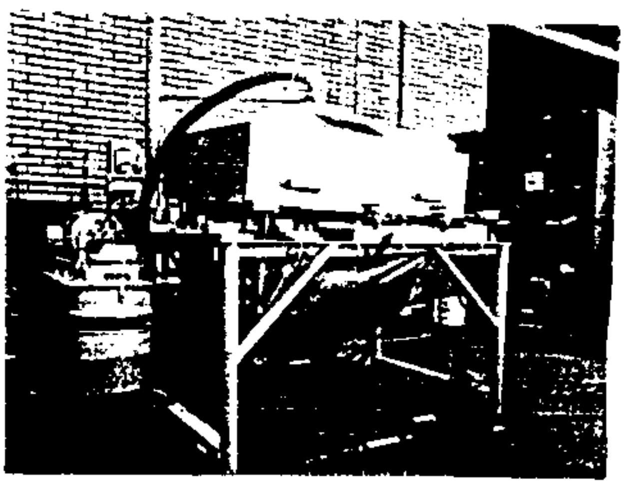

ig. 12. Canvas beneath main frame for collecting large fragments of coal.

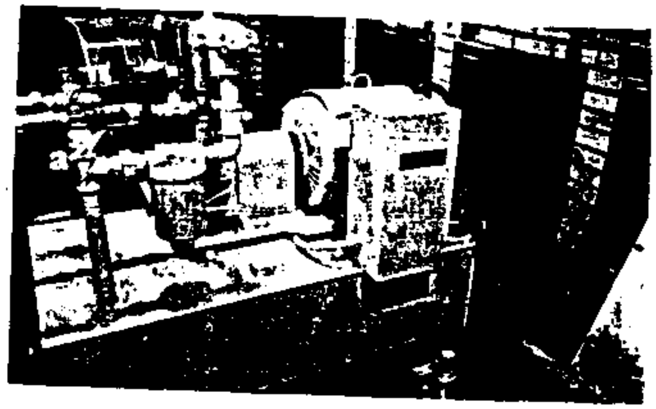

Fig. 13. Hydraulic unit (a) Flow meter.

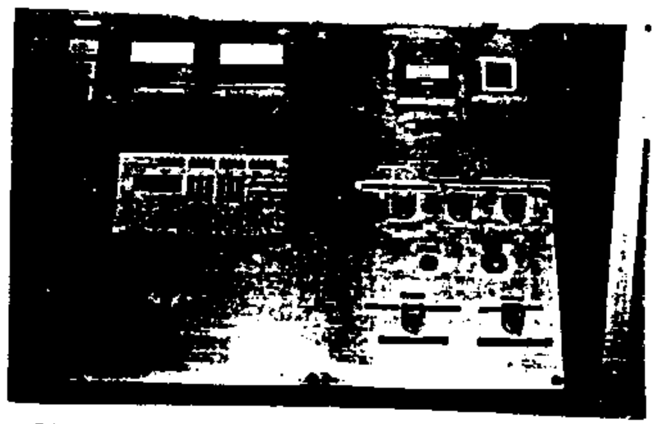

Fig. 14. ACMS control panel.

Fig. 15. Special arrangement for monitoring the speed and the revolutions of cutting drum (a) counting element, (b) rpm sensor.

STUDY OF FRACTURE MECHANISMS IN COAL SUBJECTED TO VARIOUS TYPES OF SURFACE TRACTIONS USING HOLOGRAPHIC INTERFEROMETRY*

A. Wahab Khair, Ph.D.

Associate Professor, Mining Engineering Department
West Virginia University
Morgantown, West Virginia

ABSTRACT

This paper presents an analysis of fracture mechanisms in coal subjected to bi-axial state of stresses, indentation of laterally confined coal specimen. Coal specimens were loaded to failure by the straight wedge indenters at various lateral confinement pressures. Strain distribution and acoustic emission characteristics of coal specimens under stress were recorded. The influence lines of vertical forces acting on the horizontal straight boundary of the coal specimen for each type of wedge indenter have been established using holographic interferometry technique. The effects of wedge indenter angle, confinement pressure, and coal anisotropy on fracture types, failure modes, and post-failure conditions were studied. The results indicated that combined application of holographic interferometry and acoustic emission monitoring techniques is not only suitable for studying deformability of heterogeneous and microscopically discontinuous material under stress but it also enhances the mode of fracture during the post failure stage.

INTRODUCTION

One of the relevant processes in the coal cutting technology is the application of indentation theories. Since most cutting tools in the coal industry are wedge shaped most of the indentation research is found for a wedge shaped tool.

A wide range of behavior is found in different rocks subjected to the wedge penetration. A rock which is elastic brittle at standard pressure might become elastic plastic at high confining pressure (Gnirk and Cheatham, 1963). It was also observed that some rocks will

*Prepared for presentation at the 25th U.S. Symposium on Rock Mechanics, Northwestern University, Evanston, Illinois, June 25-27, 1984.

merely be crushed and indented by a wedge whereas others will crack and form chips, furthermore the existence or non-existence of chips depends mostly on the geometry of the indenter, type of rock and the depth of penetration (Evans and Murrel, 1958). However, coal cutting technology is mostly explained by models which use rigid wedge to penetrate into a brittle material in which both crushing and chipping will occur (Evans and Murrel, 1958, 1962).

Depending upon the magnitude of the local flaws, at least three distinct regions of damage below a bit can be recognized: (a) a powdered zone adjacent to the bit (crush zone), (b) long fractures which originate in the first zone but extend to depth. These long fractures are called median vents, formed during the indenter loading, (c) an intricately fractured region in between the two above regions. Fractures in this region are called the lateral vents, which are formed during indenter unloading. It was said that lateral cracks are always associated with plastic deformation at high loads (Hartman, 1959; Johnson and Singh, 1967; Lawn and Swain, 1975).

Lundberg has conducted tests on Swedish Bohus Granite using seven indenters with angles in the range of 60° to 150°. Results here show that no chipping will occur for angles greater than 60° while crushing was predominant. However, for smaller angles chip failure was predominant (Lundberg, 1974).

The main objective of this study was to understand the fracture mechanism in coal using indentation technique with wedge shaped tools of different angles, at various confining pressures. In addition to the strain measurements, accoustic emission monitoring and holographic interferometry techniques were also used in analyzing the fracture mechanism. A brief introduction to these techniques is given here.

Microseismic techniques are based on the fact that many materials including coal, emit transient noises or vibrations. These vibrations are called microseismic activity, rock noise, seismo-acoustical, or acoustic emission (A.E. hereafter). The fact that these microseismic activities are generated from regions of instability, probably due to local failure, makes it possible to monitor failure of geologic materials (Khair, 1981). Detailed information about A.E. can be found in Hardy and Leighton, 1977 and 1980.

Holographic interferometry is a technique of measuring surface displacement. It is a photographic technique which needs no surface instrumentation, but measures displacement by superimposing a picture (hologram) of the surface in a disturbed condition over a picture of this surface in an undisturbed condition thus creating an interference pattern which describes the way that the surface has moved. This pattern is made up of contour lines of equal displacement. Closeness of these displacement lines are indicative of the severity of displacements (Khair, 1983). Detailed information about the holographic interferometry is given elsewhere in Khair, 1983.

EXPERIMENTAL STUDY

Test Specimens

Rectangular specimens of coal with approximate dimensions of 3 inches were obtained from (Coal Berg No. 2) coal blocks using a water-cooled diamond saw. The surfaces of these specimens were then ground flat and parallel, with the help of a jig attached to a surface grinder as shown in Figure 1a. After air-drying for a week, the directions of bedding, major and minor cleat planes of each specimen were identified and marked as shown in Figure 1b. At that time all of these specimens were instrumented with foil-type strain gages as shown in Figure 1(c-d). The cubical shaped specimens (Figure 1c) were used for determination of mechanical properties of coal while the plate shaped (Figure 1d) were used for the study of fracture mechanisms. In the latter case the strain gages were mounted in a position to provide strain distribution in the specimen both laterally and vertically and these gages are numbered from 1-5. Gages 1-4 are mounted to measure transverse strains, and Gage 5 measures longitudinal strain parallel to the applied load. Gage 1 is positioned on the upper edge away from

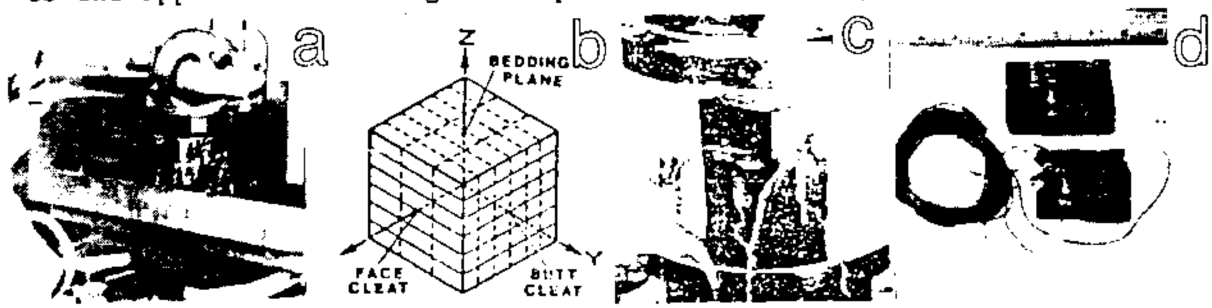

Figure 1. Illustrates: (a) specimen preparation, (b) bedding and cleat plane orientation (c) and (d) arrangements of strain gages.

the loading wedge, where Gage 2 is positioned on the upper edge right under the loading edge followed by Gage 3, 4, and 5. In order to obtain a clear hologram of the specimen a coat of white paint was used on the surface of the specimen opposite to where the strain gages were mounted.

Test Facilities

Determination of associated parameters required to utilize various equipment which, due to space limitation can only be briefly discussed.

Mechanical properties, namely compressive strength, Young's moduli, and Poisson's ratio of coal were determined using a testing machine and recording units. The facilities associated with study of fracture mechanism consisted of an optical table which acts as a vibration free surface to conduct holography, a 50 mW He-Ne laser, laser steerers and expanders. A point load tester with specially designed sperical set and loading edges was used to load the specimen to failure. An acoustic emission (A.E.) monitoring unit and recording facility was used to record deformation characteristics of the testing specimen. An overall view of experimental facilities is shown in Figure 2a. The lateral constraint was provided by a special chamber as shown in Figure 2b.

Figure 2. Shows: (a) experimental facilities; (b) confining chamber.

Test Program

The orthotropic mechanical properties of coal material were determined and are tabulated in Table 1. These mechanical properties were mostly used in determination of equivalent confining pressure. During

Table 1. Mechanical Properties of the Coal Tested

Compressive Strength (psi)			Young's Modulus (10^6 psi)			Poisson's Ratio		
C_x	C_y	C_z	E_x	E_y	E_z	ν_x	ν_y	ν_z
4688	3234	7400	0.88	1.16	0.50	0.33	0.28	0.47

an experiment the test specimen was placed in the confined chamber. While monitoring strains the specimen constrained laterally to a predetermined value. To avoid stress concentration due to lateral constraining pieces of cardboard were placed between the specimen and the chamber. Tests were carried out at four levels of equivalent confining pressures namely (0, 200, 500, and 900 psi). For each pressure level the average strain in five gages and directional elastic constants of coal were used. The specimen and the confining chamber were then placed in the loading frame, the straight edge of the wedge indenter was aligned perpendicular to the specimen and the load was applied to the specimen step by step. Two wedge indenters with angles of 20° and 45° as shown in Figure 3a-b were used. At each step the load and the strains were recorded; the holograms of the loaded specimen was obtained. Meanwhile A.E. was monitored continuously until the completion of the experiment. Following completion of the tests, the fractured specimens were photographed as in Figure 3c.

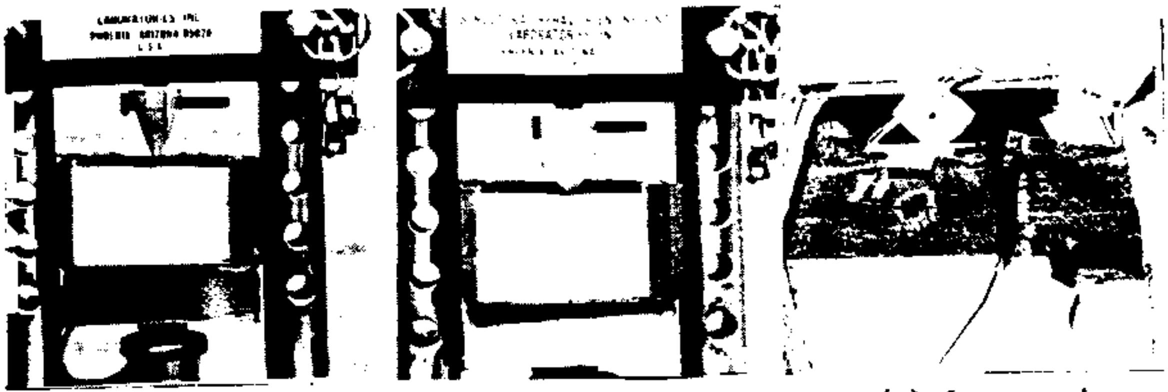

Figure 3. Shows: (a) 20°, (b) 45° wedge indenters, (c) fractured specimen.

Some typical examples of fractured specimens are shown in Figure 4.

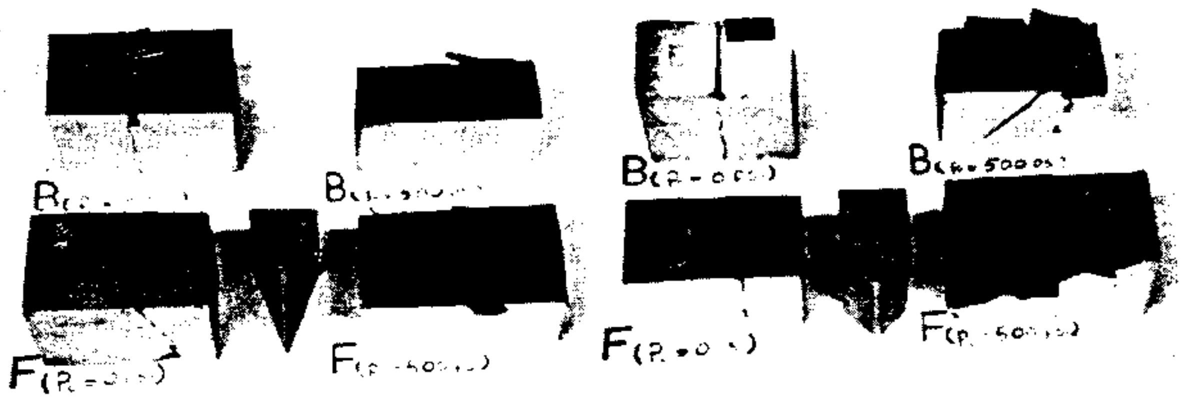

Figure 4. Shows fractured specimen by using (a) 20°, (b) 45° wedge indenters on face (F), and butt (B) cleat plane at confining pressures (P_c).

Results and Discussions

Mechanical properties of coal tested indicated directional anisotropy. Table 1 shows that compressive strength of coal in the bedding plane direction is very high in comparison to the cleat plane directions. Furthermore the value of Young's modulus in the butt cleat is much higher than the face cleat direction. Observation of fractured specimens indicated fibroidal texture resembling a stack of compressed plywood in the bedding plane direction. This feature provided rigidity in the butt cleat direction. In study of fracture mechanisms indentation forces were applied either in the direction of face cleat or butt cleat while deformation and fracture patterns were observed in the bedding plane. Table 2 shows the results of force per unit of length required to split (fracture) specimen of coal by wedge indentation under various confining conditions.

Despite the limited number of tests at each constraint condition, the following facts are clear: a) failure force per unit of length is less when using a 20° wedge than a 45° wedge, b) coal provides less

Table 2. Extension Strength of Coal, Tested in Face/Butt Cleat Plane Directions at Various Confining Pressures Using 20°/45° Wedge Indentors

Equivalent Confining Pressure (psi)	Splitting Force/Unit Length (lb/in)			
	Face Cleat		Butt Cleat	
	20°	45°	20°	45°
0	2302	2864	1744	2909
200	2183	4073	-	-
500	2099	3584	2774	5188
900	2293	4169	3087	4318

resistance when force is applied in the butt cleat plane direction than when it is applied in face cleat plane direction, c) the magnitude of failure force per unit of length is increasing with lateral constraining of the sample. This fact is quite clear when force is applied in the butt cleat direction, however the results are quite erratic at higher confining pressures and even at low pressures where the indentation force is applied in the face cleat. Change in the direction of the failure plane and the chipping of the local area under the load, as a result of high stress concentration or local flaws, could be the reasons. Observation of a failed specimen indicated more crushing and chipping when change in the direction of the failure plane occurred.

Force per unit of length-strain distribution as well as A.E. characteristics of specimen under different boundary conditions are presented in Figures 5(a-b). In general less strain in the specimens were observed prior to failure when loaded under a 20° wedge than a 45° wedge. Similarly the A.E. patterns exhibited low activity in case of a 20° wedge (Figure 5a) and high activity in the case of a 45° wedge (Figure 5b). Higher rate of A.E., indicative of higher occurrence of micro-fractures (crushing) in the specimen along the fracturing plane especially at the area of the influence of the wedge. The A.E. patterns also indicated that the rate of activity in the loaded specimens increases with confining pressures, Figures 5(c-d), as well as when the load is applied in the face cleat direction. The effects of cleat orientation, confining pressure, wedge angle, and flaws within the coal on deformation characteristics is presented in Figure 6. Figures 6(a-c) show the line of action of a 45° wedge indenter in the butt cleat direction while Figures 6(d-f) indicate the line in the direction of the face cleat plane. Comparing these two series of holograms it can be seen that a larger stress concentration zone for a given load increment is developed in the specimen loaded in the face cleat plane direction. On the other hand the line of action of the wedge indenter, applied in the butt cleat plane direction, changed throughout the specimen under each loading increment, indicative of

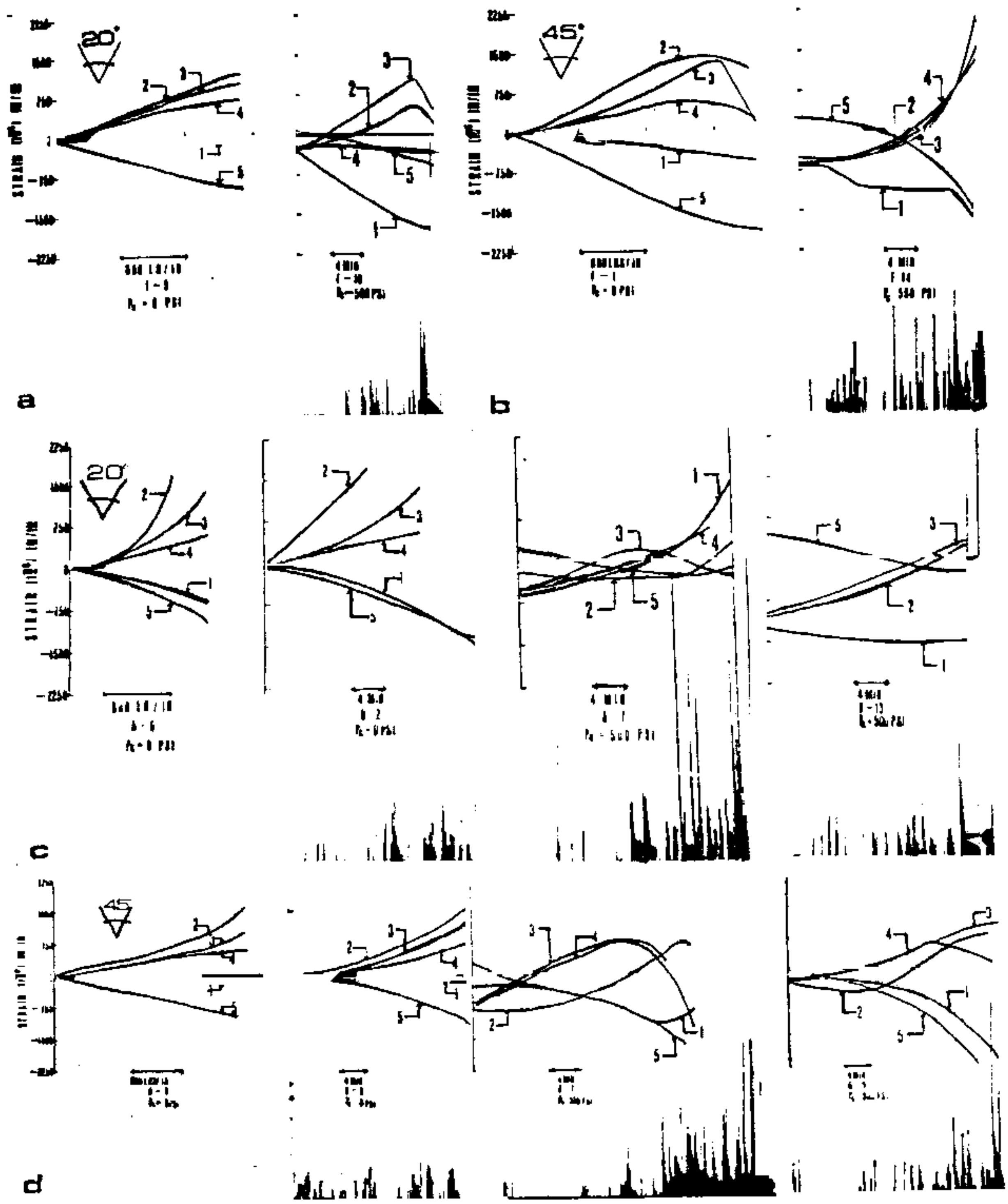

Figure 5. Shows force/unit length-strain, strain-A.E. characteristics of coal specimen under combined action of indenters and confining pressures. (A.E. set at 70 db at rate of 999 counts/0.25 sec. chart speed = 16 cm/h).

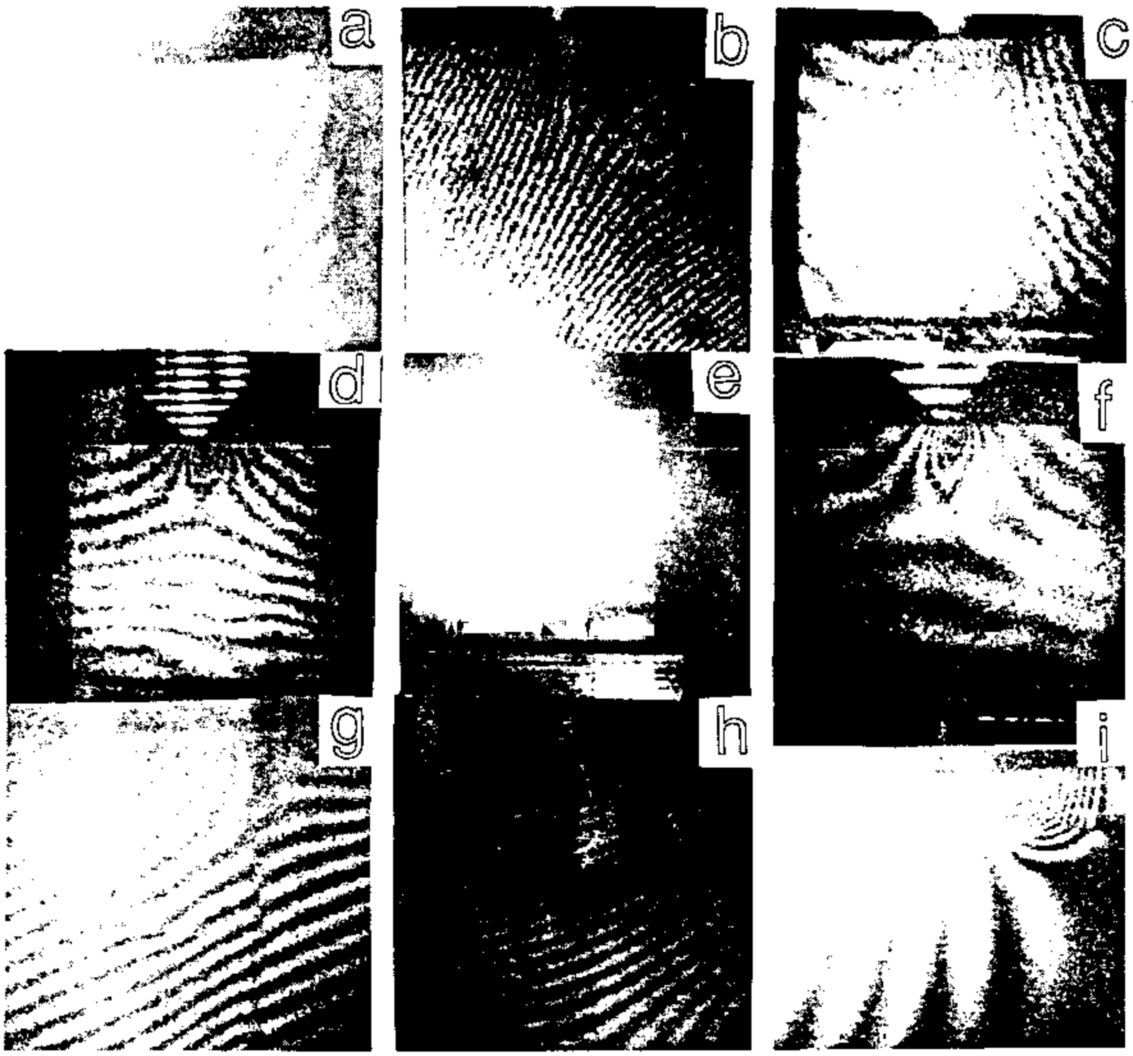

Figure 6. Shows displacement contour lines in the coal specimens subjected to incremental indentation force per unit length (F_i) in the direction of face (F) or butt (B) cleat plane. [(a-c) 45° indenter in B with P_c = 0 psi for (a) F_i = 346-433 lb/in, for (b) F_i = 519-693 lb/in, for (c) F_i = 952-1126 lb/in, (d-f) 45° indenter in F with P_c = 0 psi for (d) F_i = 1377-1463 lb/in, for (e) F_i = 2066-2151 lb/in, for (f) F_i = 1900-1987 lb/in, (g-h) 20° indenter in F for (g) P_c = 0 psi, F_i = 1379-1577 lb/in, for (h) P_c = 500 psi, F_i = 958-1057 lb/in, (i) 45° indenter in B with P_c = 500 psi and F_i = 2036-2103 lb/in].

strain redistribution in the loaded specimen. The higher the resistance provided by the specimen under failure load the larger the stress concentrated zone became. Figure 6-g exhibits lines of equal displacement in the specimen similar to Figure 6-d, however the zone of high stress concentration is much smaller due to the application of a smaller wedge angle (20°). Observation of the failed specimen, under 20° indenter, indicated less damage, crushing, and fracturing than in the case of the 45° wedge application. Figures 6(h-i) depicts the influence of local flaws in the specimen. In Figure 6-h the specimen was constrained first in the butt cleat plane direction resulting in near horizontal lines of displacements. Then the load was applied by a 20° wedge indenter. Discontinuities observed in the fringe pattern are due to local flaws. In Figure 6-i the specimen was first constrained in the face cleat direction resulting in near vertical lines of displacements. Then the load was applied by a 45° wedge indenter. The lines of action were altered by local flaws, and a combination of high confining pressure, larger wedge angle, and local flaws created high local stress concentration zone.

In summary the deformation-failure process of the coal specimen under the loading conditions described in this study can be illustrated schematically in Figure 7. As the load was applied to the specimen by the straight edge, bending of the specimen occurred as shown in Figure 7-a. This was substantiated by recorded strain in the gages. As the applied load increased to the failure load, under low confining pressure the specimen split, failed in extension, and the failure plane was parallel to the direction of wedge indenter as shown in Figure 7-b. In this case less chipping, crushing, and fragmentation were observed in the failed specimen (Figure 4-a). Under higher confining pressures and higher wedge angle when force was applied in the direction of the face cleat plane, failure in the specimens occurred in an extension mode where the failure plane was perpendicular to the direction of wedge indenter as shown in Figure 7-c. Such failure was accompanied by popping, chipping, and expulsion of material, and the failed specimen was severely damaged (Figure 4-b) resulting in higher debris and fragmentation.

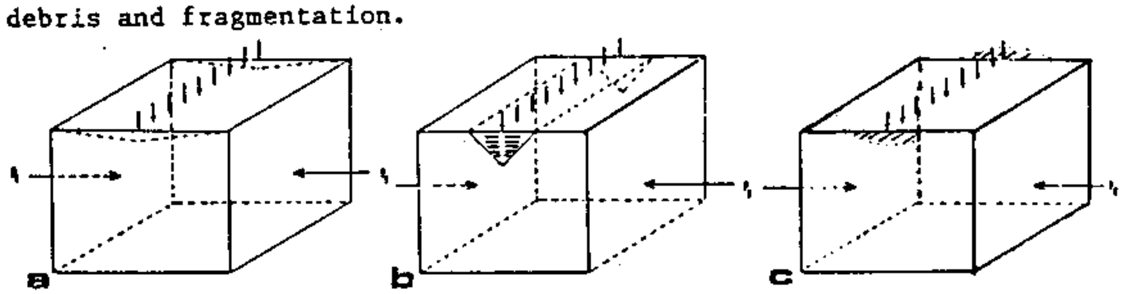

Figure 7. Depicts deformation and direction of failure plane. (a) initial stage of deformation, (b) direction of failure plane parallel to line of action of the wedge at low P_c and (c) direction of failure plane perpendicular to line of action of the wedge at high P_c.

CONCLUSIONS

In general coal samples do not behave perfectly brittle, they often exhibit some degree of ductility at the time of rupture, because they are neither homogeneous nor microscopically continuous mediums. Inherent imperfections such as porosity, cleats, joints, cracks add to the discontinuous state of coal. This discontinuity is one of the sources of permanent deformation in the coal under stress. On the other hand, discontinuities cause local stress concentration in the material when stressed, and raise stress in local areas higher than the strength of the material. This heterogeneity of the stress field causes the specimen to become locally unstable before it fails.

Results of the tests indicated that failure of coal samples under the action of a wedge indenter were in extension mode. The direction of failure plane was altered at higher confining pressure. Anisotropy of coal had a significant impact on the magnitude of load applied by the indenter to cause extension failure. Butt cleat plane direction provided the least resistance to the indenter wedge and as a result extension failure occurred in coal specimens with limited crushing zone under the straight edge of the indenter. The area of contact between the wedge and coal not only affected the size and shape of the crushed zone in the coal sample but also altered the mode of failure in the failure plane. The smaller the area of contact was, accordingly the failure was in a pure extension mode. As the area of contact increased (i.e., from 20° to 45°) the failure mode changed from bi-mode (shear-extension) to single mode (shear). The later conclusions were substantiated with two experiments as shown in Figure 8. Figures 8(a-d) show loading conditions and deformed configuration of a coal specimen subjected to a compression load applied perpendicular to the bedding plane. From Figure 8(b-d) it is obvious that deformation within the specimen is affected by the size and shape of the loading platen, especially at the boundary edge where stress is highly concentrated, resembling a punching effect. Extended loading of this specimen under the above loading conditions would have caused shear failure of the coal specimen. Figures 8(e-i) illustrate point load compression test and deformed stages of the same coal specimen. Figure 8-f shows deformed configuration of the coal specimen prior to failure load of 300 lbs. The loading condition influenced the displacement contour lines close to the contact point in a conical shape. Extended loading of the coal specimen under this type of applied load caused failure in shear-extension mode. Shear failure at the stress concentrated cone and extension failure at the tip of the cone can be observed as shown in Figures 8(g-i). Figures 8(g-i) illustrates the extent of the shearing zone, at post failure stage under subsequent incremental load. Failure zones resembling the plastic zones in ductile material. Traditional measuring techniques such as the use of strain gages would have indicated ductile failure. However these crushed zones indicated the existence of fine particles discontinued by micro-fractures, a characteristic typified by brittle failure.

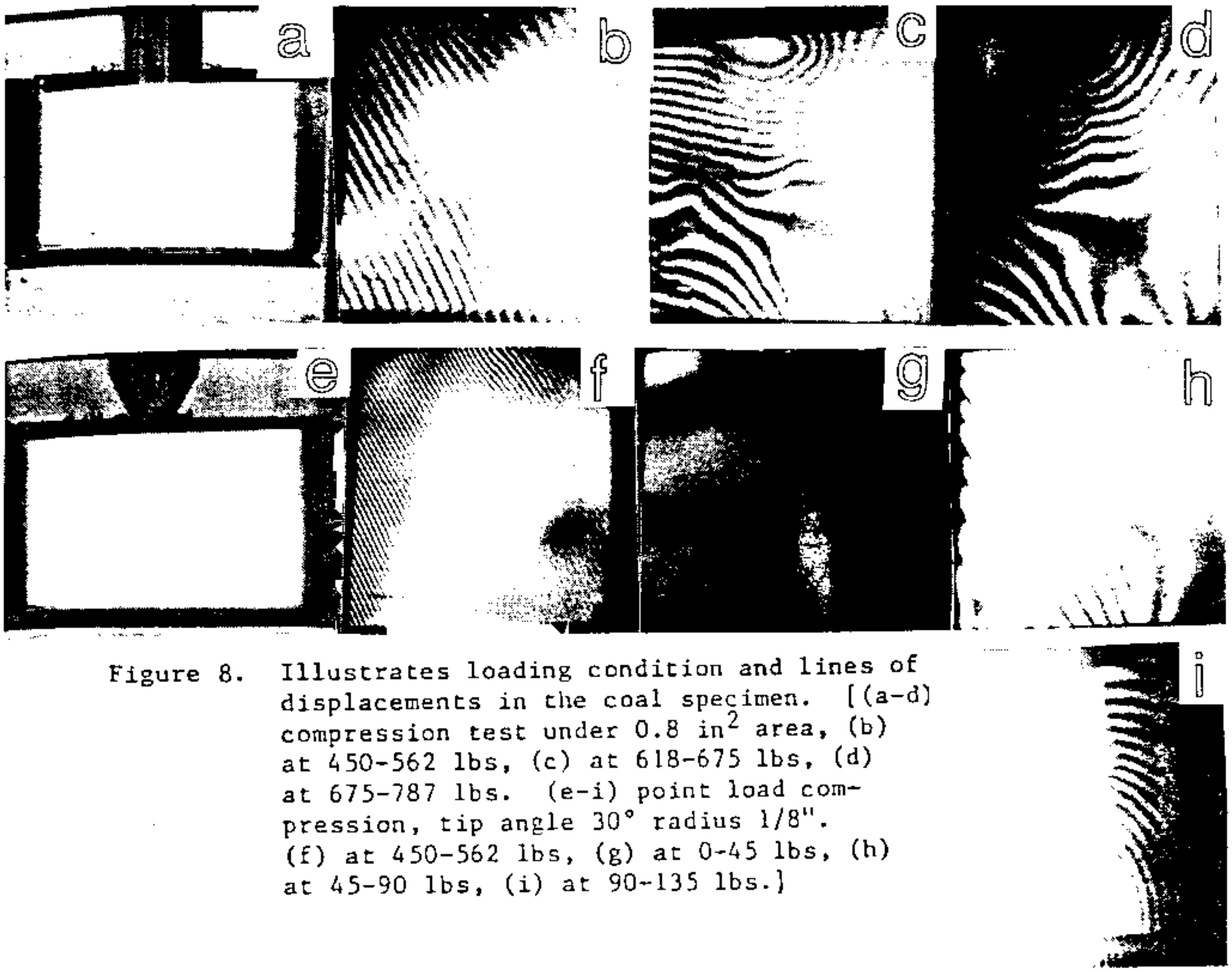

Figure 8. Illustrates loading condition and lines of displacements in the coal specimen. [(a-d) compression test under 0.8 in^2 area, (b) at 450-562 lbs, (c) at 618-675 lbs, (d) at 675-787 lbs. (e-i) point load compression, tip angle 30° radius 1/8". (f) at 450-562 lbs, (g) at 0-45 lbs, (h) at 45-90 lbs, (i) at 90-135 lbs.]

ACKNOWLEDGMENTS

The author acknowledges the assistance of R. D. Begley, G. Begley, N. P. Reddy, and N. A. Reddy, graduate students in the mining engineering department. This project was supported by funds from Generic Center associated with Respirable Dust, sponsored by Bureau of Mines under Grant Number G-1135142.

REFERENCES

Evans, I. and Murrel, S. A. F., 1958, "The Forces Required to Penetrate a Brittle Material with a Wedge Shaped Tool," Mechanical Properties of Non-Metallic Brittle Materials, Walton, W. H., ed., Interscience Publishers, Inc., pp. 432-450.

Evans, I. and Murrel, S. A. F., 1962, "Wedge Penetration into Coal," Colliery Engineering, January, pp. 11-22.

Gnirk, P. F. and Cheatham, J. B., Jr., 1963, "Indentation Experiments on Dry Rocks under Pressure," First Conference on Drilling and Rock Mechanics, January, AIME, Society of Petroleum Engineers.

Hardy, H. R., Jr. and Leighton, F. W., eds., 1977 and 1980, First and Second Conferences on A.E./M.A. in Geologic Structures and Materials, respectively, Pennsylvania State University, Trans. Tech. Publ.

Johnson, A. M. and Singh, M. M., 1967, "Static and Dynamic Failure of Rock under Chisel Loads," Transactions SME-AIME, December, pp. 366-373.

Khair, A. W., 1981, "Accoustic Emission Pattern: An Indicator of Mode of Failure in Geologic Materials as Affected by Their Natural Imperfections," Third Conference on Accoustic Emission/Microseismic Activity in Geologic Structures and Materials, Hardy, H. R., Jr. and Leighton, F. W., eds., Trans. Tech. Publ., October, 22 pp.

Khair, A. W., 1983, "Analysis of Interaction Between Models of Mine-Roof-Pillar-Floor Using Holographic Interferometry and Analytical Techniques," Proceedings of 24th U. S. Symposium on Rock Mechanics, Texas A & M University, June, pp. 107-117.

Lawn, B. R. and Swain, M. V., 1975, "Microfracture Beneath Point Indentations in Brittle Solids," Journal of Material Science, Vol. 10, pp. 113-122.

II

Dilution, Dispersion, and Collection of Dust

DUST TRANSPORT IN MINE AIRWAYS

R. V. Ramani
Professor of Mining Engineering
and
R. Bhaskar
Graduate Assistant

Department of Mineral Engineering
The Pennsylvania State University
University Park, PA 16802

ABSTRACT

The National Academy of Sciences (1) recognized the importance of studying the spatial and temporal characteristics of respirable coal mine dust atmospheres. In this paper, the progress to date of a research project on dust transportation and deposition in mine airways is presented. A mathematical model is proposed for studying the transport of dust. A source representative of dust generation in underground coal mining is defined. The influence and applicability of surface roughness, dispersivities, coagulation and reentrainment to mine dust flow are examined. A convective-diffusion model is proposed for the transport and deposition of dust in mine airways. Using the model, the spatial and temporal characteristics can be evaluated in terms of dust concentrations in the mine atmospheres.

LIST OF SYMBOLS

A' = cross sectional area of particle
c = airborne concentration
C_D = drag coefficient
C_{fx} = local stress coefficient
C = slip correction factor
d = particle diameter
D = diameter or hydraulic diameter of duct/airway
D_p = Brownian diffusivity
E_x = dispersion coefficient in x direction
f = fanning friction factor
f^* = coefficient of friction
F = resistance to the motion of settling particles
F_r = frictional force resisting movement of deposited particle
g = acceleration due to gravity
k = surface roughness height
K_{ij} = collision frequency function
i = i^{th} class of size distribution
ℓ' = mean free path of gas
L = length of airway under consideration
n_k = number of particles in size class k
N = amount of particles deposited on a surface
r_i = radius of particle in i^{th} class
R = radius of duct
Re = Reynolds number
Sc_ℓ = molecular Schmidt number
Sc_t = turbulent Schmidt number
U = flow velocity
u_* = friction velocity
V = deposition velocity of particles
V^+ = non-dimensional deposition velocity
v_t = particle settling velocity
x' = distance from leading edge of a finite surface where $x' = 0$ is the point where the flow starts
y = distance from surface of deposition
y^+ = non-dimensional $y = yu_*/\nu$
δ = rebound factor of gas from a particle's surface
ϵ = eddy diffusivity
ϵ_d = energy dissipated by turbulence
λ = coefficient of friction for smooth pipes
λ_r = coefficient of friction for rough pipes
μ = dynamic viscosity
ν = kinematic viscosity
ρ_g = density of gas
ρ_p = density of particles
τ = dimensionless particle relaxation time
τ = particle relaxation time

INTRODUCTION

The prediction of the behavior of fine particles is important in many fields of science and engineering including physics, chemistry, mining, mineral processing, and atmospheric science. In mining from the health point of view, fine coal dust is associated with the appearance of pneumoconiosis in miners exposed to the dust. Also, in addition to being a nuisance factor obscuring visibility and general mobility of miners, it can lead to sudden catastrophic incidences of explosions. This paper outlines the progress to date of a research project on dust transportation and deposition in mine airways. A mathematical model is proposed for studying the transport of dust for the various mechanisms. The dust dispersion is defined in terms of a dispersion term determined from experimental data by Skubunov (23). Coagulation is considered as one of the mechanisms that can lead to changes in the particle size distribution. Reentrainment as a possible secondary source of

Presented at the Proc. Coal Mine Dust Conference, Morgantown, W. Va., October 8-10, 1984.

dust was examined during model development but was not included in the final model.

The above factors are integrated to predict deposition rates and ambient concentrations as a function of time and distance. The transportation of dust has been modeled as a turbulent flow phenomenon in rough pipes using a convective diffusion equation solved for several particle ranges using finite difference techniques.

MODELING CONSIDERATIONS

Particle Deposition

Mass transfer resistance immediately adjacent to a surface is usually described by a deposition velocity, V, defined by Chamberlain (5) as:

$$V = N/c. \quad (1)$$

The deposition velocity equation (1) can be nondimensionalized with respect to the friction velocity u_* as follows:

$$V^+ = \frac{N}{c\ u_*} \quad (2)$$

The deposition velocity is the sum of the deposition due to various mechanisms that act on a particle. The three major mechanisms of particle deposition in turbulent flow are Brownian diffusion, eddy diffusion, and sedimentation. The other mechanisms of minor importance with reference to conditions prevailing in coal mine airways are mass transfer due to thermal gradients that exist near the surface of deposition, attraction of charged particles to deposition surfaces and inertial impaction of particles at points where the airstream undergoes abrupt changes in flow direction.

Amongst the major mechanisms of deposition, unanimity does not exist amongst researchers as to the delineation of the regimes of the different mechanisms with respect to particle sizes. For example, Gardner (11) categorizes deposition of particles into three main regimes: namely, diffusional (in the order of 0.1 microns), turbulent eddy diffusion or eddy impaction (2 to 50 microns), and particle inertia moderated regime (in the order of 10 microns). Since in the particle inertia moderated regime, the deposition process is also a turbulent impaction process it can be thought of as a continuation of the eddy diffusion-impaction process. Friedlander (9), on the other hand, adopts a simpler classification dividing deposition into convective diffusion (< 1.0 microns) and inertial deposition (> 1.0 microns). In this paper, the Friedlander classification is adopted, but the model is developed such that all three mechanisms are adequately accounted for.

Deposition by Convective Diffusion

Friedlander and Johnstone (8) did pioneering work in this area. Later workers have adopted their model assuming that particle deposition in vertical pipe flow can be described by an eddy diffusion transport followed by a final flight to the surface. Owen (17) proposed that particles are convected from the region of energetic turbulent motion outside the viscous sublayer to the wall by the occasional large eddy that encroaches the sublayer. He supports his theory by relating to a phenomenon of sporadic violent eruption from the viscous sublayer as observed by Kline et al. (13). There are not many experimental or theoretical observations on the final flight of the particles. However, regardless of the actual physical phenomena, by assuming that the particles are deposited once they reach the viscous sublayer, the general expression for the diffusion flux as proposed by Friedlander (9) and modified by Sehmel (21) can be used. This equation is

$$N = (D_p + \varepsilon)\ \frac{dc}{dy} + v_t c. \quad (3)$$

The sign of the terminal velocity, v_t, is positive for floor deposition and negative for roof deposition. For side deposition the $v_t c$ term is not included in the expression for N.

The value of the eddy diffusivity varies with distance from the boundary layer. When integrating the deposition velocity relationship, the limits of integration will have to be taken according to the applicability of the various relationships used to describe the eddy diffusivity of the particles.

Owen (18) proposed the following expression for ε/ν.

$$\varepsilon/\nu = 0.001y^{+3} \qquad 0<y^+<5 \text{ - sublayer} \quad (4a)$$

$$\varepsilon/\nu = 0.012(y^+ - 1.6)^2 \qquad 5<y^+<20 \text{ - buffer layer} \quad (4b)$$

$$\varepsilon/\nu = 0.4(y^+ - 10.0) \qquad y^+>20 \text{ - turbulent core} \quad (4c)$$

Friction velocity is calculated from the relation

$$u_* = \frac{U}{2f} \quad (5)$$

where f is the fanning friction factor and is equal to one fourth of Darcy's friction factor. This formula is more applicable than others for studies in mining as Darcy's friction factors are routinely calculated in mine ventilation studies.

Assuming that the roughness of a mine airway is in the order of the buffer layer, then the integral for the sublayer (i.e. $0<y^+<5$) will be negligible. Therefore, the integration will span the region $5<y^+<R^+$, where R^+ is the dimensionless hydraulic radius of the duct and is given by $R^+ = Ru_*/\nu$.

In this paper, the above equation is used for describing deposition rates for particles with dimensionless relaxation time (σ) between 0 and 17, where

$$\sigma = \frac{u_*^2\ \tau}{\nu} \quad (6)$$

and τ is the relaxation time, given by

$$\tau = \frac{\rho_p d^2 C}{18\mu} . \qquad (7)$$

For σ between 17 and 265, the Wood (27) approximation, matched with Liu and Agarwal data (16), is given by

$$V^+ = \frac{N}{cu_*} = 0.13. \qquad (8)$$

For $\sigma \geq 265$, the Wood empirical formula is

$$V^+ = \frac{2.6}{\sqrt{\sigma}} \left(1.0 - \frac{50.0}{\sigma}\right). \qquad (9)$$

Deposition Due to Gravity Effects

For deposition on the floor, the rate will depend upon the terminal velocity, v_t. The deposition velocity due to gravity will be

$$V_{gravity} = v_t . \qquad (10)$$

The equation describing the terminal velocity depends on the particle size range. Fuchs (10) calculated settling velocities for steady state particle motion in the various size ranges. The expression for terminal settling velocity in the 0 to 0.01 micron range is

$$v_t = \frac{F(4.5\ \delta)\ell'}{6\pi\mu r^2} \qquad (11a)$$

where,

$$F = \frac{\pi d^3 \rho_p g}{6} .$$

The value of δ depends on the way the gas molecules rebound from the surface of the particle and ranges from 1.091 to 1.175. An average of 1.13 is assumed here.

For particle diameters from 0.01 to 8 microns, Fuchs equation is (21)

$$v_t = \frac{\rho_p d^2 g}{18\mu} \left[1.0 + A\frac{\ell'}{r} + Q\frac{\ell'}{r}\exp\left(-\frac{br}{\ell'}\right)\right]. \qquad (11b)$$

The values of the coefficients A, Q and b are 1.246, 0.42 and 0.87, respectively.

For particle diameters greater than 8 microns and less than 15 microns, Stokes formula is considered applicable (21).

$$v_t = \frac{\rho_p d^2 g}{18\mu} . \qquad (11c)$$

A general equation for particle sizes greater than 8 microns is (21)

$$v_t = \left(\frac{2F}{\rho_g r^2 C_D}\right)^{1/2} . \qquad (11d)$$

The drag coefficient C_D is calculated as follows (21):

$$C_D = \frac{24}{Re}\left[1.0 + (a + bRe + cRe^2 + dRe^3 + eRe^4)(Re^f)\right] \qquad (12)$$

where,

$a = -1.1204909 \times 10^{-3}$
$b = 0.112008758$
$c = -2.0444472 \times 10^{-4}$
$d = 2.9734145 \times 10^{-7}$
$e = -1.2782079 \times 10^{-10}$
$f = -0.2121004 \times 10^{-1}$.

In this paper, equations 11a and 11b are used for the calculation of terminal velocity of the particles of size up to 8 microns. For particles over 8 microns, equation 11c is used instead of 11d since the results from the latter do not compare well with other data (7).

Coagulation

The interaction of particulate matter plays an important role in the determination of airborne particle size distribution and thus the amount deposited on the surfaces of the airways. Smoluchowski (6) proposed a model for the rate of change of the number of particles in any size range as

$$\frac{dn_k(t)}{dt} = \frac{1}{2}\sum_{\substack{i=1 \\ i+j=k}}^{k-1} K_{ij} n_i n_j - n_k \sum_{i=1}^{\infty} K_{ik} n_i \qquad (13)$$

where $n_k(t)$ is the number of particles of size k at time t and K_{ij} is the collision frequency function between particles of sizes i and j. The first term on the right side represents the gain to size k from collisions between particles i and j and the second represents loss from the k^{th} class by collisions of particles of size k with all other particles. The factor of 1/2 is introduced because each collision is counted twice in the summation.

The efficiency of sticking is probably dependent on shape, nature of the surface of the colliding particles, size, as well as electrostatic and Van der Waals forces. In the absence of definite literature, theoretical or experimental, the efficiency of sticking is usually assumed to be 1.

In a modified form of the Smoluchowski equation (6) the consideration of porosity of agglomerated particles is ignored. The modified rate equation used in the model is:

$$\frac{dn_k(t)}{dt} = \frac{1}{2}\sum_{\substack{i=1 \\ i+j+k}}^{k-1} K_{ij} n_i n_j + n_k \sum_{i=1}^{\ell} K_{ik} n_i - n_k \sum_{i=\ell+1}^{\infty} K_{ik} n_i$$

(14)

Collision Mechanisms

Coagulation of particles occurs when two particles intercept each other. Assuming that all particles that intercept one another adhere to each other, then the number of particles that coagulate or coalesce with time is given by a collision frequency function. The collision frequency function depends on the physical processes involved. The processes involved can be Brownian motion, turbulent motion of the fluid, differential shear of the fluid due to velocity gradient, and differential settling. It is assumed that the particles are non-interacting, i.e., the forces of attraction between them are negligible except on contact, when they are large enough to hold them together.

Saffman and Turner (20) developed a comprehensive model that took into account the motion of the drops with the air, sedimentation and also relative motion due to the air. The formula proposed is:

$$K_{ij} = 2(2\pi)^{1/2}(r_i+r_j)^2[(1-\frac{\rho_g}{\rho_p})^2(\frac{\overline{Du}}{Dt})^2(\tau_1-\tau_2)^2 + \frac{1}{3}(1-\frac{\rho_g}{\rho_p})^2(\tau_1-\tau_2)^2 g^2 + \frac{1}{9}(r_i+r_j)^2\frac{\epsilon_d}{\nu}]^{1/2} \quad (15)$$

where $(\frac{\overline{Du}}{Dt})^2 \approx 1.3\nu^{-1/2}\epsilon_d^{1/2}$ as shown by Batchelor (4).

Reentrainment

Particles of dust deposited on a surface may become airborne through the process of reentrainment. Reentrainment occurs when the dispersing force acting on the particle overcomes the forces of adhesion. Reentrainment can take place by three mechanisms, namely, mechanical concussion, explosive dislodgement and aerodynamic dispersement. In a duct flow, the dominating mechanism is the removal of particles by airflow and the turbulence caused by it, i.e. aerodynamic dispersement.

According to Bagnold and others (2,12) when the shear due to airflow exceeds adhesive forces, then the particles roll over the other grains, a process known as saltation. As the particles gather momentum, their paths will consist of little bumps over other particles or the surface. If the bumps are slightly violent, then the particles may jump above the viscous sublayer. The turbulent fluctuation of the airflow may now act carrying the particle clear off the surface. In the absence of any conclusive evidence, it is presumed that once the particles are reentrained they are carried into the airstream.

Bagnold (2) suggested that a static threshold velocity is necessary to overcome the adhesive forces which hold the particle to the surface. This velocity depends on the history of the exposed surface and turbulence. Punjrath and Heldman (19), based on the Bagnold hypothesis, proposed that the particle reentrainment rate can be derived from a force balance equation. The aerodynamic force F acting on a deposited particle can be written as:

$$F = \frac{C_D \rho_g U^2 A'}{2}. \quad (16)$$

At the boundary layer where the surface has an effect on flow conditions near it, the drag coefficient can be replaced by a local shear stress coefficient (19). The frictional force (F_r) can be defined as:

$$F_r = \rho_p f^* g \frac{\pi d^3}{6}. \quad (17)$$

Reentrainment occurs when the local aerodynamic force exceeds the frictional force, i.e.,

$$(\frac{\pi d^2}{4})(C_{fx}\rho_g\frac{U^2}{2}) \geq \rho_p f^* g(\frac{\pi d^3}{6}). \quad (18)$$

Assuming the roughness height of the surface to be the same as the diameter of the particles, the Schlichting definition (22) of C_{fx} is

$$C_{fx} = (2.87 + 1.58\log x'/k)^{-2/5}, \quad 10^2<\frac{x'}{k}<10^6 \quad (19)$$

thus expressing the stress coefficient as a function of the distance x' from the leading edge.

Assuming that the surface roughness can be represented by roughness height, reentrainment occurs if

$$U \geq (\frac{4\rho_p d f^* g}{3\rho_g})^{1/2}[2.87+1.58\log(\frac{x'}{d})]^{5/4}, \quad 10^2<\frac{x'}{d}<10^6 \quad (20)$$

where d is the median diameter of the particle.

It must be realized that the above derivations are valid only for reentrainment from horizontal surfaces. This aspect had attracted the attention of scientists studying movement of desert sands and resuspension and transportation of radioactive material from the earth's surface after a nuclear fallout. No such analyses have been made for reentrainment from the roof and sides of ducts. Little is known about the forces that hold these particles once they are deposited. It is possible that electrostatic forces, Van der Waals forces, surface tension and chemical bonds may be the dominant or contributing mechanisms. Due to the absence of saltating forces which are the dominating mechanisms on horizontal surfaces, the amount of reentrainment from the side and roof is probably not significant. As mentioned earlier, the equations are based on the physical interpretation of Bagnold. No account is taken of other possible adhesive mechanisms such as electrostatic forces. Reentrainment may be ignored as a source-sink since its effect can be dominant only at high air velocities and not at the 2 to 4 m/s maximum velocities normally encountered in mine workings.

Diffusion and Dispersion of Dust

Skubunov (23) proposed the following relationship for the longitudinal dispersion coefficient, E_x.

$$E_x = 15.6\ UDSc_l^{-0.6}\ Sc_t\ \sqrt{\lambda/\lambda_r}\ . \qquad (21)$$

To translate the dispersion coefficients proposed by Skubunov to the transfer of aerosols in a turbulent medium, the relation between particle acceleration and fluid motion has to be considered as the density of the medium (ρ_g) and of the particles (ρ_p) become important. When the particle is very light, ρ_g and ρ_p are nearly equal, i.e., the ratio $(\frac{\rho_g}{\rho_p})$ approaches 1.0, then the particle can be expected to very nearly follow the fluid motion. On the other extreme, where ρ_g/ρ_p approaches zero, the particle will tend to remain nearly fixed in space, and the fluid will flow around it.

A fundamental problem in turbulent flow is whether the motion of particles can be considered identical to that of the medium. On the basis of theoretical studies, Tchen (12) showed that the coefficients of turbulent diffusion of particles are equal to that of the medium. While particles possess a smaller fluctuation velocity than the medium, their velocities are more persistent. Thus their time scale of turbulence and the diffusion steps are larger than those of the elements of the fluid. Similar conclusions were later drawn by Soo (25) and Liu (15). Soo also carried out experiments (26) which confirmed these conclusions.

Skubunov (24) consolidated the results of a number of researchers to determine the coefficients of turbulent transfer. A major conclusion of his work is that the coefficients of turbulent transfer agree irrespective of the nature of the flowing fluid or the diffusing impurities. These relate to workings with a steady, uniform velocity profile in the transverse direction. Where the velocity profile is not uniform, the coefficient of longitudinal diffusion may be higher.

NUMERICAL MODELING OF DUST FLOWS

Turbulent transfer of particulate matter in airflow lends itself to numerical analyses. Particulate analyses differ from that of dispersion studies of gaseous matter in that the dominant physical mechanisms are size dependent.

The properties of a turbulent fluid are observed to spread maintaining a nearly gaussian distribution, and a statistical equation for turbulent diffusion of a parabolic form has often been applied (12). For incompressible flows the equation in generalized form can be expressed as:

$$\frac{\partial c}{\partial t} = \frac{\partial}{\partial x}(E_x \frac{\partial c}{\partial x}) + \frac{\partial}{\partial y}(E_y \frac{\partial c}{\partial y}) + \frac{\partial}{\partial z}(E_z \frac{\partial c}{\partial z}) - U(x)\frac{\partial c}{\partial x} - U(y)\frac{\partial c}{\partial y} - U(z)\frac{\partial c}{\partial z} + \text{sources} - \text{sinks} \qquad (22)$$

where c is the average concentration; x, y and z are the axes; E_x, E_y, and E_z are turbulent dispersion coefficients; and U(x), U(y) and U(z) are the velocities in the three directions respectively.

Assuming that the concentration remains rather constant as one traverses from the core of the duct to the boundary with most of the change taking place in the boundary layers, and basing deposition equations on such an assumption, the population balance one-dimensional equation for constant velocity in the direction is:

$$\frac{\partial c_i}{\partial t} = E_x \frac{\partial^2 c_i}{\partial x^2} - U \frac{\partial c_i}{\partial x} + \text{sources} - \text{sinks} \qquad (23)$$

where for a particle range with representative diameter i,

$\frac{\partial c_i}{\partial t}$ = rate of growth of concentration

$U \frac{\partial c_i}{\partial x}$ = net gain due to convective transfer

$E_x \frac{\partial^2 c_i}{\partial x^2}$ = loss due to turbulent diffusion.

The size distribution of the particles is divided into a number of size classes. This equation is solved for various size classes using representative particle diameters. The general behavior of a particular size distribution is obtained as a sum effect of that of the individual size classes.

To solve the equation one initial and two boundary conditions are required. The initial condition can be of the form:

$$c(x,t) = 0 \text{ for } t = 0,\ 0<x<L \qquad (24)$$

where L is the length of the airway under consideration. Assuming a dominative convective transfer and that the concentration gradient at the point L does not vary, it can be

$$\frac{dc}{dx} = 0 \qquad (25)$$

This would mean that at the artificial boundary, L, the concentration is in the asymptotic region of the falling concentration curve, an assumption that would be reasonable when considering long airways.

Source Term

Recognizing the fact that the rate of emission of dust varies with the mode of operation of the continuous miner, a step type source function is assumed (Figure 1) given by:

$$s(x,t) = \delta(t-t_1)A_1 + \delta(t-t_2)A_2 \ \ldots \qquad (26)$$

where $\delta(t-t_i)$ is the direct delta function and A_i is the emission when in mode i of the miner's operation.

The Thomas algorithm for solution of diagonally dominant tridiagonal matrices is used in the computer program for solving the finite differences approximation of the convective-diffusion equation developed by Bandopadhyay (3).

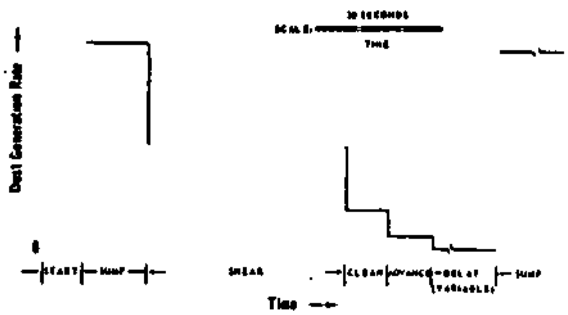

Figure 1. Dust Generation Rate of a Continuous Miner.

Preliminary Analyses of Model

Validation of mathematical models of environmental systems is difficult due to a number of reasons. For one, the boundaries of environmental systems are ill defined. Secondly, there are too many parameters of the model to carry out controlled validation experiments. Thirdly, model validation experiments can also be very expensive.

A preliminary test of the model was done using published data (14). The mine section in which the data was collected is shown in Figure 2. Due to the lack of data on all the parameters needed for validation, it was possible to compare only the deposition patterns of the model and not absolute values. This was done by taking the ratio of the deposition at all points with respect to point 1. Figure 3 shows the results of the deposition pattern obtained from the model. The experimental data points are also shown in the figure. As can be seen in the figure, the deposition pattern is in general agreement with the experimental points. The discrepancy with points 2 and 3 could probably be due to the assumption of an average velocity in the model while the velocities varied from point to point as well as during the course of the experiment. The experimental deposition data also showed some variation at the 30.48 m station. At points where more than one samples was taken, an average value was assumed. One of the reasons for discrepancy at the last point may be the assumption of an artificial boundary condition in the model. The last point is located close to this boundary.

It is recognized, however, that more than one set of data can lead to similar curves. A more complete and organized data collection is necessary to validate these types of environmental models.

SUMMARY

A mathematical model has been developed that is designed to evaluate:

1. Dust deposition in a straight section of a roadway. Both total dust as well as respirable dust values are output for the various points in the roadway.
2. ambient concentration, including concentration in the respirable range. Time averaged and instantaneous values can be determined.
3. effect of varying source emission rates on the dust exposure values at the various points.

On the basis of the validation test, the model for dust deposition and transport is considered representative of the phenomenon of deposition. Complete and controlled experimental studies will have to be performed for fully validating ambient

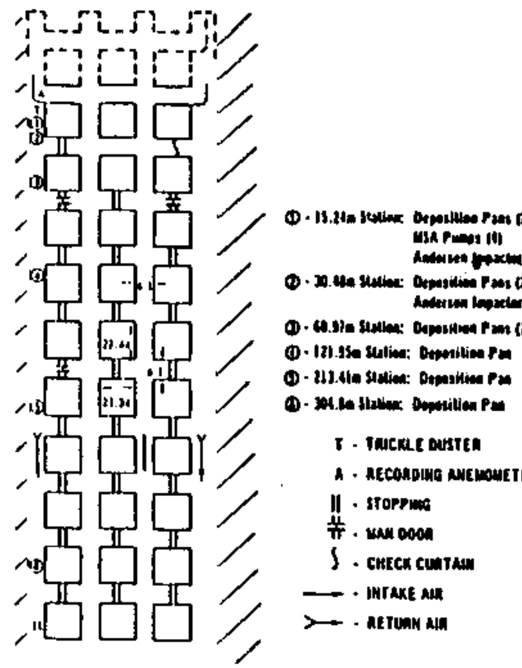

Figure 2. Sampling Locations in a Mine Section Return (after Kost, Colinet and Shirey, 1981).

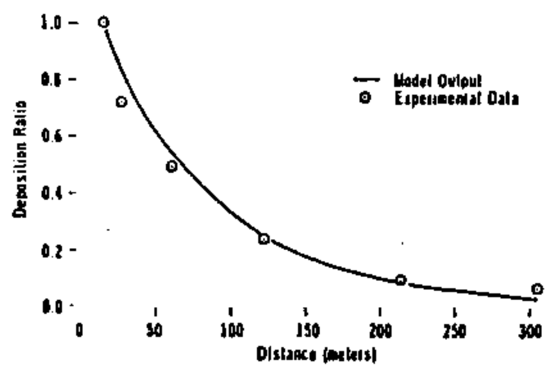

Figure 3. Plot of Model Output and Experimental Data.

concentrations and deposition together. The model incorporates several dominant physical mechanisms that are not part of presently available models for mine dust flow.

The amount of dust a miner is exposed to when working at any location is determined, at present, by actual measurements. However, these measurements are known to have a high coefficient of variation. One way of complementing these experimental data is to develop mathematical models that attempt to explain the transport characteristics of dust clouds generated by mining machines. In fact, as the understanding of the physical mechanisms that act on these clouds increases, premining investigation can be made of dust hazard in proposed mining work areas. Appropriate measures can then be taken, if necessary, to reduce dust exposures. Towards that effort, a mathematical model for predicting the behavior of dust clouds in mine airways under the action of controlled flow has been developed.

ACKNOWLEDGMENTS

The work reported here is a part of an ongoing research project in the Generic Technology Center for Respirable Dust at The Pennsylvania State University. The Center is supported by a grant from the U.S. Bureau of Mines. Support and assistance from the Bureau of Mines and The Pennsylvania State University are appreciated.
Grant Number G1135142

REFERENCES

1. Anon., "Report of the Committee on Measurement and Control of Respirable Dust," NMAB-363, National Academy of Sciences, 1980.

2. Bagnold, R. A., The physics of blown sand and desert dunes, Methuen, London, 1962.

3. Bandopadhyay, S., "Planning with diesel powered equipment in underground mines," Ph.D. Thesis, The Pennsylvania State University, 1982.

4. Batchelor, G. K., "Pressure fluctuations in isotropic turbulence," Proc. Camb. Phil. Soc., Vol. 47, pp. 359, 1951.

5. Chamberlain, A. C., "Transport of lycopodium spores and other small particles to rough surfaces," Proc. Royal Soc. A296, pp. 1444, 1967.

6. Chung, H. S., "Coagulation processes for fine particles," Ph.D. Thesis, The Pennsylvania State University, 1981.

7. Davies, C. N., "Definitive equations for the fluid resistance of spheres," Proc. Physical Society, Vol. 57, pp. 259, 1945.

8. Friedlander, S. K. and H. F. Johnstone, "Deposition of suspended particles from turbulent gas streams," Ind. Engrg. Chem., Vol. 49, p. 1151, 1957.

9. Friedlander, S. K., Smoke, Dust and Haze, Fundamentals of Aerosol Behavior, John Wiley and Sons, 1977.

10. Fuchs, N., The Mechanics of Aerosols, Pergamon, 1964.

11. Gardner, G. C., "Deposition of particles from a gas flowing parallel to a surface," Int. Jl. Multiphase Flows, Vol. 2, pp. 213-218, 1975.

12. Hidy, G. M. and J. R. Brock, Dynamics of Aerocolloidal Systems, Pergamon, 1970.

13. Kline, S. J., W. C. Reynolds, F. A. Schraub, and P. W. Runstadler, "The structure of turbulent air flows," Jl. Fluid. Mech., Vol. 30, pp. 741, 1967.

14. Kost, J. A., J. F. Colinet and G. A. Shirey, "Field survey of float dust in coal mining operations," USBM Mineral Research contract report, Contract No. J0308030, Bituminous Coal Research Inc., March 1981.

15. Liu, V. C., "Turbulent dispersion of dynamic particles," Jl. Meteor, Vol. 13, pp. 399, 1956.

16. Liu, B. Y. H. and J. K. Agarwal, "Experimental observation of aerosol deposition," Jl. Aerosol Sci., Vol. 5, No. 2, 1974.

17. Owen, P. R., "Pneumatic Transport," Jl. Fluid Mech., Vol. 39, 1969.

18. Owen, P. R., "Dust deposition from a turbulent airstream," in Aerodynamic Capture of Particles, Ed. Richardson, 1969.

19. Punjrath, J. S. and D. R. Heldman, "Mechanisms of small particle reentrainment from flat surfaces," Aerosol Sci., Vol. 3, pp. 429-40, 1972.

20. Saffman, P. G. and J. S. Turner, "On the collision of drops in turbulent clouds," Jl. Fluid Mech., Vol. 1, pp. 16, 1956.

21. Sehmel, G. A., "Particle eddy diffusivities and deposition velocities for isothermal flow and smooth surfaces," Jl. Aerosol Sci., Vol. 4, No. 2, 1973.

22. Schlichting, H., Boundary Layer Theory, McGraw Hill, New York, 1955.

23. Skubunov, V. V., "Turbulent diffusion of exhaust gases in a transportation working," Soviet Mining Science, No. 4, July-August 1970.

24. Skubunov, V. V., "Turbulent transport coefficients for mine workings and tunnels," Soviet Mining Science, No. 4, pp. 402, 1973.

25. Soo, S. L., "Statistical properties of momentum transfer in two phase flow," Chem. Engrg. Sci., Vol. 5, pp. 57, 1956.

26. Soo, S., C. Tien, and V. Kadambi, "Determination of turbulence characteristics of solid particles in a two phase stream by optical autocorrelation," Rev. Sci. Instr., Vol. 30, pp. 821, 1959.

27. Wood, N. B., "The mass transfer of particles and acid vapor to cooled surfaces," Jl. Inst. of Energy, June 1981.

SOME FACTORS INFLUENCING THE AIRBORNE DUST DISTRIBUTION IN LONGWALL FACE AREA

H. S. Chiang, S. S. Peng, G. C. Sun, and Y. F. Zhao
Department of Mining Engineering
College of Mineral and Energy Resources
West Virginia University
Morgantown, WV 26506

ABSTRACT

Dust sampling was performed in two longwall faces working in two separate seams. Instantaneous dust samples were measured by RAM's for various locations in the longwall faces. Preliminary analysis of the data shows that in addition to the shearer's haulage speed, there are four major factors that influence the airborne dust distribution in longwall face areas: locations with respect to the position of the shearer's cutting, hardness of the materials, characteristics of water spray, and roof conditions. This paper presents the effects of those four parameters in detail.

INTRODUCTION

A research project was initiated in September 1983 to measure and construct a dust distribution map for the longwall face. During the first year, airborne dust samplings were performed in two longwall panels located in northern and southern West Virginia and working in the Pittsburgh and Eagle Seams, respectively. The physical parameters and equipment employed for both panels are listed in Table 1. Figure 1 shows the detailed characteristics of the coal seams. Notice in both panels floor cutting was involved either to gain sufficient mining height or to reduce the adverse effects associated with a soft floor.

The purpose of the research is to define the dust distribution at any instance in the longwall face area so that proper working positions can be determined and/or effective dust control techniques can be developed.

This paper presents the partial results obtained during the first year.

SAMPLING METHODOLOGY

In order to understand the diffusion and flow of dust-laden air generated from various dust sources and construct the dust distribution maps, the arrangments of the sampling points for various locations in the face area are designed as follows. Note two real-time aerosol monitors (Model RAM-1) are used and three operators are required:

A. Along the Whole Face Area

The sampling points in the longitudinal cross-sections (i.e., along the face advancing direction) is shown in Figure 2. The same sampling point will be repeated every five shields starting from the headentry T-junction. There are two schemes of sampling arrangement in each cross-section. The 3-row arrangment (Fig. 2A) is suitable for the period immediately before shearer's cutting while the 4-row arrangement (Fig. 2B) is immediately after the cutting but before the support advance.

B. Shearer's Cutting

The sampling point around the shearer and shearer operators are shown in Fig. 3. In order to determine the dust distributions around both leading and rear drums, samplings were taken around the circumferences of both drums near the gobside end of the drums.

C. Support Advance

Three or four sampling points underneath the roof and parallel to the canopy were arranged for measuring dust concentrations before, during, and right after support advancing (Fig. 4). The hydraulic leg pressures of the support before and after support advance were also recorded.

D. Coal Transportation

The airborne dust produced by coal transportation can be divided into the following five parts:

a. During coal conveying by AFC, the sampling cross-sections were taken every 5 or 10 shields between headentry T-junction and the shearer. The sample points in each cross-section is similar to that shown in Fig. 2.

b. At the transfer point where the AFC emptied into the stage loader, the dust concentrations were monitored around the headentry T-junction transfer point.

Presented at the Proc. Coal Mine Dust Conference, Morgantown, W.Va., Oct. 8-10, 1984.

c. During coal traveling along the stage loader, the sampling points were arranged as shown in Fig. 5 for every 10 ft. interval.

d. At the discharge point from the stage loader to the tail-piece of the belt conveyor, two sampling cross-sections were taken immediately before and behind the transfer point.

e. Along the belt conveyor in the headentry, the sampling cross-section was taken every 100-150 ft. as shown in Fig. 6.

RESULTS AND DISCUSSION

Based on the data obtained so far, four major factors that control the airborne dust distribution in longwall faces have been identified, i.e., locations with respect to the positions of the cutting shearer, hardness of the materials being cut, water spray system, and roof conditions.

It must be noted that all data presented in this paper are instantaneous dust concentration and each data point is a mean value of from 30 to 90 measurements. For simplicity, only the dust concentrations along the walkway are presented unless otherwise stated in the text.

(1) Location with Respect to the Positions of the Cutting Shearer

Dust concentration at any point at any instance varies with the movement of the shearer.

Figures 7 and 8 show the airborne dust distributions around the shearer under different cutting directions at panel #2, and panel #1, respectively. Generally, the leading drum cuts the full drum height and generates the majority of the dust measured while the trailing drum makes much less amount due to lesser amount of coal cut. When the shearer is cutting from headentry to tailentry (Fig. 7), the shearer is moving downwind. Dust concentration increases rapidly on the downwind side beginning with the leading drum. Within the shearer, the lowest dust level occurs near the rear drum operator's position. It increases on both directions, i.e. both toward the rear drum and leading operator. When the shearer is cutting upwind (Fig. 8), the dust concentration at the leading operator is higher. It decreases continuously on the downwind side (i.e. even at the rear operator's position) and reaches the lowest level at two-support distance downwind from the rear drum. It then increases gradually away from the shearer.

Therefore under both conditions, the rear operator's position and his immediate neighborhood have the lowest dust concentration which are approximately 50-60% lower than that around the leading drum operator. This can be attributed to the following two factors:

(1) Water spray - the use of shearer clearer system with water sprays located and oriented strategically confines the dust-laden air on the face side of the shearer (Fig. 9).

(2) The air speed near the shearer increases significantly due to the reduction in cross-sectional area available for air flow. Higher air speeds tend to dilute the airborne dust concentration (Table 2).

However, after this low concentration area in the return air side of the shearer, the dust concentration increases gradually until it reaches the highest level which is generally 2-3 times higher than that around the leading drum operator (Fig. 10). Beyond that point, dust concentration decreases away from the shearer. The distance between the point of highest dust concentration and the shearer depends on the dust concentration of the dust-laden air flow, air speed, size and weight of the airborne dust particles. The higher is the airborne dust concentration and the lower is the air speed, the shorter is the distance between the point of highest dust level and the shearer. For example, the average dust concentration near the shearer in panel #1 is less than 2 mg/m^3 and the local air speeds are more than 800 fpm at the shearer's position and 400-500 fpm behind the shearer in the return air side, the highest dust concentration (4.5 mg/m^3) occurs at the 26th shield (130 ft.) behind the shearer, whereas in panel #2, the highest dust concentration (19.8 mg/m^3) appears only 50 ft. behind the shearer. In comparison with panel #1, the average dust concentration is much higher (5 mg/m^3) and the air speed is much lower (i.e. 238 ft. at the shearer's location and 210-240 fpm behind the shearer on the return air side).

Figure 11 shows the dust distribution around the drums. The higher dust concentration occurred near the top side of the leading drum during cutting while during the clean-up trip, the higher concentration always occurred near the bottom of the drum.

(2) Hardness of the Material to be Cut

The amount of dust generated during cutting is proportional to the hardness of the material to be cut (e.g. soft vs.

hard coal and coal vs. rock). For instance the Hardgrove Grindability Index (HGI) for the Eagle seam is higher than that for the Pittsburgh seam (Fig. 1), the dust concentration generated in the Eagle seam is much higher that that in the Pittsburgh seam (Fig. 10).

Furthermore, in order to make a mining height of 6 ft. for optimum support operation in panel #2, sometimes, the shearer has to cut the floor about 1 ft. deep. Airborne dust concentration during floor cutting increases significantly and reaches up to 12 mg/m^3 which is 4-6 times higher than those during coal cutting (Fig. 12).

(3) Water Spray

At present water spray on the shearer is the most important and effective technique for reducing airborne dust level. Figures 8 and 13 indicate the significance of water spray in dust reduction. Once the water spray on the shearer was completely turned off during cutting, the airborne dust concentration increases suddenly reaching up to 12 mg/m^3 for the softer Pittsburgh seam (Fig. 8) and 42 mg/m^3 for the harder Eagle seam (Fig. 13) which is 6 and 12 times, respectively, more than those for normal cutting with water sprays. The effects of water spray system under four working conditions (Fig. 8) on the effectiveness of dust reduction was conducted in panel #1 using GCA RAM-1. Obviously the internal water sprays which were mounted on the cutting drum near the cutting bits were most effective. The dust concentrations when the external water sprays were turned off (i.e., only internal water sprays were operating) were only 30-60% of those when the internal water sprays were turned off (i.e., only external water sprays were operating). Table 3 shows dust concentrations at various positions under the four working conditions. Note that for panel #1, the water was supplied at 452 psi and 115 gpm whereas for panel #2, it was 300 psi and 80 gpm.

A dust curtain was mounted lengthwise across the shearer's body in panel #2. Figures 14 and 15 show that a dust curtain is an effective method for reducing the dust concentration on the gobside. This is particularly true for the rear operator's position (Fig. 14). The effectiveness reduces toward the downwind side between the rear and the leading operators (Fig. 15).

(4) Support Advance under Various Roof Conditions

Support advance is a neglected dust source in modern longwall face, although it contributes to the airborne dust generation for only a short period of time. The amount of airborne dust generated by support advance depends on the immediate roof conditions. Figure 16 shows a systematic result of airborne dust concentration and variations during support advancing process under various immediate roof conditions. Dust concentration under various steps of support advancing (i.e., leg lowering, support advance, and leg rising for resetting) are different. The airborne dust concentrations measured under crushed roof condition are 2 times (for support advance and resetting) to 8 times (for leg lowering) more than that under stable roof conditions. Therefore some effective dust control techniques are necessary when the immediate roof is unstable or crushed.

Summary

There are many factors that affect the dust generation and distribution in the longwall faces. Those generic to all longwall faces are shearer's cutting, support advancing, immediate roof condition, cutting drum's rotational speed, shearer's haulage speed, coal conveying by AFC, method of ventilation, air speed, effectiveness of water spraying, hardness of the material to be cut and coal cutting methods, etc.

The first year's results have clearly demonstrated that shearer cutting is the primary source of airborne dust generation while support advancing is the secondary source (especially under crushed roof condition) although it occurred in a short period of time. Airborne dust generated by AFC and/or belt transportation is rather limited, generally 0.1-0.3 mg/m^3 depending on the loaded length of the conveyor. Therefore the study of dust distribution in longwall faces equipped with DERDS (double-ended ranging drum shearer) should focus on the location with respect to the position of the shearer's cutting drums.

ACKNOWLEDGEMENTS

This research has been supported by the Department of the Interior's Mineral Institute program administered by the Bureau of Mines through the Generic Mineral Technology Center for Respirable Dust under grant number G1135142.

ANALYSIS OF AN AIRBORNE DUST STUDY MADE FOR A SOUTHWESTERN PENNSYLVANIA UNDERGROUND BITUMINOUS COAL MINE

Robert L. Grayson and Syd S. Peng
Department of Mining Engineering
College of Mineral and Energy Resources
West Virginia University
Morgantown, WV 26506

ABSTRACT

An airborne dust study was undertaken at a Southwestern Pennsylvania underground bituminous coal mine by the Pennsylvania Department of Mines and Mineral Industries in 1964 for the purpose of making recommendations and requirements regarding compliance with health and safety aspects of The Bituminous Coal Mining Laws of Pennsylvania, approved by the legislature on July 17, 1961. The study was designed to accurately represent the airborne dust conditions of the subject mine. Sampling by midget impinger of specific worker locations throughout the mine was accomplished. Sample analyses yielded dust concentrations in mppcf, particle size determinations in cumulative per cent less than specified cut-off diameters, and determinations of free silica percentages in total dust samples. The data from this study is further analyzed, and the results are presented.

INTRODUCTION

The Bituminous Coal Mining Laws of Pennsylvania, enacted in 1961, prompted a study of respirable coal mine dust by the Department of Mines and Minerals Industry in 1964. In recognition of their obligation for ensuring the health and safety of bituminous coal miners, the department set out to characterize the airborne dust of mines throughout the commonwealth. The purpose of the studies was to make recommendations and requirements for compliance with the law and for control of airborne coal mine dust in Pennsylvania mines.

One such study was undertaken at an underground bituminous coal mine operating in the Pittsburgh Seam in Southwestern Pennsylvania. The study was designed to sample specific worker locations throughout the mine site and characterize the respirable dust relative to each of them. A midget impinger was used to gather respirable range dust samples during an 8-hour shift. Continuous miner operator, roof bolter, stoper bolter, loading machine operator, shuttle car operator, gathering motorman, mainline motorman, and rotary dumper jobs were sampled underground. In addition, barge mover, coal sampler, fine coal operator, heavy media operator, and boiler room attendant occupations were sampled on the surface. The surface sampling was over a 7½-hour shift because of UMWA contract provisions.

DESCRIPTION OF THE MINE AND MINING SYSTEM

Coal was extracted at this mine by the room-and-pillar method, utilizing a 6-entry system. A 6CM continuous mining machine equipped with 8 to 10 water sprays ripped the coal from the face and dumped it on the bottom. It mined a 4-foot pass and the roof bolters would next install anchor bolts. The roof bolting apparatus, including a dust collector system, was an integral part of the 6CM. Supplemental bolting was done with a pneumatic stoper bolter. An 11BU loading machine loaded coal dumped on the bottom into alternating 10SC shuttle cars. The shuttle cars trammed an average distance of 425 feet to a ramped dumping point. Here the shuttle cars dumped their payload into 6-ton mine cars which were supplied to the section via a continuous loop track system (40-pound rail). A car mover, controlled by the shuttle car operators, was placed between the rails at the dumping point to move wagons as they were loaded.

Two 13-ton gathering locomotives were used on a section to transport loaded 30-wagon trips out of and take empty trips of 30 wagons back into the section. Main-line 50-ton tandem locomotives were used to pull 50-wagon trips to the mine bottom, approximately 4.5 miles away. The rotary dumper dropped wagon payloads into two 12-ton skip buckets (alternating) which were hoisted to bins at the preparation plant.

In the preparation plant, coal was washed and sampled for quality. A yield of approximately 80% resulted from the beneficiation process. Heavy media washing by rotary processors, fine coal washing by drag tank and rheo launders, and elaborate washing by froth flotation were performed in the plant. The product was loaded into 1000-ton barges at a loading tipple on the nearby river.

Presented at the Proc. Coal Mine Dust Conference, Morgantown, W. Va., October 8-10, 1984.

METHOD OF SAMPLING

As mentioned previously, midget impingers were used to sample the respirable range dust existing at specific work locations. A team consisting of two state mine inspectors, a company industrial hygienist, and a company dust sampler gathered the samples. The impinger was located in close proximity to each worker position sampled on separate days. A 20-minute sample was taken each hour during the shift. Thus, 8 samples were obtained for each underground job sampled, and 7 samples were obtained for each surface job sampled due to a 7½-hour work day. In addition to the impinger samples, a drop cloth sample of total dust was obtained for analysis of silica. A total of 162 20-minute samples were gathered during the study, consisting of 120 underground samples and 42 surface samples. Twenty-one drop cloth samples were taken, one for each work position.

SAMPLE ANALYSES AND RESULTS

Each 20-minute sample obtained had a particle count analysis (200 particles by micro-projector) made on it, and a determination of number concentration was made (in mppcf). The 8 20-minute samples (7 for surface work position) obtained for a work position on a day were then combined into a weighted number concentration. A size analysis was also made. Table 1 shows the results of these analyses for weighted number concentration in mppcf and average per cent of particles less than 1 micrometer diameter for each worker position sampled. The geometric standard deviation and count median diameter are also given to fully describe the particle size distribution. Analysis of the drop cloth sample for per cent silica is also listed. The worst number concentration during the shift is given to show the relative maximum deviation from the weighted number concentration.

Threshold limit values (TLV's) for maximum permissible number concentration in 1964 were dependent upon the per cent silica in the dust. For less than 50% silica, 50 mppcf was allowed. For silica content greater than 50%, a TLV of only 5 mppcf existed. Number concentrations which exceeded the existing TLV for any work position sampled are boxed in Table 1. Two samples were out of compliance according to these TLV's. A roof bolter and a stoper bolter were over the maximum allowable number concentration value of 20 mppcf for dust containing from 5% to 50% silica. It is interesting to note that if the silica content of the dust was less than 5% in all cases, then not a single noncompliance would have occurred.

Needless to say, the dust study was very favorable for this mine. The two bad samples could have been easily brought into compliance by simple alteration of the dust collector systems of the roof bolter and the stoper bolter according to the dust study committee. Comparison with dust standards existing today, however, gives quite a different result.

FURTHER STATISTICAL ANALYSIS

Using original particle size distributions and number concentrations, further statistical analyses were made on the samples. The resulting mass concentrations and MRE equivalent mass concentrations were then evaluated in accordance with modern dust standards. Using the geometric standard deviation (GSD) and count median diameter (CMD) for each size distribution, the mass median diameter (MMD) was calculated using

$$MMD = CMD_e(3 \ln^2 GSD).$$

The total percentage of mass which would have been deposited on a filter following a 10 mm cyclone separation of the atmospheric dust was then computed using the ACGIH curve for the 10 mm cyclone collection efficiency and the cumulative mass distribution curve described by the MMD and GSD for a specific worker position.

By using the particle size statistics, the particle diameter of average mass was determined from

$$d_m = CMD_e(1.5 \ln^2 GSD)$$

and then the total dust mass concentration was computed using

$$C_m = C_N \frac{\rho\pi}{6} d_m^3 .$$

This total dust mass concentration was then multiplied by the percentage of total mass collected by the 10 mm cyclone to arrive at a respirable mass concentration. Finally, the respirable mass concentration was multiplied by 1.38 to obtain the MRE equivalent mass concentration which is the benchmark for determination of compliance with present statutes contained in 30 CFR 70.100 and 70.101.

It is important to note here again that the maximum allowable respirable mass concentration is dependent upon the quartz content of the respirable sample. Whenever the percentage of quartz exceeds 5%, that number is divided into 10 to get the total respirable dust threshold limit value. Table 2 reflects the results of these computations. Again, boxed concentrations represent those which would have been out of compliance with current law.

COMPARISONS AND CONCLUSIONS

The results summarized in Table 2 present a totally different perspective on the dust conditions at this mine. Seven of fifteen underground samples of work positions are out of compliance according to the MRE equivalent mass concentrations. Three of the ten are nearly out of compliance because of the quartz content of the total dust. Six out of eleven face worker samples are out of compliance. The roof bolter who was determined out of compliance in the original study is found to be in compliance with respect to mass concentration. The shuttle car operator and one of the CM operators sampled were in compliance under either analysis. Two of three CM operators, one loading machine operator, and three of four roof/stoper bolters are out of compliance. All three locomotive operators are found nearly out of compliance primarily due to silica content of total dust. This may or may not hold true if the respirable dust were analyzed for quartz content. All surface work positions were in compliance originally and are found in compliance upon further analysis.

No problems have occurred at this mine in complying with modern standards for respirable dust concentration. It is obvious from this analysis that much was done to achieve compliance. A more effective water spray system was necessary to gain consistent compliance for CM operators. A better dust collector system is now used to aid in compliance for roof bolters. Loading machines are no longer used in the mining cycle at this mine, so no comparison will be made, nor will discussion on improvement methods be addressed. Stoper bolting is rarely used now, generally only for bolting over falls construction work, or on the haulage for supplemental support. The motormen have stayed in compliance with present standards although no dust control improvements have been effected. This perhaps has resulted from more favorable quartz content determinations as analyzed from the respirable mass collected.

Table 1. Results of Dust Analyses - 1964

Worker Position	Type Mining	C_N (mppcf)	% < 1 μm	CMD	GSD	Worst Hour H_N	Silica Content
CM Operator	RET	15.26	52.0	0.961	2.99	35.86	3%
LM Operator	RET	10.59	57.5	0.869	2.71	34.71	2%
Roof Bolter	DEV	31.60	44.0	1.375	3.86	66.19	5%
SC Operator	DEV	3.77	57.0	0.877	2.07	7.03	3%
CM Operator	DEV	29.96	54.0	0.926	3.03	53.51	2%
Roof Bolter	DEV	26.80	49.5	1.238	2.73	53.37	3%
Stoper Bolter	DEV	30.87	46.0	1.145	2.58	76.30	13%
Stoper Bolter	DEV	8.41	40.0	1.576	2.41	26.09	20%
LM Operator	DEV	13.62	47.5	1.909	1.45	28.74	6%
CM Operator	RET	9.12	54.0	0.926	4.13	20.64	4%
SC Operator	RET	4.77	57.5	0.869	3.35	7.16	3%
G. Motorman	-	3.27	59.0	0.847	2.98	5.62	21%
Dumper	-	4.25	57.0	0.877	3.37	6.54	4%
ML Motorman	-	4.14	69.0	0.735	2.59	10.68	22%
ML Motorman	-	4.33	71.5	0.699	2.42	6.98	22%
Boiler Attnd.	-	2.84	47.0	1.176	4.59	7.67	10%
Slate Picker	-	10.30	61.5	0.813	3.82	17.17	4%
Barge Mover	-	0.965	56.0	0.893	2.73	1.45	4%
Sampler	-	5.99	53.5	0.933	2.88	11.05	5%
Hvy Media Opr.	-	6.09	53.0	0.943	4.34	10.15	4%
Fine Coal Opr.	-	4.49	73.0	0.685	2.43	5.94	3%

Table 2. Results of Further Analyses

Worker Position	Type Mining	C_N (mppcf)	Silica Content	C_m (mg/m^3)	MRE Equiv. C_m	
CM Operator	RET	15.26	3%	1.63	2.25	
LM Operator	RET	10.59	2%	1.31	1.81	
Roof Bolter	DEV	31.60	5%	0.95	1.31	
SC Operator	DEV	3.77	3%	0.22	0.30	
CM Operator	DEV	29.96	2%	2.99	4.13	
Roof Bolter	DEV	26.80	3%	4.59	6.33	
Stoper Bolter	DEV	30.87	13%	5.32	7.34	
Stoper Bolter	DEV	8.41	20%	2.05	2.03	
LM Operator	DEV	13.62	.6%	1.45	2.01	
CM Operator	RET	9.12	4%	0.19	0.26	
SC Operator	RET	4.77	3%	0.26	0.36	
G. Motorman	-	3.27	21%	0.32	0.44	vs. 0.4[illegible]
Dumper	-	4.25	4%	0.13	0.18	
ML Motorman	-	4.14	22%	0.38	0.52	vs. 0.4[illegible]
ML Motorman	-	4.33	22%	0.31	0.43	vs. 0.4[illegible]
Boiler Attnd.	-	2.84	10%	0.10	0.14	
Slate Picker	-	10.30	4%	0.06	0.08	
Barge Mover	-	0.965	4%	0.10	0.14	
Sampler	-	5.99	5%	0.71	0.98	
Hvy Media Opr.	-	6.09	4%	0.03	0.04	
Fine Coal Opr.	-	4.49	3%	0.31	0.43	

ACKNOWLEDGEMENTS

This research has been supported by the Department of the Interior's Mineral Institute program administered by the Bureau of Mines through the Generic Mineral Technology Center for Respirable Dust under grant number G1135142.

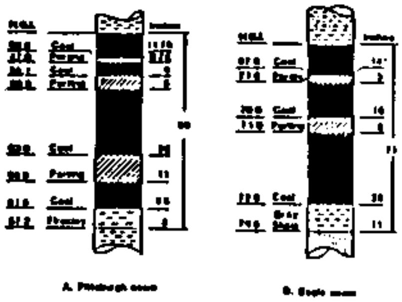

Fig. 1. Detailed characteristics of the coal seams.

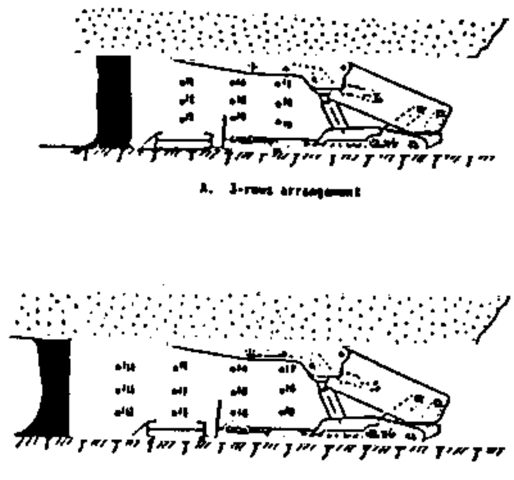

f_1, f_2, ... f_{12} - Measuring points arranged in each cross-section.

Fig. 2. Arrangement of sampling points in each cross-section along the longwall face.

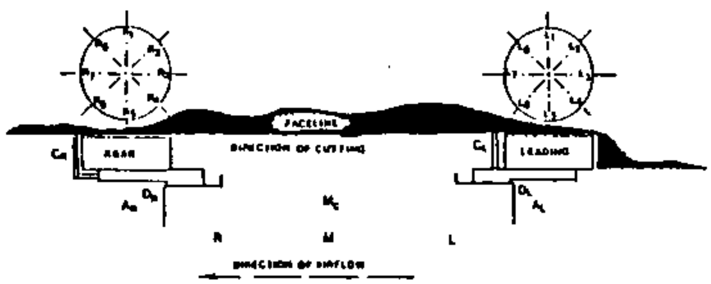

L - Leading operator; R - Rear operator; M - Between O_L and O_R; M_C - Body Center;

C_L - Behind the cowl of leading drum; C_R - Behind the cowl of rear drum;

O_L - Discharging window from leading drum onto AFC; O_R - Discharging window from rear drum onto AFC;

A_L - Near sprays-arm of leading drum; A_R - Near sprays-arm of rear drum;

L_1, L_2, ... L_8 - Measuring points around leading drum; R_1, R_2, ... R_8 - Measuring points around rear drum.

Fig. 3. Arrangement of sampling points around the shearer.

S_1, S_2, S_3 - Measuring points underneath roofline.

Fig. 4. Arrangement of sampling points during support advance.

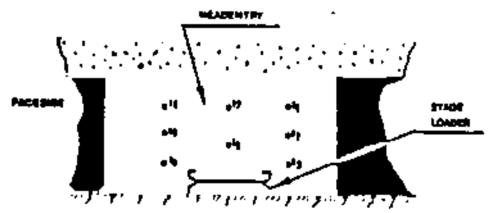

t_1, t_2, ... t_8 - Measuring points around the stage loader in each cross-section.

Fig. 5. Arrangement of sampling points in each cross-section along the stage loader.

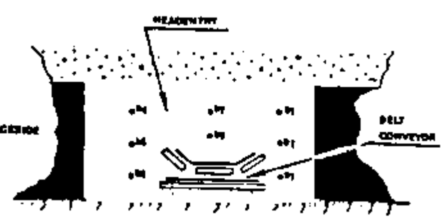

b_1, b_2, ... b_8 - Measuring points around the belt conveyor in each cross-section.

Fig. 6. Arrangement of sampling points in each cross-section along the belt conveyor.

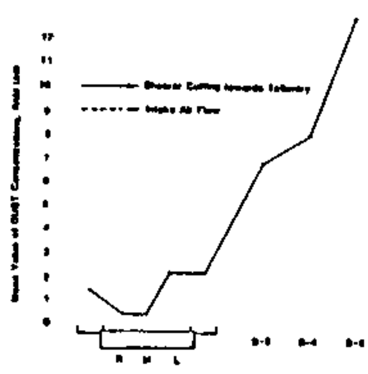

Fig. 7. Airborne dust distribution around the shearer measured at Panel #2, Mine #2.

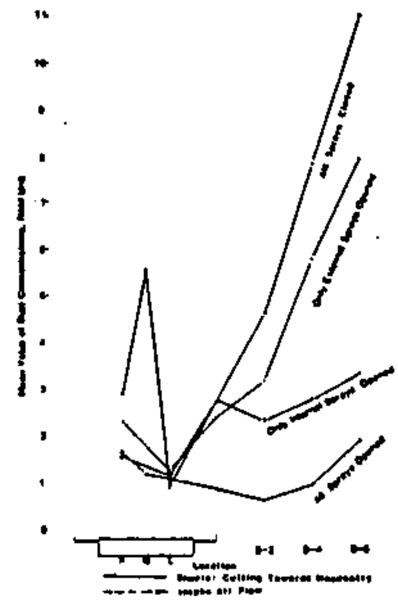

Fig. 8. Airborne dust distribution around the shearer measured at Panel #1, Mine #1.

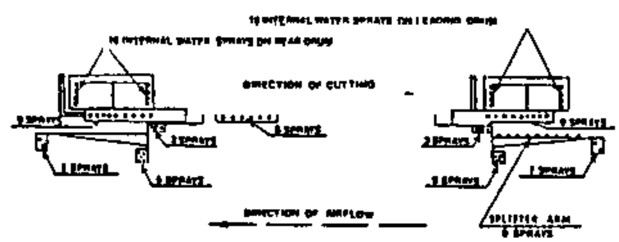

Fig. 9. Arrangement of water sprays for Model BERS-480 shearer employed in Panel #1, Mine #1.

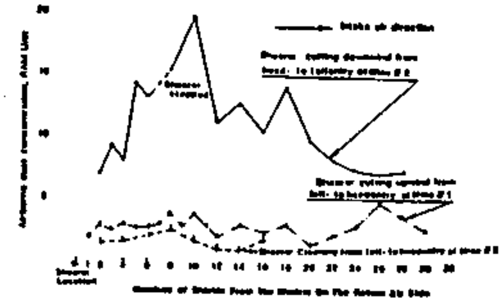

Fig. 10. Airborne dust distribution at various distances downwind from the shearer measured along the walkway.

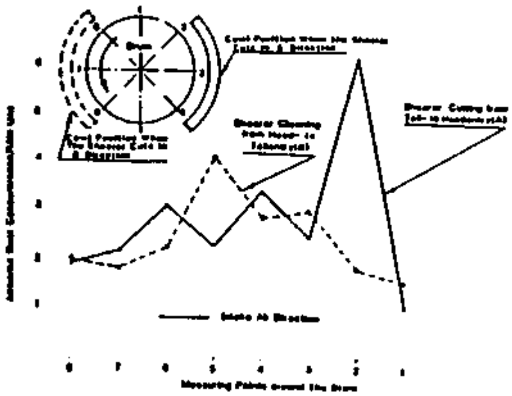

Fig. 11. Airborne dust distribution around the leading drum of the shearer employed in Panel #1, Mine #1.

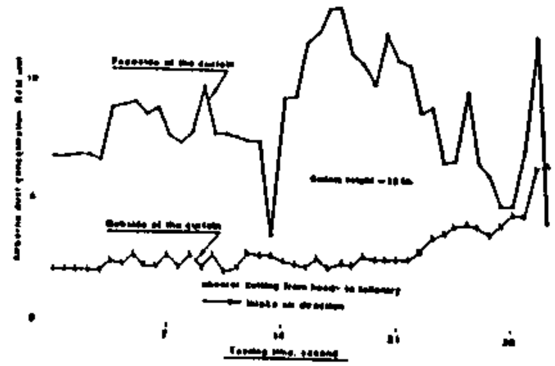

Fig. 14. Variations of airborne dust concentration at both sides of the shearer curtain measured near the rear drum operator of the shearer at Panel #2, Mine #2.

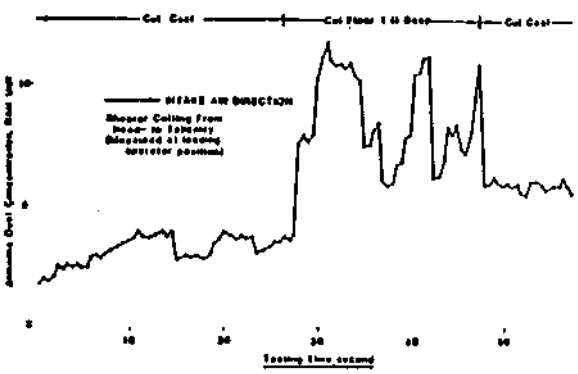

Fig. 12. Variations of airborne dust generation under different cutting conditions at Panel #2, Mine #2.

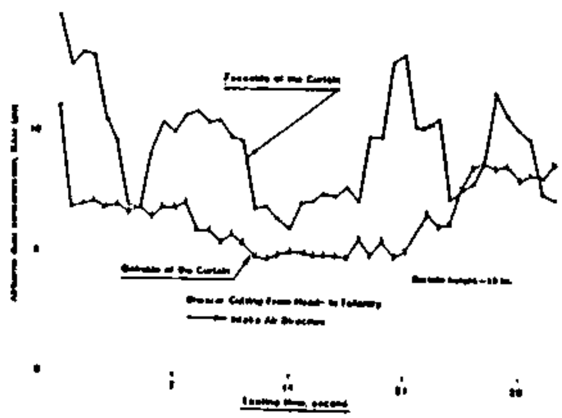

Fig. 15. Variations of airborne dust concentration at both sides of the shearer curtain measured at the middle point between both operators of the shearer at Panel #2, Mine #2.

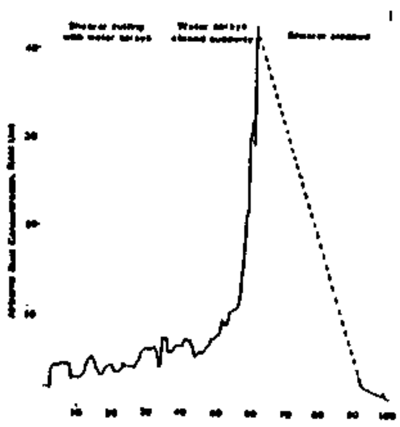

Fig. 13. Variations of airborne dust concentration under different working conditions measured near the leading drum at Panel #2, Mine #2.

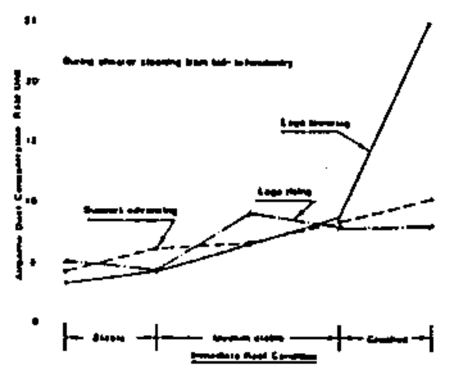

Fig. 16. Airborne dust concentration and variations measured under various roof conditions during support advancing process at Panel #2, Mine #2 (behind the shearer 10-12 supports).

Table 1. Physical Parameters and Equipment Employed in Longwall Panels.

Panel Number	#1	#2
Mine Number	#1	#2
Coal Seam	Pittsburgh	Eagle
Depth, ft.	750	1100
Thickness, in.	72-76	60-66
Panel Layout		
Panel length, ft.	3760	2400
Panel width, ft.	550	590
Number of Entry	4	Head 4/Tail 3
Entry width	13'10"	20'
Size of chain pillar, ft. x ft.	100 x 115	Head 80 x 80/Tail 40 x 80
Ventilation System	Antitropal	Antitropal
Powered Support	Shield	Shield/chock shield/shield
Type	Gallick-Dobson 2-leg	WS1.7/BS2.1/Dowty 4-leg
Setting: psi/tons	4500/342	4135/240; 420; 480
Yield: psi/tons	7020/535	7255/420; 5440/550; 7150/760
Number of Units	112	101 + 5 + 12 = 118
Cutting Machine	DERS	DERS
Type	Eickhoff EDW-150-2L	Sagem
Haulage (chainless)	Eickhoff Rack	Eickhoff Rack
Haulage speed		
cutting, ft/min.	13-18	10-15
cleaning, ft./min.	30-40	15-25
Cutting pattern	Tail-to-Head	Head-to-Tail
Cutting web, in.	30	30
Cutting drum rotational speed (rpm)	45	45
AFC		
Type and chain strand	H & B, DCCS	Westfalia Lunen, DCCS
Chain size, mm.	26	26
Motors, HP	2 x 200	3 x 175
Stage Loader	Long-Airdox	H & B

Table 2. Air Speed at Various Locations Along the Face.

Location	Local Air Speed, fpm	
	Panel #1	Panel #2
Headentry	561	273
Shield #1	431	-
Shield #10	423	-
Shield #30	418	233
Shield #50	424	214
Shield #70	423	213
Shield #90	414	232
Shield #110	464	240
Headentry side operator	895	338
Tailentry side operator	915	340
Tailentry	418	224

Table 3. Dust Concentrations under Four Working Conditions for Panel #1

Testing Condition	Position*	Airborne Dust Concentration, mg/m^3			
		Maximum	Minimum	Mean	Standard Deviation
All sprays closed	M	7.8	2.8	5.54	1.551
	L	4.5	2.9	3.82	0.419
	R	1.6	0.6	0.91	0.285
	B_2	6.[illegible]	2.9	4.66	1.003
	B_4	12.7	5.7	7.84	0.097
	B_6	13.4	9.5	11.06	1.514
Only external sprays opened	O_L	3.3	1.6	2.30	0.395
	O_R	1.6	0.9	1.29	0.294
	A_R	5.1	0.9	2.39	0.864
Only internal sprays opened	O_L	2.3	1.1	1.59	0.337
	O_R	2.6	1.0	1.19	0.293
	A_R	4.6	1.6	2.77	1.106
	B_2	3.6	1.6	2.38	0.521
	B_4	4.2	1.8	2.79	0.668
	B_6	4.5	2.7	3.37	0.550
	C_R	1.3	0.5	0.80	0.283
All sprays opened	M	1.4	1.1	1.22	0.109
	L	2.9	1.2	1.67	1.120
	R	2.5	0.6	1.11	0.214
	A_R	1.4	0.4	0.9	0.313
	B_2	0.8	0.6	0.68	0.100
	B_4	1.2	0.9	1.01	0.100
	B_6	2.8	1.0	1.95	0.550

*L - Leading shearer operator; R - Rear shearer operator; M - Between L & R; A_R - Near the sprays arm of the rear drum; B_2, B_4, B_6 - at 2, 4, 6 shields from the rear drum of the shearer during shearer cutting from tail- to headentry.

III

Dust Characterization

INSTRUMENTATION FOR THE MEASUREMENT OF RESPIRABLE COAL MINE DUST

Virgil A. Marple, Professor
Kenneth L. Rubow, Research Associate
University of Minnesota
125 Mechanical Engineering Building
111 Church Street
Minneapolis, MN 55455

INTRODUCTION

Respirable dust is defined as the dust which penetrates to the alveolated regions of the lungs. Due to the size selective nature of the particle removal mechanisms in the nasal passages and lung airways, criteria defining respirable particles must be a function of the particle size. Three criteria defining respirable particle penetration are shown in Figure 1. These criteria have been defined by the British Medical Research Council (BMRC), the American Conference of Governmental Industrial Hygienists (ACGIH) and German TBF 50-II (1).

The quantity of respirable particles in an aerosol can be measured by use of two-stage samplers. The first stage consists of a particle preclassifier with penetration characteristics corresponding to one of the respirable penetration curves in Figure 1. The large nonrespirable dust particles are removed from the airstream in the preclassifier and the smaller respirable dust particles pass on to some device which can measure their concentration (the respirable dust concentration).

Instrumentation for the measurement of respirable coal mine dust has been limited by the severe conditions existing within the coal mine. The conditions of particular importance are the methane atmosphere, high humidity, and the general non-laboratory type environment. The most severe of these conditions is the methane atmosphere since any electronic or electric powered instrumentation must be intrinsically safe to operate in such an atmosphere.

In spite of the difficulty of sampling respirable dust within the mines, many instruments have been developed for in mine use. Although these instruments operate under a variety of principles, they generally fall within two categories: personal samplers and area samplers.

A personal sampler is worn by the miner while he is performing his duties in the mine. These devices are generally small, light weight and require little power so as not to interfere with the miner's ability to work.

Area monitors, on the other hand, are larger but yet portable instruments which are generally located at fixed positions and sample dust from a specific area of the mine. These devices normally operate on the same principles as the personal samplers but are larger in size and often are more versatile in their functions.

The more powerful sophisticated instruments used for analyzing powders and instruments to measure atmospheric aerosol particles are normally not intrinsically safe and cannot be taken into the mine. Even if the instruments were to be made intrinsically safe they are usually too large and cumbersome to be transported easily to the work place and from location to location within the mine. For these instruments to be used in analyzing coal mine dust particles, the particles must be collected within the mine and brought to the surface for analysis.

In this paper the most common personal and area samplers are reviewed and the adaptation of the recently developed aerodynamic particle sizer to measure the size distribution of coal mine dust collected in the mine and transported to the surface is described. A general discussion of these different types of samplers as well as specific descriptions of several

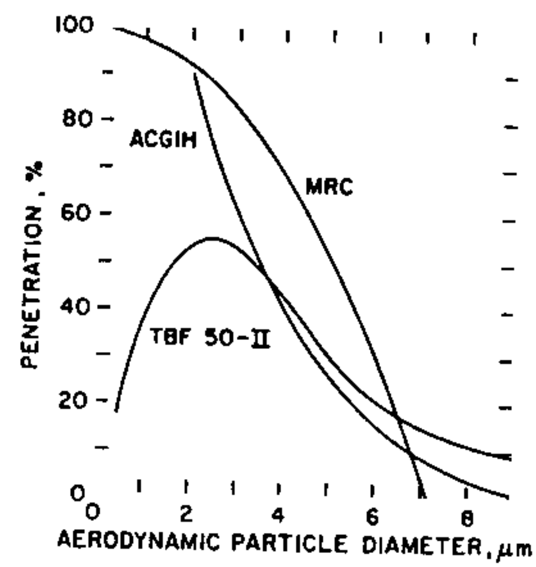

Figure 1. ACGIH, BMRC and TBF 50-II respirable dust criteria.

Presented at the Coal Mine Dust Conference, Morgantown, W. Va., October 8-10, 1984.

samples and instruments can be found in the book Air Sampling Instruments (1) and the report "Measurement and Control of Respirable Dust" (2).

PERSONAL SAMPLERS

Personal samplers are worn by the individual workers in an attempt to measure the concentration of the respirable dust to which the worker is exposed. Most personal samplers are simple devices consisting of a particle classifier, filter collector for the respirable particles and a pump. However, the recently developed MINIRAM is a compact photometer which can be worn by the worker as a respirable dust sampler.

Of the classifier/filter type samplers, the Dorr-Oliver cyclone followed by a filter is the most common (3-6). At a flow rate of 1.7 or 2 liters per minute depending upon the dust, the classification characteristics of this cyclone approximate the ACGIH respirable curve. Thus the large nonrespirable particles are removed in the cyclone and the smaller respirable particles penetrate the cyclone to be collected on the filter. The filter is weighed before and after a test and the mass of particles collected on the filter determined gravimetrically. The air is pulled through the cyclone and filter by an intrinsically safe personal sampling pump.

A similar device, the SIMPEDS, has been used in Britain (7). This unit again has a cyclone for a preclassifier and collects the particles upon a filter.

Recently, inertial impactors designed in such a manner as to provide penetration characteristics which are similar to either the ACGIH or the British MRC respirable dust curves have been developed (8). These devices are very similar to the cyclone filter devices with the exception that the cyclone has been replaced by an inertial impactor. The advantage is that the impactor can be designed for any sample flow rate. Thus the only limit on the flow rate is set by the sampling pump.

The GCA MINIRAM (GCA Corp. Bedford, MA) is a small photometer which makes use of the optical system to discriminate against the large nonrespirable particles and is only sensitive to the respirable fraction of the aerosol (9). Therefore, this photometer does not require the use of a classifier and no pump is needed. The MINIRAM is designed in such a fashion that the air currents carry the particles through the sensing cavity of the photometer. The MINIRAM has the advantage of electronic data aquisition and can provide the mass concentration as a function of time. The disadvantage of such a device is that calibration of the instrument is required since it is not measuring the mass of the particles directly but the light scattered from an aerosol cloud.

AREA SAMPLERS

Area samplers are designed to be located in a specific area of the mine and measure the mass concentrations of the aerosol in that area. These instruments are usually portable so they can be moved easily from location to location but are toolarge to be used as personal samplers. Many of the area samplers use a preclassifier in much the same manner as personal samplers. One of the oldest of these samplers is the British MRE Gravimetric Dust sampler using a horizontal elutriator as a preclassifier to model the British MRC respirable curve (10). The particles which penetrate the elutriator are considered respirable and are collected upon a filter. In more recent developments, this horizontal elutriator has been used as a preclassifier for photometers as in the SIMSLIN II sampler.

The Dorr-Oliver 10mm nylon cyclone has also been used as a classifier on area samplers such as for the GCA RDM-101, RDM-301 and RAM-1 instruments. For the GCA RDM-101 and RDM-301, particles which penetrate the cyclone are collected at an impactor stage and the mass of the particles measured by beta attenuation through the deposit (11-16). The 10mm cyclone is also used as a preclassifier on the RAM-1 which is a photometer (9, 17-19). Since the aerosol is passed through the Dorr-Oliver cyclone, the photometer is now measuring the concentration of the respirable particles as defined by the ACGIH criteria whereas the SIMSLIN II (Rotheroe & Mitchell Ltd., Ruislip, Middlesex, England) photometer is measuring the concentration corresponding to the British MRC criteria (16-20).

Yet another photometric device utilizes the wave length of the light source and the angle of the optics to discriminate against the large nonrespirable particles. This device is the Tyndallometer TM Digital Sampler (Ernst Leitz GmbH, Wetzlar, West Germany), which is designed to detect the particles according to the TBF 50-II respirable criteria (16, 19-21).

As indicated above it is important to be aware of the various respirable dust criteria and choose a sampler with respirable classification of the criteria of interest. However, if a personal cascade impactor such as the Marple Model 298 (Anderson Samplers, Inc., Atlanta, GA) is used, the mass size distribution of the aerosol will be measured and any of the above mentioned respirable criteria can be applied. The use of this personal cascade

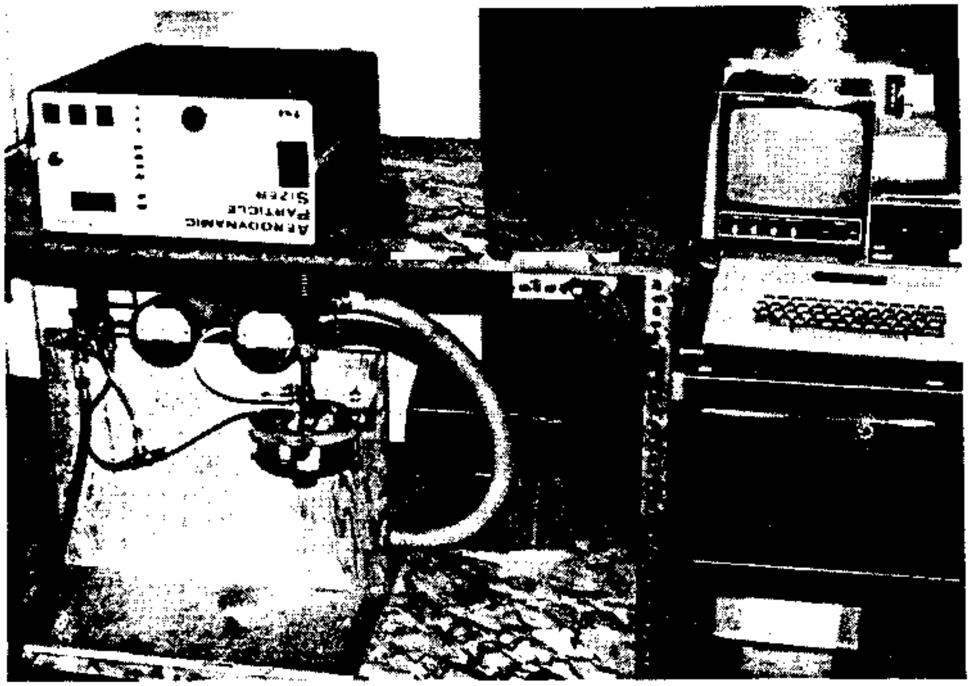

Figure 2. The aerodynamic particle sizer system.

impactor will therefore yield more information than a single stage respirable classifier.

THE DUST AERODYNAMIC PARTICLE SIZER

Recently a new instrument for measuring the aerodynamic particle size of aerosol particles has been developed by TSI Inc., 500 Cardigan Road, Shoreview, MN 55112. This instrument, called the Aerodynamic Particle Sizer (APS), Model 3300, is essentially a high technology inertial impactor (22-24). The aerosol particles are accelerated through a nozzle in much the same manner as in an inertial impactor. However, instead of the jet of particles impinging upon an impaction plate as in an impactor the particles are passed through a split laser beam. The APS measures the velocity of the particles between the two beams. Since the airflow is accelerating through the nozzle there is a lag in the particle velocity compared to the air velocity. Since particles with higher inertia (larger particles) have lower acceleration, the velocity of the larger particles will be less than the velocity of the smaller particles. Therefore, by measuring the velocity of the particles at the exit of the nozzle the aerodynamic diameter of the particles can be determined.

The APS is automated to present the aerodynamic diameter particle size distribution in much the same manner as an optical particle counter. That is, a histogram of the concentration of particles as a function of particle size.

To utilize this device to measure the size distribution of coal dust particles a dust dispersion system was developed as an accessory to the APS. A photograph of the system is shown in Figure 2. The main components of the system are the dust disperser, the APS, microcomputer data acquisition and analysis system and the excess particle dump. It may be noted in this figure that the APS is operated in an inverted position so that the particles can be aerosolized and transported vertically upward directly into the inlet of the APS. The APS can operate in the inverted position without any modifications to the instrument.

A schematic diagram of the system is shown in Figure 3. The procedure to analyze a dust is to place the dust on a sample plate from where it is picked up by air stream flowing upward in a small capillary tube. This tube operates as a small vacuum cleaner passing over the sample plate. The air is drawn up the capillary tube at the rate of 2 liters per minute by a venturi aspirator. This is accomplished by placing the outlet of the capillary tube near the throat of the venturi. The accelerated velocity of the air creates a low pressure in this region which draws flow up the capillary tube. From the outlet of the capillary tube dust is transported upward to the inlet of the APS where a small fraction is sampled and the aerodynamic diameter of the particles

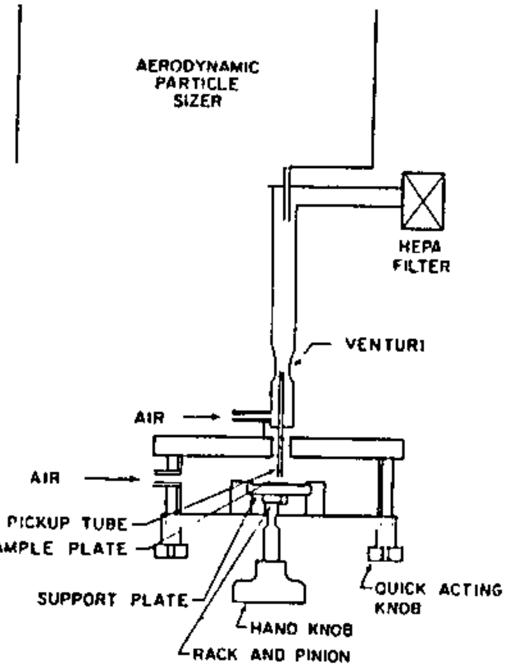

Figure 3. Schematic diagram of the dust aerodynamic particle sizer system.

measured. The particles which are not measured by the APS are passed through a filter (particle dump).

There are two important criteria for this dust dispersion system. First, the particles must be dispersed in a steady manner such that no "puffs" of particles are introduced into the APS. If puffs of particles were sampled by the APS, it would become overloaded and erroneous results obtained. Second, the particles must not be agglomerated when they enter the APS or the APS will measure the aerodynamic diameter of the agglomerated particles rather than the individual particles. Thus the dust dispersion system must disperse the particles in a steady manner without puffs and must thoroughly deagglomerate the particles.

The steady dispersion of the dust was obtained by using a rough surface (sandpaper) sample plate. To prepare a sample plate the powder is placed upon the rough surface and then spread over the surface with the edge of a glass slide. The powder particles are now in the crevices of the rough surface. As this rough surface is passed under the inlet of the capillary sampling probe, the dust particles are sucked out of the crevices and transported up the tube. If the surface of the sample plate is not rough, the powder will be drawn into the capillary tube as clumps which results in puffing of the dispersion system. Several types of rough surfaces were tested in our laboratory and ordinary sandpaper surfaces were found to work best.

The aerosol particles were deagglomerated in the venturi throat. This is achieved by the shear forces generated between the high velocity gas through the venturi and the low velocity gas particle stream coming from the exit of the capillary tube in the venturi throat. The gas passing through the venturi throat not only tends to break up the agglomerates due to shear forces but also acts as a sheath around the aerosol stream in the throat section of the venturi so as to reduce particle losses (particles deposited upon the walls of the venturi). Several tests were performed with different size venturi nozzles and different flow rates. It has been found that good operation is obtained with flow rates of 12 L/m through the venturi and 2.0 L/m through the capillary tube.

Figure 4 shows a photomicrograph of coal dust particles that have been dispersed in the system. Note that essentially all of the particles are completely deagglomerated and that the APS would be measuring the aerodynamic diameter of the individual particles.

The particle induced signals from the APS are processed by the microcomputer to provide number, surface area and mass size distributions of the aerosol particles and histograms are displayed. The calculations for the surface area and mass size distribution assume that the particles are spherical. Several samples of coal dust particles have been analyzed in our laboratory and a typical size distribution is shown in Figure 5. Any particular size distribution of an aerosol can be stored internally in the microcomputer and used as a standard to compare to other size distributions measured by the APS. This routine divides the number of particles in each size range by the number of particles in corresponding size ranges of the standard distribution. This is a convenient mode of operation for checking the reproducibility of the APS in that a comparison should give identical values for this ratio in all of the size ranges. Such a comparison is shown in Figure 6. Note that the value of the number concentration ratio is nearly equal in all channels indicating that the size distribution was the same for both runs.

In the system as shown in Figure 3 the aerodynamic particle size distribution of a powder sample can be measured. A powder sample must be collected in the mine and a size distribution measured by the APS at a remote location. However, the APS would be much more useful if it could measure the aerodynamic diameter of the airborne particles in a mine. To achieve this, a variation of the dust aerodynamic particle sizer was developed. The principle of

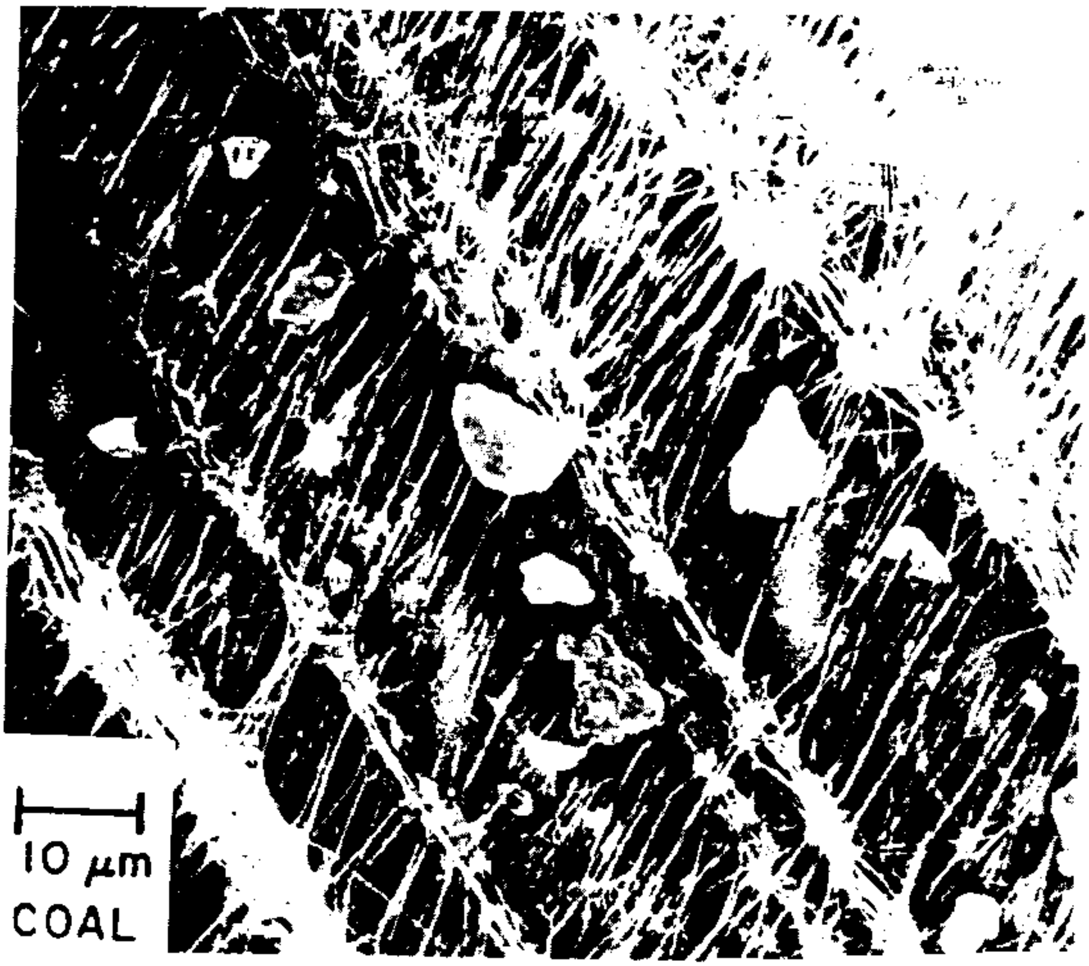

Figure 4. Photomicrograph of dispersed coal dust particles.

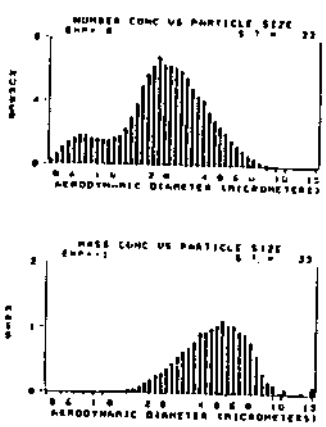

Figure 5. Typical coal dust size distribution.

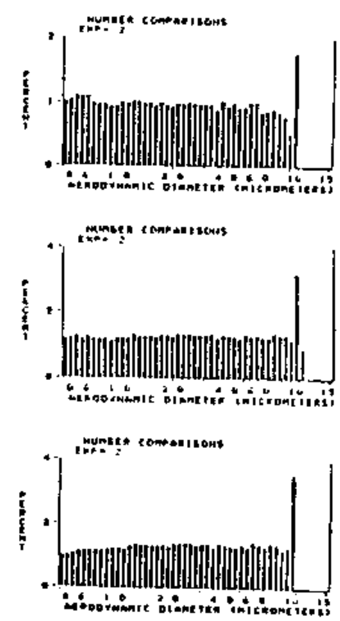

Figure 6. Comparison of the coal dust size distributions from several consecutive tests.

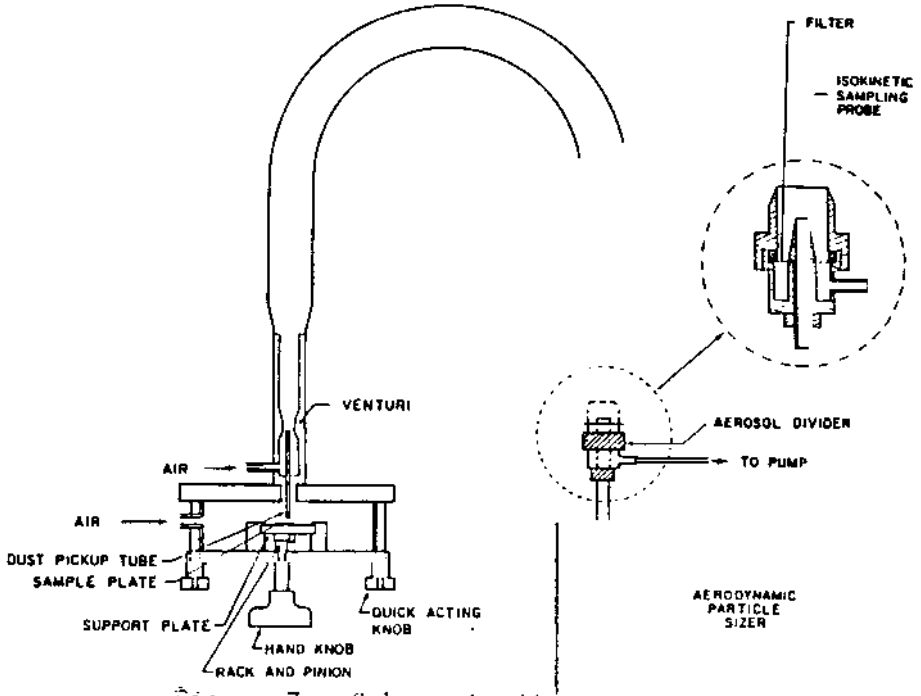

Figure 7. Schematic diagram of the dust areodynamic particle sizer system and precision aerosol divider test setup.

this variation is to collect the airborne particles in the mine on a filter and then redisperse the dust particles from the filter and measure the aerodynamic diameter size distribution with the APS. This has the added advantage in that the mass concentration of particles collected on the filter can be determined gravimetrically before the particles are analyzed by the APS. Thus the mass concentration and the size distribution of the particles can be measured from one filter sample.

To investigate the redispersion of the particles from the filter the system was configurated as shown in Figure 7 with the APS in the upright position and a precision aerosol divider (25) placed on the inlet of the APS. The precision aerosol divider is essentially a filter holder with a sampling probe penetrating the center of the filter. The aerosol being sampled by the filter is then split isokinetically into two streams. One of the streams passes through the central probe to the APS. The other stream passes through the filter where the particles are collected. Since the distance between where the aerosol stream is sampled isokinetically to the position where the particles are collected on a filter or sampled by the APS is very short, there are low losses in the system and a good split of the particles is obtained.

In this program, coal dust particles were first dispersed from the sandpaper sample plate and the particles passed through the precision aerosol divider and APS. The size distribution was measured by the APS and saved in its memory. The filter was then removed from the precision aerosol divider and placed upon the sample plate with two sided sticky tape. This filter was then placed below the capillary dust pickup tube and the particles were vacuumed from the filter. The size distribution of the particles redispersed from the filter were again measured by the APS. A comparison of this size distribution was made to the original size distribution and the comparative graphs from two tests shown in Figure 8. Note that the relative concentration of the particles in the redispersed dust was approximately 2% of the concentration of the powder in the original dust. The comparison between the size distribution indicates that the size distribution of the redispersed dust is nearly the same as the size distribution of the original dust. The variations shown in the comparison graphs are probably due to statistical fluctuations since the number of the redispersed particles was quite small.

Due to the results of this test, it is felt that it is possible to take filter samples, obtain the mass concentration and then redisperse the dust into the APS to

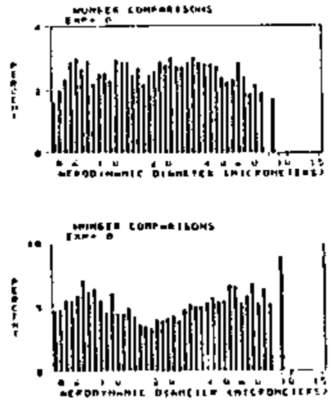

Figure 8. Comparison of the size distributions of coal dust particles redisperse from a filter to the original size distribution.

obtain particle size distribution. Further testing will be required to verif this hypothesis and the limitations of this technique ascertained. It is obvious, for example, that the particles will not disperse well from a filter which has been collected under high moisture conditions which will cake the particles.

One final feature of the dust dispersion system is that the venturi capillary tube section of the dust disperser can be removed from the frame and used as a wand. The source of the vacuum in the capillary tube is in the venturi. Thus, if air is passing through the venturi, there will be an air flow up the capillary tube. Figure 9 shows this mode of operation. Here the disperser is being operated by hand to remove the particles from a filter on the sample plate. This particluar feature of the dust disperser adds to its versatility in that now the wand can be used to probe the particles from surfaces not suitable for insertion in the dust dispersion chamber.

Figure 9. Dust dispersion system being used as a wand.

REFERENCES

1. Lioy, P. J., Air Sampling Instruments, American Conference of Governmental Industrial Hygienists, Cincinnati, Ohio, 1983.

2. "Measurement and Control of Respirable Dust in Mines," National Academy of Sciences, NM AB-363, 1980.

3. Lippmann, M., "Size-Selective Sampling for Inhalation Hazard Evaluations," Fine Particles: Aerosol Generation, Measurement, Sampling, and Analysis, edited by B. Y. H. Liu, Academic Press, New York, 1976.

4. Lamonica, J. A. and H. N. Treaftis, "The Effect of Pulsation Damping on Respirable Dust Collected by Coal Mine Dust Personal Samplers," BuMines, Report of Investigations 7636, 1972.

5. Almich, B. P. and G. A. Carson, "Some Effects of Chargind on 10-mm Nylon Cyclone Performance," Amer. Ind. Hyg. Assoc. J., Vol. 35, 1974, p. 603.

6. Caplan, K. J., L. J. Doemeny, and S. D. Sorenson, "Performance Characteristics of the 10 mm Cyclone Respirable Mass Sampler; Part I: Monodisperse Studies; Part II: Coal Dust Studies," Am. In. Hyg. Assoc. J., Vol. 38, 1977, pp. 83-95, 162-173.

7. Maguire, B. A., D. Barker and D. Wake, "Size Selection Characteristic of the Cyclone used in the SIMPEDS 70 MK2 Gravimetric Dust Sampler," Staub-Reinhalt Luft, Vol 33, 1973, pp. 95-98.

8. Marple, V. A. and J. E. McCormack, "Personal Sampling Impactors with Respirable Aerosol Penetration Characteristics," Am. Ind. Hyg. Assoc. J., Vol. 44, 1983, pp. 916-922.

9. Marple, V. A. and K. L. Rubow, "Respirable Dust Measurement," draft final report on Contract No. USDI/BOM J0113042, March, 1984.

10. Dunmore, J. H., R. J. Hamilton and D. S. G. Smith, "An Instrument for the Sampling of Respirable Dust for Subsequent Gravimetric Assessment," J. Sci. Instr., Vol. 41, 1964, p. 669.

11. Lilienfeld, P. and J. Dulchinos, "Portable Instaneous Mass Monitor for Coal Mines Dust," Am. Ind. Hyg. Assoc. J., Vol. 33, 1972, p. 136.

12. Marple, V. A. and K. L. Rubow, "An Evaluation of the GCA Respirable Dust Monitor 101-1," Am. Ind. Hyg. Assoc. J., Vol. 39, 1978, pp. 17-25.

13. GCA Corporation Information Bulletin (Precision Scientific Group), Recording Respirable Dust Monitor - Model RDM 301 for Both Short- and Extended-Time Measurements, 1977.

14. Volkwein, J. C. and P. T. Behum, "Laboratory Evaluation of a Recording Respirable Mass Monitor," Am. Ind. Hyg. Assoc. J., Vol. 39, 1978, p. 945.

15. Fairchild, C. I., M. I. Tillery and H. J. Ettinger, "An Evaluation of Fast Response Aerosol Mass Monitors," Los Alamos Scientific Laboratory, LA-8220, 1980.

16. Thompson, E. M., H. N. Treaftis, T. F. Tomb, A. I. Bechert and A. I. Bero, "Laboratory Evaluation of Instantaneous Reading Dust Monitors," Am. Ind. Hyg. Assoc. J., Vol. 42, 1981, pp. 191-197.

17. Rubow, K. L. and V. A. Marple, "An Instrument Evaluation Chamber: Calibration of Commercial Photometers," Aerosols in the Mining and Industrial Work Environment. V. A. Marple and B. Y. H. Liu, eds., 1983, pp. 777-798.

18. Marple, V. A. and K. L. Rubow, "Instruments and Techniques for Dynamic Particle Size Measurement of Coal Dust," final report on Contract No. USDI/BOM H0177025, January, 1981.

19. Kuusisto, P., "Evaluation of the Direct Reading Instruments for the Measurement of Aerosols," Am. Ind. Hyg. Assoc. J., Vol. 44, 1983, pp. 863-874.

20. Blackford, D. B. and G. W. Harris, "Field Experience with Simslin; II: A Continuously Recording Dust Sampling Instrument," Ann. Occup. Hyg., Vol. 21, 1978, pp. 301-313.

21. Breuer, H., J. Gebhart and K. Robock, "Photoelectric Measuring Apparatus for Determination of the Fine Dust Concentration," Staub Reinhaltung der Luft (in English), Vol. 33, 1973.

22. Remiarz, R. J., J. K. Agarwak, F. R. Quant and G. J. Sem, "A Real-Time Aerodynamic Particle Size Analyzer," Aerosols in the Mining and Industrial Work Environments, Vol. 3 Instrumentation, V. A. Marple and B. Y. H. Liu editors, Ann Arbor Sciences, Ann Arbor, Michigan, USA, 1983.

23. Agarwal, J. K., R. J. Remiarz, F. R. Quant and G. J. Sem, "Real-Time Aerodynamic Particle Size Analyzer," J. Aerosol Sci., Vol. 13, 1982, pp. 222-223.

24. Baron, P. A., "Sampler Evaluation with an Aerodynamic Particle Sizer," Aerosols in the Mining and Industrial Work Environments, Vol. 3 Instrumentation, V. A. Marple and B. Y. H. Liu editors, Ann Arbor Sciences, Ann Arbor, Michigan, USA, 1983.

25. Marple, V. A., K. T. Whitby, B. R. Olson and J. L. Wolf, "Precision Aerosol Divider," Am. Ind. Hyg. Assoc. J., Vol. 37, 1976, pp. 69-72.

ACKNOWLEDGEMENTS

This research has been supported by the Department of the Interior's Mineral Institute program administered by the Bureau of Mines through the Generic Mineral Technology Center for Respirable Dust under grant number G1135142.

PULMONARY SURFACTANT INTERACTION WITH RESPIRABLE DUST

By

W.E. Wallace, Jr., M.J. Keane, V. Vallyathan, T-M. Ong, V. Castranova
National Institute for Occupational Safety and Health
944 Chestnut Ridge Road
Morgantown, WV

Inhalation of certain forms of silica, asbestos and some other respirable dusts can result in pulmonary fibrosis, characterized by destruction of the surfaces of alveoli and respiratory bronchioles. Fibrous thickening of the alveolar septa decreases the lung's capacity for gas exchange.

Pulmonary macrophage damage by respired dust may initiate the fibrotic response. In one proposed mechanism, dust particles interact with the plasma membrane of a macrophage. This damages the cell or induces some hyperactivity of the cell, resulting in excessive release of lysosomal enzymes and reactive forms of oxygen (1). These reactive enzymes or radicals then damage the alveolar surface epithelial cells. A second mechanism has also been proposed (2,3) in which dust damage to the macrophage causes the release of mediator substances which induce pulmonary fibroblast cell proliferation and increased collagen synthesis. This produces fibrous tissue in the terminal air spaces (4,5).

Mineral surface interactions with plasma membrane lipoproteins have been proposed as a mechanism of lytic damage of pulmonary cells by silica dust in numerous models (6,7). The significance of dust surface properties has been further revealed in studies showing significant changes in dust induced cytotoxicity as a function of dust surface crystallinity and organic or inorganic contamination or coating of mineral surfaces (8,9). Such modification of the mineral surface might interfere with surface sites responsible for the toxicity of dusts for pulmonary macrophages, thus interrupting the early stages of the process of fibrosis.

In vitro cellular assay systems using erythrocyte hemolysis or the release of macrophage cytosolic or lysosomal enzymes following dust challenge, have been used to analyze the initial mechanism of dust damage to cells. However the ability of these assays to predict the pulmonary disease producing potential of various dusts is imperfect owing to some "false positive" results. These assays as performed are therefore questionable models for the initial lesion in pneumoconiosis or silicosis. In particular, kaolin frequently is found to have comparable biological activity to silica quartz in these assays (10,11).

Silica and kaolin have distinctly different fibrogenic potentials. Silica is highly fibrogenic, resulting in both acute and chronic silicosis (12). Some epidemiological data and animal experimentation data have indicated that long term exposure to kaolin can result in pneumoconiosis; however, kaolin is relatively benign as compared to silica (13-18). Kaolin is also of interest because it is one of the major mineral inclusions in Eastern U.S. bituminous coals. We have observed that exposing respirable sized native silica or kaolin for two hours to pulmonary macrophages results in a greater enzyme release for kaolin exposures, on a dust mass basis. Exposure of erythrocytes to the dusts also results in greater levels of hemolysis by kaolin for equal mass respirable dust doses. Therefore, these results do not correlate positively with known disease inducing potentials of the two dusts.

Characterization of physical and chemical surface properties of dusts involved in occupational exposures, and characterization of the alteration of those surface properties which are likely to occur upon deposition of the dust in the lung, should improve the identification of respiratory disease hazards.

Inhaled dust particles deposited in the lower respiratory tract will come in contact with pulmonary surfactant. This surfactant forms a surface film on and emulsion in the liquid hypophase coating of the alveoli and respiratory bronchioles. The primary constituent of this pulmonary surfactant is the lipid diacyl glycerophosphorylcholine, lecithin (19). Because this lipid is also a major component of cell membranes, it is possible that surfactant can interact with mineral

Presented at the Proc. Coal Mine Dust Conference, Morgantown, W. Va., October 8-10, 1984. National Technical Information Service Report PB86 169380/AS Springfield, Va.: NTIS

dust to alter its interaction with macrophages and other pulmonary cells and, thus, its pathogenicity.

Adsorption of dipalmitoyl lecithin from emulsion in physiological saline by kaolin, a layered alumino-silicate, does occur. (20) In addition, silica also exhibits the capacity to absorb surfactant-like material.(21)

Our earlier research quantified the adsorption of dipalmitoyl lecithin emulsion in physiological saline at 37°C by a kaolin respirable sized dust of 26 m^2/g specific surface area. In the concentrated emulsion range, up to 18 weight % lecithin to kaolin was adsorbed.

It has been suggested that such adsorption of lipids may alter the cytotoxicity of dusts (22,23,24). We have been studying this question, using dipalmitoyl lecithin in physiological saline to pretreat dusts to model the initial contact of respired dust with pulmonary surfactant. First, we monitored cytotoxicity using two assay systems. The release of three enzymes from pulmonary macrophages were used as indicators of cell death or damage following dust exposure *in vitro*. Lactate dehydrogenase (LDH) and two lysosomal enzymes, beta-glucuronidase (β-GLUC) and beta-N-acetyl glucosaminidase (β-NAG) , were measured in the external cell medium following dust exposure and compared with total intracellular levels for unexposed controls. Second, hemolysis of erythrocytes was used as a specific indicator for external cell membrane lysis by dusts. These assays were used with native silica and kaolin dusts in contrast to experiments using lecithin treated silica and kaolin.

We present here some representative data obtained in studies of silica and kaolin respirable sized dusts. Complete data will be reported elsewhere.

Crystalline silica (Min-U-Sil) was fractionated using a Donaldson classifier and the 80% < 5 μm particle diameter fraction collected. The silica was at least 98.5% pure as determined by x-ray energy spectrometric (XES) analysis. It had a median area equivalent diameter of 1.24 μm. The specific surface area of the size fractionated silica was 2.97 m^2/g as determined by BET Nitrogen adsorption.

Kaolin from Georgia Kaolin Mills was similarly size fractionated to obtain a fraction 90% < 5 μm particle diameter. This kaolin was at least 96% pure and contained no crystalline silica as determined by XES analysis. The specific surface area of this kaolin fraction was 13.25 m^2/g, as determined by BET nitrogen adsorption.

Stock dipalmitoyl lecithin (DPL) emulsions of 10 mg of DPL (Calbiochem) per ml of physiological (0.165M) saline were made by sonication. Silica and kaolin dusts were exposed to DPL by vortexing the sized, untreated dusts into DPL emulsion at 7.5 mg dust per ml emulsion and incubating the mixtures for one hour at 37°C. This provided ample DPL for kaolin surface coverage as estimated from the adsorption isotherm data extrapolated to the surface area of the kaolin used. Silica and kaolin controls were similarly incubated in physiological saline without DPL. Following incubation the mixtures were centrifuged for ten minutes at 990 xg and each dust resuspended in Dulbecco's phosphate buffered saline (PBS); this procedure was performed twice. The stock suspension of 2 mg dust per ml PBS was diluted to make sample dust suspensions used. Dust suspension and DPL emulsification did not change the osmolarity of 296 ± 1 mOsm or the pH of 7.3 of the saline system.

As one index of cytotoxicity, hemolysis by the native and treated dusts was measured. Sheep blood erythrocytes were prepared as a 4% by volume suspension in PBS after three washes in PBS with centrifugation at 990 xg. Aliquots of this suspension and the dust suspensions were mixed in equal volumes to make samples of 2% by volume erythrocytes with treated or native dust concentrations from 0.1 to 1.0 mg/ml. Hemolysis assays were performed using the method of Harrington et al. (25), with minor changes. Native silica or kaolin and DPL emulsion-treated silica or kaolin suspensions with erythrocytes were incubated at 37°C for one hour, and then centrifuged at 990 xg for ten minutes. Negative controls contained only erythrocytes in PBS. Standard lysate controls were made by lysing erythrocytes in PBS with 0.5% Triton X-100. All samples were read at 540 nm on a spectrophotometer against distilled H_2O.

Alveolar macrophage enzyme release studies were carried out using alveolar macrophages harvested from male Sprague Dawley rats weighing 250-275 grams. Following sacrifice, lungs were lavaged repetitively (10-12 times) with calcium and magnesium free Hank's balanced salt solution. Macrophages were sedimented by centrifuation at 990 xg from the pooled lavages and suspended in HEPES buffer at pH 7.4. Cell counts were made by trypan blue dye exclusion test(26). From 85 to 90 percent of the cells counted were viable, based on this test. Approximately 95% of the cells obtained by lavage were alveolar macrophages.

Suspensions of native or DPL-treated silica or kaolin were mixed with the macrophage suspension to produce 2 x 10^6 cells per ml of suspension and dust concentrations of 1 mg per ml of suspension. All samples were incubated for 2 hours at 37°C in a shaking water bath. Following incubation all samples were centrifuged at 500 xg for 10 minutes and total and released activities of 3 enzymes were determined in duplicate tests. For estimation of total enzyme released, one set of controls of cells without dust were lysed with 0.2% Triton X-100 at the end of incubation. LDH activity was determined according to the method of Reeves and Fimignari (27). ß-GLUC activity was measured using p-nitrophenyl--D-glucuronide as the substrate, according to the method of Lockart and Kenedy (28). ß-NAG was assayed according to the method of Sellinger et al. (29). Percentages of enzymes released were calculated relative to the Triton lysed samples.

Representative hemolysis data shown in Figure 1 indicate that the silica and kaolin have comparable cytotoxicities for erythrocyte hemolysis on a dust mass or specific surface area basis. However, the cytotoxicity of both silica and kaolin is almost completely suppressed by incubation of the dust with lecithin emulsion in physiological saline.

Representative data on the release of three enzymes from pulmonary macrophages are shown in Figure 2. Both dusts show comparable cytotoxicity for pulmonary macrophages as indicated by comparable macrophage release of the three enzymes. Once again, lecithin pretreatment reduces the macrophage cytotoxicity, for these two hour incubations of treated dust with the macrophages, to background levels.

Suppression of the toxicities of both dusts by lecithin pretreatment in these assays may represent a prompt *in vivo* physiological response. No fibrosis occurs in the early stages of silica exposure. To the extent that such lecithin treatment is a representative model of one interaction of respired dusts *in vivo*, the assay results imply that the pulmonary surfactant system may constitute a defense system against prompt lytic damage to pulmonary cells by respired dusts. This is not inconsistent with the *in vivo* phenomena of lipidosis, an early response of the lung to silica exposure, in which alveolar type II cells release greater than normal amounts of pulmonary surfactant (30).

The comparable short-term suppression of the cytotoxicity of both dusts by lecithin does not correlate with known relative dust pathogenicity since silica quartz is highly fibrogenic. If relative pathogenicities of silica and other silicates originate in dust damage of the macrophage, then, that damage must manifest itself over a longer time period, that is, after phagocytosis of the dust by pulmonary macrophages. If a dust particle does not promptly lyse and kill the macrophage it will be phagocytized and taken into a phagolysosome. There it will be exposed to lysosomal enzymes, among which are lipases capable of digesting lipids. Pulmonary macrophage phagolysosomal digestion of serum protein from the surface of phagocytized silica has been reported (31).

We are investigating a research premise that after phagocytosis and formation of the secondary lysosome, the protective surfactant surface coating on silica may be enzymatically digested, re-toxifying the dust within the macrophage. As a corrollary, such processes may be quantitatively or qualitatively different for dusts which are not so pathogenic as silica *in vivo*, i.e., kaolin. As a first step we are studying the *in vitro* ability of a specific lipid active enzyme, phospholipase A_2, known to be present in macrophage lysosomes, to affect a lecithin coating on silica quartz, and on kaolin.

Representative data for the restoration of cytotoxicity of lecithin treated silica and kaolin dusts by phospholipase A_2 treatment are shown in Figure 3; the assay used was erythrocyte hemolysis. Commercial phospholipase A_2, obtained from *Crotalus adamanteus* venom, was *dissolved in PBS* supplemented with 1 mM $CaCl_2$, and made up to 2 mg/ml, equivalent to 400 units/ml. This solution was diluted 1:4 and 1:400. Enzyme solutions were kept on ice until used.

As additional controls, dusts which had not been lecithin treated, were subjected to phospholipase A_2 treatment.

Silica and Kaolin dusts were first incubated with dipalmitoyl lecithin for 15 hours, following the same procedure as discussed above. Then they were washed and incubated *in vitro* with phospholipase A_2 for *one hour* at 37° with lipase concentrations adequate to provide enzyme activities ranging from 2 unit-minutes to 44000 unit-minutes. The high activity point in Figure 3 is an exception to this; incubation time was 22 hours using the same enzyme concentration used for the 2000 unit-minute point. Dusts were then incubated with erythrocytes for one hour. Representative data are shown for silica in Figure 3.

The Figure 3 ordinate shows the phospholipase A_2 restored cytotoxicity of lecithin treated silica or kaolin as a precentage of native (non-lecithin treated) silica or kaolin cytotoxicity. The abscissa shows the activity of phospholipase A_2 used in the one hour incubations. The final point is the "theoretical equivalent" activity of the 22 hour incubation.

The data indicate that treatment with phospholipase A_2 can restore the cytotoxicity of lecithin pre-treated silica to levels approximately equal to native or bare-surface silica levels, shown by the "100% retoxification" level. This implies that the lecithin component of a pulmonary surfactant defense system against the lytic effects of respired particles, may be undone by the pulmonary macrophage phagocytic defense system against bacterial challenge. Similar studies using full pulmonary surfactant and pulmonary macrophage lysosomal enzymes are required to further investigate a research premise, that the deleterious effects of respired silica begin after phagocytosis when the protective surfactant coating is digested and desorbed by lysosomal enzyme activity.

The results for kaolin retoxification are qualitatively different from the silica results, as shown in Figure 3.

Using the lecithin-kaolin adsorption isotherm data extrapolated by specific surface area to the kaolin used here, and using the homogenous phase enzymatic activity of the phospholipase A_2 used in these studies, the phospholipase activity between 20 unit-minutes and 200 unit-minutes is the approximate activity in homogeneous phase reaction needed to digest the amount of lecithin coating the kaolin. Figure 3 shows that in this activity region the restored hemolytic cytotoxicity goes from near the totally suppressed levels for lecithin coated kaolin to levels greater than the cytotoxicities of native (non-lecithin treated) kaolin. The restored cytotoxicity, therefore, may not be due to digestion and removal of the lecithin from the kaolin. That is, unlike the case with silica, the phospholipase treatment may not bare the kaolin surface. Treating kaolin with lysolecithin and using this dust in erythrocyte hemolysis assays results in cytotoxicity levels comparable to the lecithin-phospholipase treated kaolin levels. Treating silica with lysolecithin results in hemolysis assay results comparable to those using lecithin-phospholipase treated silica.

Further research is underway to determine if lysolecithin, with palmitic acid the product of phospholipase A_2 digestion of dipalmitoyl lecithin, remains bound to the kaolin surface following phospholipase treatment of lecithin coated kaolin, and if phospholipase stays associated with the kaolin surface. Preliminary thin layer chromatographic analyses of chloroform elution of the lecithin and phospholipase treated kaolin show that lysolecithin is associated with the kaolin surface after phospholipase digestion.

These preliminary studies indicate a quantitative and qualitative difference in the restoration of hemolytic potency of lecithin treated silica and kaolin following phospholipase digestion *in vitro*. The results indicate *that the* lecithin coating on silica may be digested and desorbed by lipase, restoring silica toxicity. Further research using mixed component pulmonary surfactant in longer term macrophage exposures and studies using full macrophage lysosomal enzyme treatment of full surfactant treated dusts is required to determine if similar digestion and desorption within macrophage phagolysosomes might occur to retoxify silica within the macrophage.The lecithin protective coating on kaolin may be partially hydrolyzed but may be removed incompletely; and therefore kaolin may not be restored to its original toxicity during phagocytosis. This may correlate with the different pathogenicities of silica and kaolin, if kaolin coated with lecithin and lysolecithin or other digestion products is not lytic to the interior phagolysosomal membrane.

These results provide the following research premise which is now under investigation: a) pulmonary surfactant coats silica and aluminosilicate and protects the lung against immediate lytic damage by the dusts; b) after phagocytosis of the dusts by macrophages the lysosomal enzymes digest the surfactant coating; c) this bares the surface of silica which then lyses the lysosomal membrane and thus damages or kills the macrophage; d) some surfactant and products of surfactant digestion by lysosomal enzymes, which are not toxic within the interior of the lysosome, stay bound to the surface of kaolin and continue to suppress its toxicity.

While surfactant may provide a natural defense system to minimize the prompt toxicity of inhaled particles, the emulsifying properties of surfactant may also enhance the toxicity of particles which are coated with or consist of organic compounds, by assisting the in vivo solubilization of these toxic organics. (32-34) The solubilizing effect of pulmonary surfactant may affect the release of toxic materials from respired particles into the alveolar hypophase, the clearance of those solubilized toxicants, and the partitioning of toxicants into alveolar cells. In this area current NIOSH research is directed to studies of the pulmonary surfactant extraction (a simulated in vivo process) of mutagenic materials from respirable diesel exhaust particulate. As measured by Ames assay for reverse mutation in Salmonella typhimurium (35), extraction of mutagenic materials does occur and results in some cases, in slightly greater mutagenic activity than that of standard organic (dichloromethane) extraction products.

Figure 4 shows representative results of S. typhimurium TA98 histidine reversion mutagenicity assays for a diesel exhaust soot extract. Dichloromethane, physiological saline, and lecithin in physiological saline were used in equal liquid volume to extract the soot. Samples of each of the three extracts were applied to the tester strain, pre-incubated for 90 minutes at 37° C and then plated. Plates were incubated for 48 hours at 37° C. Revertant colonies were counted on an electronic colony counter (ARTEK). As shown, the lecithin extract resulted in somewhat higher activity than the organic solvent.

Results indicate that the surface properties of respirable particles and their interaction with pulmonary surfactant are important considerations for predicting the eventual toxicities of particles to the lung.

REFERENCES

1. Weiss, S.J. and LoBuglio, A.F., Laboratory Investigations. 47, 5 (1982).

2. Allison, A.C., Archives of Internal Medicine. 128, 131 (1971).

3. Brain, J.C., Environmental Health Perspectives. 35, 21 (1980).

4. Heppleston, A.G. and Styles, J.A., Nature. 214, 521-522 (1967).

5. Bittermen, P.B., Rennard, S.I., Hunninghake, G.W., and Crystal, R.G., Journal of Clinical Investigations. 70, 806-822 (1982).

6. Langer, A.M., Quarterly Reviews of Biophysics. 11, 543 (1978).

7. Nolan, R.P., Langer, A.M., Harington, J.S., Oster, C., and Selikoff, I.J., Environmental Research 26, 503 (1981).

8. Marks, J., British Journal of Industrial Medicine. 14, 81 (1957).

9. Stalder, K. And Stober, W., Nature. 207, 874 (1965).

10. Brown, R.C., Chamberlain, M., Davies, R., Morgan, D.M.C., Pooley, F.D., and Richards, T., in "The In Vitro Effects of Mineral Dusts", Edited by R.C. Brown, et al., p 47 (1980).

11. Daniel, H., and LeBouffant, L., in "The In Vitro Effects of Mineral Dusts", edited by R.C. Brown, et al., p 33 (1980).

12. Morgan, W.K.C., and Seaton, A., "Occupational Lung Diseases", (1975).

13. Hamilton, A. and Hardy, H.L., "Industrial Toxicology", p 448 (1974).

14. Parker, W.R., "Occupational Lung Disorders", p 338 (1974).

15. Hunter, D., "The Diseases of Occupations", p 992 (1975).

16. Sheers, G., British Journal of Industrial Medicine, 21, 218 (1964).

17. Warraki, S., and Herant, Y., British Journal of Industrial Medicine, 20, 226 (1963).

18. Lynch, K., and McIver, F.A., American Journal of Pathology, 30, 1117 (1954).

19. Clements, J.A., Nellenboyer, J., and Trahan, H.J., Science 169, 603 (1970).

20. Wallace, W.E., Jr., Headley, L.C., and Weber, K.C., Journal of Colloid and Interface Science. 51, 535 (1975).

21. Light, W.G., and Wei, E.T., "The In Vitro Effects of Mineral Dusts", Edited by R.C. Brown, et al., p 140 (1980).

22. Jurand, M.D., Magne, L., and Bignon, J., British Journal of Industrial Medicine. 36, 113 (1979).

23. Emerson, R.J., and Davis, G.S., Environmental Health Perspectives. 51, 81 (1983).

24. Adamis, T., and Timar, M. "The In Vitro Effects of Mineral Dusts:, edited by R.C. Brown et al., p 139 (1980).

25. Harington, J., et al., Environmental Research, 4, 95-117 (1971).

26. Phillips, H.J., in "Tissue Culture Methods and Applications", p.406, ed. by P.R.Kruse Jr. and M.K.Patterson Jr., Academic Press, N.Y. (1973).

27. Reeves, W.J., and G.M. Fimignari, J. Biol. Chem., 238 3853 (1963).

28. Lockard, V., and Kennedy, R., Lab. Inv. 35, 501-6.

29. Sellinger, O.Z., et al., Biochem. J. 74, 450-6.

30. DeShazo, R.C., Journal of Allergy and Clinical Immunology, 70, 41-49 (1982).

31. Allison, A.C., in "Respiratory Defense Mechanisms", Part II, p 1075-1102, ed. by J.D. Brain, D.F. Proctor, and L.M. Reid. Marcel Dekker Inc., NY (1977).

32. Falks, H.L., Miller, A., and Kotin, P., Science. 127, 474 (1957).

33. King, L.C., Kohan, M.J., Austin, A.C., Claxton, L.D., and Huisingh, J.L., Environmental Mutagenesis. 3, 109 (1981).

34. Buddingh, F.B., Bailey, M.H., Wells, B., and Haesemeyer, J., American Industrial Hygiene Association Journal. 42, 503 (1981).

35. Ames, B.N.,McCann, J., and Yamasaki, E., Mutation Research, 31, 347 (1975).

ACKNOWLEDGEMENTS

This research has been supported by the Department of the Interior's Mineral Institute program administered by the Bureau of Mines through the Generic Mineral Technology Center for Respirable Dust under grant number G1135142.

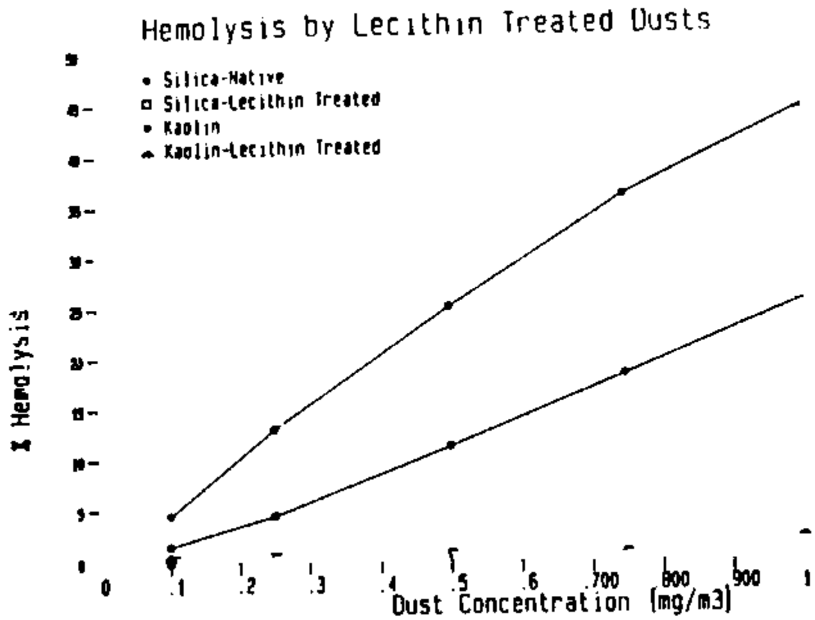

Figure 1 Erythrocyte Hemolysis by Native and Dipalmitoyl Lecithin Treated Silica and Kaolin Dusts

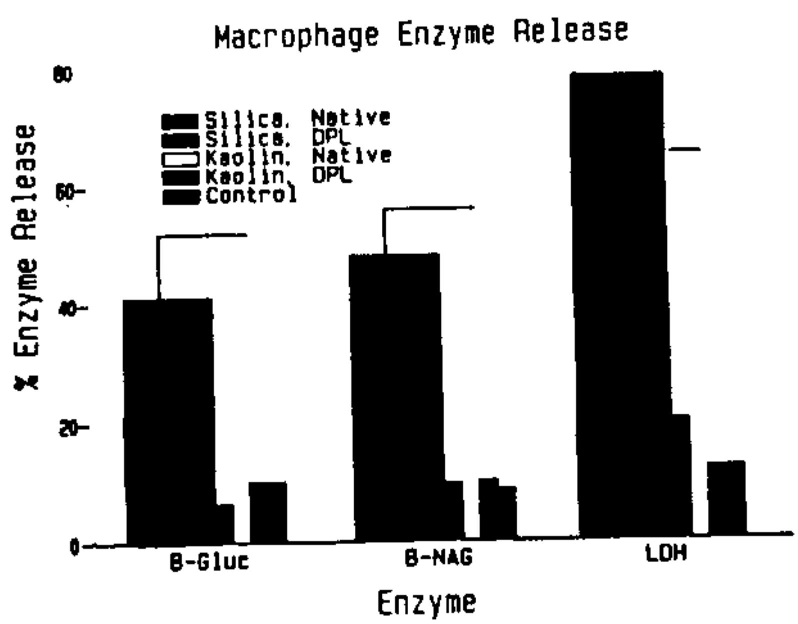

Figure 2 Murine Pulmonary Macrophage Release of β glucuronidase, β-N-acetyl glucosaminidase, and Lactate Dehydrogenase following Exposure to Native and Dipalmitoyl Lecithin Treated Silica and Kaolin dusts

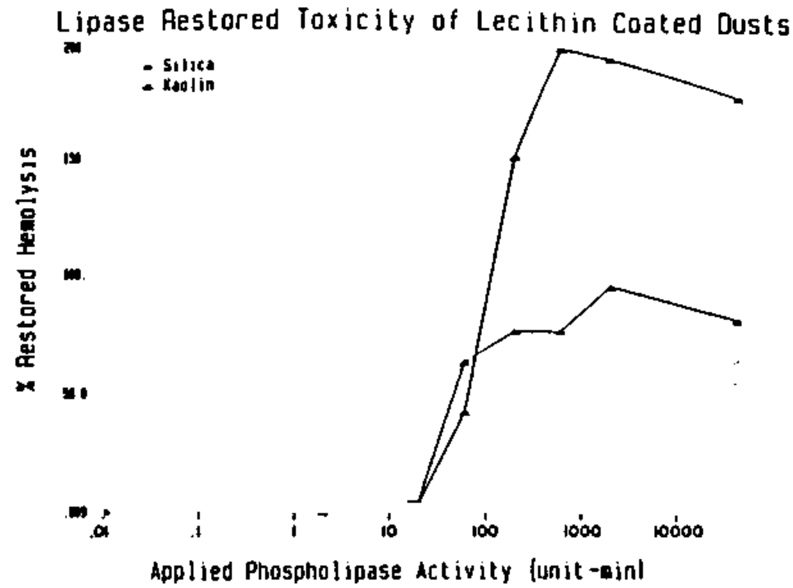

Figure 3 Cytotoxicity (Erythrocyte Hemolysis) of Dipalmitoyl Lecithin Pretreated Silica and Kaolin Dusts Following Incubation with Phospholipase A_2

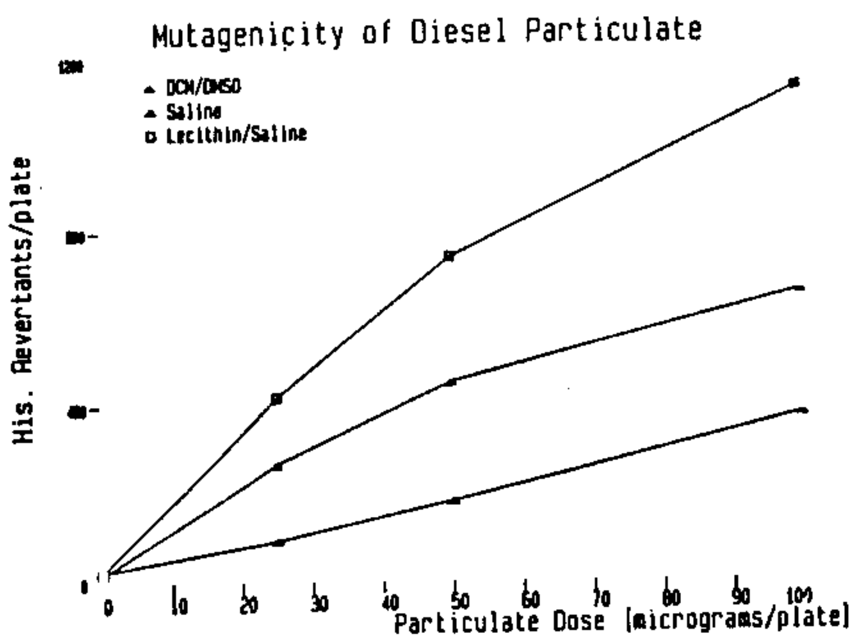

Figure 4 Mutagenicity of Diesel Soot Particulates Extracted or Dispersed in Dichloromethane/ DMSO, Physiological Saline, and Dipalmitoyl Lecithin in Physiological Saline

IV

Dust Lung Interaction

THE DEVELOPMENT OF AN ELECTRO-OPTICAL TECHNIQUE TO MEASURE SUPEROXIDE RELEASE FROM PULMONARY ALVEOLAR MACROPHAGES EXPOSED TO COAL DUSTS

Kevin A. DiGregorio, Graduate Research Assistant
Eugene V. Cilento, Associate Professor of Chemical Engineering/Anatomy
R. Clark Lantz, Assistant Professor of Anatomy

Departments of Chemical Engineering and Anatomy
West Virginia University
Morgantown, West Virginia 26506

ABSTRACT

A microscope-based spectrophotometer has been developed to measure superoxide release from single pulmonary alveolar macrophages (PAM) or other phagocytes in culture. Results indicate that PAM respond to stimulation by phorbol myristate acetate (PMA). It appears that some PAM do not release O_2^- upon stimulation by PMA; however, those that do release O_2^- show differences in: (1) the total amount of O_2^- released, (2) the rate of release of O_2^-, and (3) the time delay for release of O_2^-. The significance of measuring O_2^- release from single cells is two-fold. It allows the simultaneous study of O_2^- release and electrical potential changes across the membrane of PAM and it allows the study of differences in O_2^- release among cells. Thus, the function of normal PAM and the dysfunction of PAM exposed to coal dusts can be more closely studied on single cells.

INTRODUCTION

Pulmonary alveolar macrophages (PAM), free cells found in the lungs, protect the lungs by removing inhaled foreign debris and bacteria. The macrophages do this by engulfing and then internalizing the foreign matter (phagocytosis). Stimulation of PAM causes the release of superoxide radical (O_2^-) which has been shown to be the primary metabolite involved in the killing of bacteria by phagocytes (3,8,12). The superoxide radical is highly reactive and is spontaneously or enzymatically converted to other antibacterial oxidants, including hydrogen peroxide (H_2O_2), singlette oxygen ($^1O_2$), hydroxyl radical (OH^-), and hypochlorous acid (HOCl) (2, 3,8,11,12).

Exposure of PAM to dusts may lead to dysfunction of this cell-type and to a greater risk of lung damage or infection upon subsequent exposure to toxic dusts. To date, much of the research with this cell-type has used cytotoxicity (cell death) as a measure of dysfunction. Although this is an important end point, PAM dysfunction may occur at doses below those which lead to cell death. In addition, dysfunction has been measured using large numbers of cells. In order to obtain a clear understanding of the mechanisms involved in dysfunction, measurements should be made on single cells. As mentioned earlier, one of the major roles of this cell type is its antibacterial actions. Therefore, asessment of release of superoxide radical in single cells is important in determining the functional behavior of PAM before and after exposure to dusts. Since measurements of O_2^- production have not been made on single cells the purpose of this study is to develop the methodology needed to study release of O_2^- from single cells.

Recent studies have suggested that a relationship exists between the release of O_2^- and changes in the electrical properties of phagocytes. The change in membrane potential is thought to be the initial step in superoxide production (6, 9). Stimulants which cause O_2^- release also cause changes in the transmembrane potential of phagocytes (9) and in the permeability of the cell membrane to ions (6). For example, stimulants which cause the release of O_2^- from neutrophils have also been shown to increase the membrane transport of Na^+, K^+, and Ca^{+2} and stimulation of macrophages leads to increases in Na^+ and perhaps Ca^{+2} permeability with a subsequent change in membrane potential. In some cases, phagocytic activity has been shown to depend upon the extracellular concentrations of these ions (6). Holian and Daniele (7) have shown evidence that the redistribution of cellular Ca^{+2} in alveolar macrophages is an initial step leading to O_2^- release. In order to provide direct evidence that O_2^- production is related to electrical changes across the plasma membrane of phagocytes, these two phenomena must be analyzed simultaneously on single cells. Ultimately, measurements of O_2^- release using the methodology developed in this study will be combined with electrophysiological techniques to study both superoxide release and membrane potential changes simultaneiously on single PAM, and to examine the effects of coal and mineral dusts on their physiological function.

METHODS

Cell Isolation. The PAM used in this study were obtained from male Long-Evans hooded rats weighing between 250-300 g using the tracheal lavage method developed by Myrvik, et al. (10). Alterations in membrane potential and superoxide release have been shown to occur upon appropriate stimulation of groups of these cells in culture (9).

The animals were anesthetized with sodium pentobarbital (0.2 g/kg body weight) and exsanguinated by cutting the abdominal aorta. The lungs were lavaged 10 times with a total of 80 ml of an ice cold calcium-free solution containing 145 mM NaCl, 5 mM KCl, 1.9 mM NaH_2PO_4, 9.35 mM Na_2HPO_4, and 5.5 mM glucose (pH = 7.4). Cells were separated from the lavage fluid by centrifugation at 500 g for five minutes and then washed twice with ice cold HEPES buffered-medium

Presented at the Proc. Coal Mine Dust Conference,
Morgantown, W. Va., October 8-10, 1984.

(140 mM NaCl, 5 mM KCl, 1.5 mM $CaCl_2$, 10 mM Na-HEPES), (N-2-hydroxyethyl piperazine-N'-2-ethane sulfonic acid), and 5.5 mM glucose (pH = 7.4). After washing, the cells were resuspended in ice cold HEPES buffered-medium and kept in an ice bath. An aliquot (2 ml) of the ice cold cell suspension (100,000 cells/ml) was then withdrawn and placed in a tissue culture dish (35 mm Falcon type 3001); the remaining cell suspension being kept on ice until needed.

Data Recording. The culture dish was placed on a heating element for approximately 30 minutes to preheat the cells to 37°C and to allow the macrophages time to adhere to the bottom of the dish. Nonadherent cells were then removed along with the HEPES resuspension fluid by washing the dish three times with preheated (37°C) HEPES buffered-medium. Finally, preheated (37°C) HEPES buffered-medium containing 1 mg/ml nitro-blue tetrazolium (NBT) was added to the dish. In the presence of a strong reducing agent, such as O_2^-, soluble NBT is reduced to a formazan precipitate which can be measured spectrophotometrically at 550 nm. The culture dish was placed on the stage of an inverted light microscope where the cell culture was maintained at 37°C for the remainder of the experiment.

PAM were transilluminated at 550 nm and visualized using an Olympus inverted microscope and a low light-level Cohu silicon-vidicon television camera.

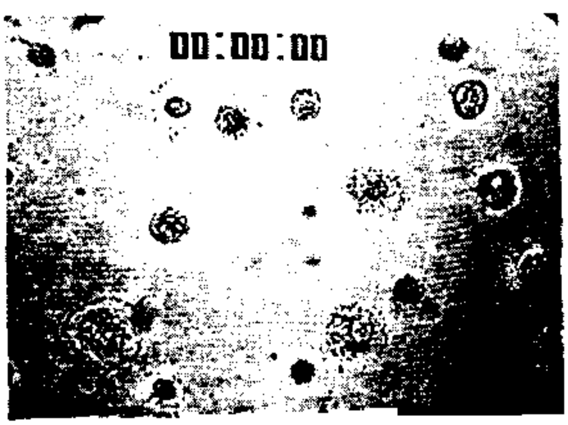

Figure 1. Representative microscopic field showing pulmonary alveolar macrophages before stimulation. Picture was taken of a single videoframe from image on monitor.

The televised image of the cells in a microscopic field was videotaped for approimately 40 minutes using a 3/4" Sony videocassette recorder (VCR).

PAM were stimulated to release O_2^-, following four minutes of baseline recording, by adding 10 ug/ml of phorbol myistrate acetate (PMA) to the culture medium. PMA has been shown to cause superoxide release and membrane potential changes in rat alveolar macrophages (9). Although other stimulants also result in stimulation of PAM, PMA was used in this study to compare results obtained here with results of Miles and coworkers (9). In addition, PMA is a soluble stimulant and therefore did not interfere with measurements of reduced NBT.

Data Analysis. Images recorded on videotape were played back through an IPM video photometric analyzer (model 204A) which generates two windows (boxes) in the televised scene.

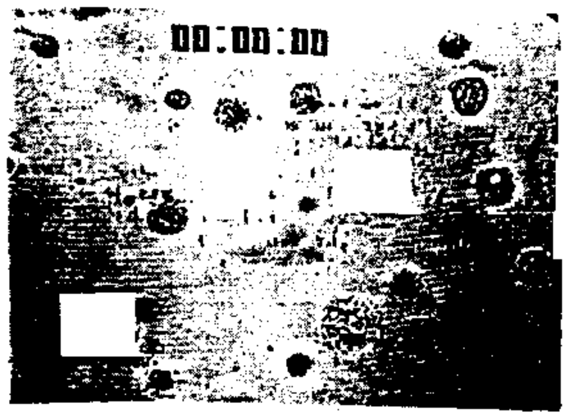

Figure 2. Same image shown in Figure 1 but with windows from photoanalyzer positioned over two cells. The size and position of the windows within the video images is user-selectable.

These windows, acting as phototransistors, are sensitive to changes in the average light intensity in the box area. The output of the photometric analyzer is a 0-1 voltage output proportional to this average light intensity. The box size and position are selected by the user. This system was used to measure the optical denisty (OD) change that occurs due to the reduction of NBT by superoxide. To do this, a window was positioned over a single PAM for a total of 40 minutes and the output voltage from the photoanalyzer digitized (12 bit) every ten seconds uisng a Keighley Data Acquisition System (model 520) and stored on an IBM PC-XT microcomputer for data analysis. These data provided a light intensity versus time curve for the 40 minute experiment.

The change in optical density was calculated using the Beer-Lambert Law which relates the OD change to the log ratio of the initial light intensity, I(0), and the light intensity at any time t, I(t). I(0) was determined by averaging the baseline voltage measurements, taken every ten seconds, for four minutes prior to stimulation of the PAM. I(t) was then measured every 10 seconds following stimulation for 36 minutes.

Camera background was also recorded by closing the beam splitter of the microscope so that no light was transmitted to the camera. Background voltage (VC) produced by the camera was subtracted from both I(0) and I(t) so that the calculation of OD included only voltages related to light intensity actually illuminating the cell. This is analogous to spectrophotometry where the transmittance is initially set to zero (infinite absorbance) when no light is transmitted through the sample. In addition, the maximum transillumination was set such that the camera output voltage did not saturate; that is, the video output did not exceed one volt. The Beer-Lambert Law was then modified as follows:

$$OD = \log((I(0)-VC)/(I(t)-VC))$$

Measurement of background light intensity changes was made in microscopic fields of the cell culture which did not contain cells. Preliminary studies have shown that the videotape background changed very slightly and linearly over the 40 minutes. Thus, I(t) may actually be changing very slightly during the experiment because of background variation. To correct for this, the tape background measurements were used to correct for the temporal change in I(t) that occurs due to the background. The linear change calculated in background at a time t was determined by fitting a straight line to the background measurements. The slope (m) of this line multiplied by the time t was then used to correct for background variation by subtracting the change (m*t) from I(t). The final modified form of the Beer-Lambert Law used for these experiments then becomes:

$$OD = \log((I(0)-VC)/(I(t)-VC-m^*t))$$

Calibration. The light microscope spectrophotometer was calibrated with neutral density filters which reduce, by a given amount, the transmitted light intensity without changing the spectral characteristics of the light. Several filters of known optical density values were placed on the microscope stage, one at a time, in increasing steps of optical density. Thus, the transmitted light (550 nm) illuminating the camera was progressively decreased. Images were videotaped and analyzed with the photometric analyzer analogous to an NBT reduction experiment. This provided a calibration curve of known OD which was used to determine the actual OD change that occured due to NBT reduction by superoxide. The calibration curve obtained using neutral density filters showed that the system responded linearly over the OD range of 0.1 to 1.0 OD.

RESULTS AND DISCUSSION

System Reliability. The first test of the system involved comparisons between on-line and off-line measurements. Data was obtained from live (on-line) measurements of light intensity from PAM and background. Simultaneously, these experiments were videotaped and measurements identical to those obtained on-line were made from the recording (off-line). The light intensity data was then used to determine the temporal changes in optical density. The results showed no significant differences between on-line and off-line determination of OD, thus, further analyses were made off-line.

Microscopic focus changed very slightly at various times during the experiments, and it was monitored and adjusted to keep the PAM in focus. However, adjustments were made "by eye" and were not always made immediately. Thus, the effect of focus changes was examined by moving the plane of focus above and below the cells with the fine and coarse adjustment. Results obtained for background measurements showed that OD remains constant through both fine and coars adjustments.

One of the most significant erros in microspectrophotometry is the distributional error, which is a result of the light-absorbing material (precipitate) not being uniformly distributed over the measurement field. The most widely accepted procedure for avoiding this error consists of dividing the measurement area into a large number of smaller regions and determining the OD of each smaller region separately. The OD results from each smaller region are then summed to obtain the OD of the original measurement area. In this study, the area measured is much larger than ideal, and distributional errors may exist. In general, if such errors exist, the OD measurements are conservative. In this study, distributional errors limit our ability to determine the actual OD of the precipitate, but do not interfere singificantly with relative comparisons of O_2^- release among PAM (1,4).

To test the effect of different-sized windows, several cells were analyzed with either small boxes (approximately 5% of cell area), medium boxes (approximately 20% of cell area), or large boxes (approximately 50% of cell area). In addition, cells were analyzed with single boxes of various sizes ranging from approximately 80% to 120% of the cell area. For each box size, the OD calculated was multiplied by the box area to account for the difference in area. In all cases, the results showed no significant differences among the window sizes used and therefore further analyses were made with a box area approximately equal to the area of the cell being measured.

A final test of system reliability and accuracy involved repeatability of measurements. Several repeated measurements were made from the same PAM and/or background. These results also showed no significant difference in the OD versus time curves.

Superoxide Release. Results obtained to date were acquired during the development of the methodology. Thus, all data obtained during different stages of the development can not be compared directly, but can be used to make some general conclusions about O_2^- release from single rat PAM.

The most interesting findings were that O_2^- release measured with this system varies significantly among PAM and that more than half of the PAM respond to stimulation (Figure 3). Figure 3 shows four frames of video which demonstrate the types of responses which are seen and the variability between cells. Cells were stimulated with PMA at the 4 minute mark and then followed for an additional 36 minutes. As can be seen, after stimulation, a gradual darkening sppears over and around some, but not all cells. This is the superoxide-reduced NBT precipitating around cells. Also, even among the PAM that respond, there were differences in the apparent rates as observed visually. From computer analysis of individual cells, the differences in rates,

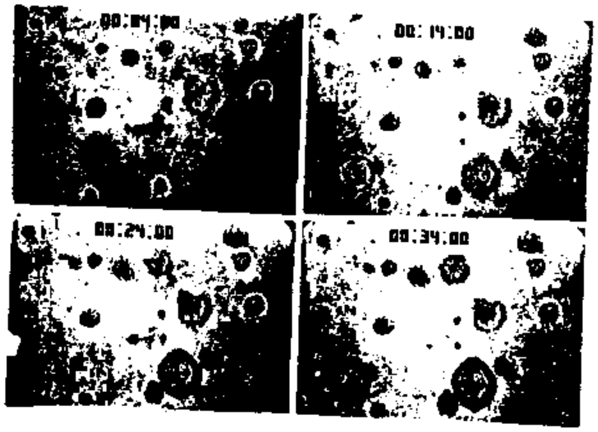

Figure 3. Four videoframes showing progressive reduction of NBT by superoxide following stimulation of macrophages with PMA. Cells were stimulated at 4 minutes.

amounts, and lag times can be determined (Figure 4). Of the cells that do release O_2^-, variation appears to occur in: (1) the total amount of O_2^- released, (2) the rate of release of O_2^-, and (3) the lag time before release of O_2^-. In terms of OD units, the total amount of O_2^- released ranged from 0.2 OD units to 1.3 OD units, and the rate of O_2^- release ranged from approximately 0.001 OD units/minute to 0.1 OD units/minute. This suggests an order of magnitude difference in both the total amount of O_2^- released and the rate of release. The delay time after stimulation ranges from nearly instantaneously (few seconds) to 12 minutes.

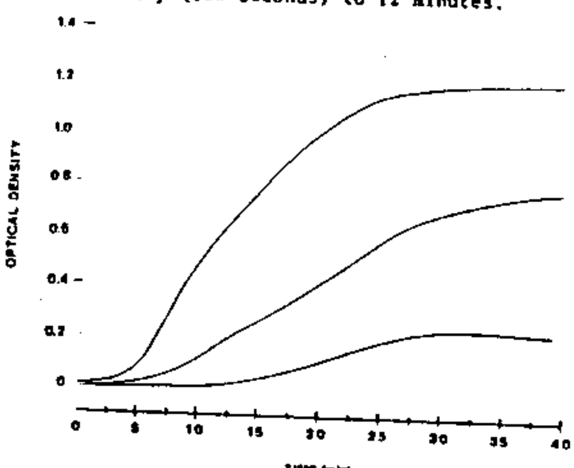

Figure 4. Temporal changes in OD for three different macrophages stimulated with PMA. Differences are noted in the total reponse, the rate of response, and the lag time between stimulation and initiation of a response. Stimulation was started at 4 minutes.

Differences in the response of individual macrophages measured in this study may be due to heterogeneity among macrophages. Heterogeneity of PAM has been demonstrated in previous work where large numbers of PAM have been subdivided either on the basis of their density or as a function of their lavage fraction (5,3,14). Differences within the subpopulations were found in their ability to respond to test stimulants with a respiratory burst and in their release of superoxide. Further study of individual PAM with the methodology described here will permit determination of the factors responsible for the degree of heterogeneity observed among control and dust-exposed animals.

Another explanation is that distributional errors account for the differences in measured response among macrophages. If distributional errors exist and if the cellular distribution of superoxide release varies among cells than differences in the measured rates of release and lag time for release could be a consequence of the present method for measurement of optical density. This problem can only be alleviated if distributional errors can be measured. However, elimination of distributional errors is beyond present equipment capabilities and can not be assessed until more sophositicated video instrumentation is acquired.

In summary, although the methodology described here shows promise in being able to answer questions about function and dysfunction of single PAM which can not be answered using other techniques. Questions about heterogeneity, mechanism(s) of dysfunction, and correlation of function with biochemical and morphological data can only be addressed using data obtained from individual cells. Continued development of this technique will give much useful information on the ability of this important cell-type to respond to dust exposures and to function following exposure.

BIBLIOGRAPHY

1. Altman, F.P. The Quantification of Formazans in Tissue Sections by Microdensitometry, III. The Effect of Objective Power and Scanning Spot Size. Histochem. J., 8:507-511; 1976.

2. Babior, B.M. Oxygen Dependent Microbial Killing by Phagocytes (parts 1 and 2). New England J. Med. 298:659-667; 1978.

3. Babior, B.M. The Enzymatic Basis for O_2^- Produced by Human Neutrophils. Can. J. Physiol. Pharmacol. 60:1353-1358; 1982.

4. Bitensky, L. Microdensitometry. Excerpta Medica O; Trends in Enzyme Histochemistry and Cytochemistry. 181-202; 1980.

5. Drath, D.B., P. Davies, J.M. Shorey, N.S. Gibrans, P.J. Simpson, and G.D. Huber. Characterization of a Postlavage, In situ Pulmonary Macrophage Population. J. Cell Physiol. 111:97-103; 1982.

6. Holian, A. and Daniele, R.P. Formyl Peptide Stimulation of Superoxide Anion Release from Lung Macrophages: Sodium and Potassium Involvement. J. Cell Physiol. 113:413-419; 1982.

7. Holian, A. and Daniele, R.P. The Role of Calcium in the Initiation of Superoxide Release from Alveolar Macrophages. J. Cell Physiol. 113:87-93, 1982.

8. Klebanoff, S.J. Oxygen Metabolism and the Toxic Properties of Phagocytes. Ann.Int.Med. 93:480-489; 1980.

9. Miles, P.R. and Bowman, L. Transmembrane Potential Changes During Phagocytosis in Rat Alveolar Macrophages. J. Cell Physiol. 106: 109-117; 1981.

10. Myrvik, Q.N., Leake, E.S., and Fariss, B. Lysozyme Content of Alveolar and Peritoneal Macrophages from the Rabbit. J. Immunol. 86: 133-136; 1961.

11. Root, R.K. and Metcalf, J.A. H_2O_2 Release from Human Granulocytes during Phagocytosis. J. Clin. Inves. 60(126):1279; 1977.

12. Singh, A. Chemical and Biochemical Aspects of Superoxide Radicals and Related Species of Activated Oxygen. Can. J. Physiol. 60:1330-1345; 1982.

13. Somerville, T.D., M.R. Van Scott, P.R. Miles, and V. Castranova. Heterogeneity of Alveolar Macrophages: Relationships Between Cellular Properties and Lavage Number. Am. Rev. Resp. Dis. 129:A6; 1984.

14. Van Scott, M.R., T.D. Somerville, R.C. Lantz, P.R. Miles, and V. Castranova. Heterogeneity of Rat Pulmonary Macrophages: Relationship to Lavage Number. Submitted to J. Appl. Physiol.

ACKNOWLEDGEMENTS

The authors wish to thank Cindy A. Phillips and Victoria C. Bruhn for the preparation and typing of this manuscript. Supported in part by the WVU Energy Research Center (ST84-CM141) and Generic Respirable Dust Center (G1135142).

V

Relationship of Mine Environment, Geology and Seam Characteristics To Dust Generation and Mobility

AN ANALYSIS OF COAL AND GEOLOGIC VARIABLES RELATED TO COAL WORKERS' PNEUMOCONIOSIS

Jan M. Mutmansky
Associate Professor of Mining Engineering
and
Changwoo Lee
Graduate Assistant

Department of Mineral Engineering
The Pennsylvania State University
University Park, PA 16802

ABSTRACT

This paper results from the research at The Pennsylvania State University into establishment of standard procedures for characterization of respirable coal dust performed by the Generic Mineral Technology Center for Respirable Dust and supported by the U.S. Bureau of Mines and the Mining and Mineral Resources Research Institute at The Pennsylvania State University. The research performed within this particular project is oriented primarily toward standard methods of sampling and characterizing respirable coal mine dust underground so that the chemical, physical, and morphological characteristics are known and can be related to the incidence of coal workers' pneumoconiosis (CWP) in Pennsylvania.

The research was initiated by conducting a search of the literature to determine what coal and geologic variables may be related to CWP. The effects of coal rank, free silica content, the mass of respirable dust, and the level of trace elements were the major variables studied. It seems to be evident that the free silica content, the rank of coal, and the mass of respirable dust are the major concerns in defining the causes of CWP. However, based on the literature survey, the authors have concluded that verification of the causes of CWP is a multivariate problem and must be analyzed in an appropriate statistical manner.

The results of a multivariate analysis of ten trace elements recorded on Pennsylvania coals are presented. Five of these trace elements were found to be of use in differentiating one coalfield from the others. Of these five elements, chromium and zirconium showed a strong positive correlation with the rank of coal while strontium showed a negative correlation.

The design of the field sampling work and its application in future research is the final topic discussed. The sampling plan is oriented toward continuous miner sections with eight-stage impactors as the collection equipment. All of the field work will be conducted in the coal measures of the Allegheny Formation and above with both dust and channel samples being collected in the same mines.

INTRODUCTION

Coal workers' pneumoconiosis has been an important topic of concern to miners, mining engineers, and epidemiologists for decades. The general cause of the disease, the inhalation of coal mine dust, is well known, but the specific coal and geologic variables that affect the incidence and severity of the disease are still subject to debate and study. The primary objective of this study is to identify those variables of Pennsylvania coals that contribute to the CWP problem. To accomplish this task, a field sampling program is to be conducted to relate the characteristics of the coal dust, the coal seam properties, and the geologic variables to the occurrence of CWP.

The first year of this study has been involved with both a literature review and experimental work oriented toward identification of causal variables related to CWP. The results of this work are presented here along with plans for implementation of the findings in future research.

REVIEW OF THE LITERATURE

The previous studies of CWP causal variables have been conducted by scientists, engineers, and medical personnel. Many different types of studies have been performed with emphasis on interpreting the effects of dust mass concentration, mineralogy of the coal, the rank of the coal, and trace element concentrations upon the incidence of CWP in various coalfields. Most of the research has been conducted during the last two decades, with the British Isles, West Germany, and the United States being the primary countries involved.

The review of the literature was conducted to determine which variables are likely to warrant further study in Pennsylvania. Previous research studies have related CWP to free silica and other mineral content, the rank of coal, the mass of dust in the working place, and the trace elements in the coal and lung dust. In the following sections, each of these topics will be discussed and analyzed.

Presented at the Proc. Coal Mine Dust Conference, Morgantown, W. Va., October 8-10, 1984.

It should be noted that no attempt is being made here to include all the references related to the individual topics or to discuss all the references listed in any detail. Instead, the topics will be covered by tabular summaries that will attempt to provide the major conclusions of each investigating team. A complete reference list will be provided for those interested in a more detailed analysis of the individual research projects.

Free Silica and Other Mineral Content

It has been known for many decades that miners subjected to metal mine dusts high in free silica content are likely to incur a higher incidence of silicosis than similar miners subjected to respirable dust containing lesser percentages of free silica. Many studies corroborate this fact in metal mines. In coal mines the relationship between CWP and the free silica content is not quite as certain. In part, this is probably due to the fact that coal seams contain less quartz than metal ores. A second complicating factor is that silica often comes from sources outside the coal seam (e.g., roof and floor) making the free silica content of the respirable dust in a coal mine a function of variables external to the seam.

During the 1960s and 1970s, a number of studies were performed that attempted to relate the effects of free silica content of coals and the incidence or severity of CWP. Many of these studies are listed in Table 1. A majority of the

Table 1. Studies Relating Free Silica Content and CWP.

Reference	Sites of study	Conclusions
Leiteritz et al. (1)	Ruhr and Saar districts in West Germany	a. Stronger changes of the lung tissue were observed in cases of high quartz and dirt contents. b. The lowest quartz contents were found in the lungs of face workers; the highest quartz contents from the lungs of miners who worked mostly in rock drifts or in coal seams with high dirt contents. c. An important factor in the size distribution of the respirable dust is the amount of mineral matter.
Jacobsen et al. (2)	Britain	a. Quartz in mixed coal mine dust does not have a clear effect on the chances of developing CWP.
McLintock et al. (3)	Britain	a. No clear relationship between quartz content and prevalence of CWP.
Naeye et al. (4)	312 Appalachian miners	a. The association of CWP with the rank of coal in Appalachia is probably fortuitous. b. The level of exposure to free silica plays a more important role.
Morgan (5)	Not available	a. The silica content of coal mined seems to have little or no effect on the prevalence of CWP. b. There exists a relationship between the prevalence of CWP and the rank of coal.
Sweet et al. (6) Carlberg et al. (7) Keenan et al. (8) Crable et al. (9) Crable et al. (10)	Raleigh County, West Virginia	a. A monotonically increasing trend in means of Mg, Be, V, free-silica, coal dust and total dust with increasing degrees of lung damage. b. No relationship between the severity of CWP and Cr, Cu, Fe, Mn, Ni, Ti, Zn and noncoal dust.
Walton et al. (11)	Britain	a. The quartz content of airborne dust is low when high-rank coal is mined and higher in low-rank coalfields. b. The probability of progressive massive fibrosis appears to fall with mineral content.
Reisner (12)	West Germany	a. There is no clear relationship between the quartz content and the chances of developing CWP.
Hurley et al. (13)	2,600 miners over a period of 20 years in Britain	a. Cumulative exposure to quartz is highly correlated ($r=0.77$) with exposure to mixed dust overall. b. A clear relationship between cumulative dust exposure and the prevalence of pneumoconiosis. c. Among men with similar cumulative dust exposures, those who have worked longer hours in coal mining have higher prevalence of CWP. d. Little evidence that exposure to quartz influenced the chance of developing CWP. e. No evidence of association of the prevalence of CWP with contents of ash and kaolin-plus-mica in respirable dust. f. Weak correlation between the prevalence of CWP and the rank of coal.

research projects seem to indicate a statistical consensus that the incidence or severity of the disease is related to the free silica content of the coal. However, other researchers reported different conclusions, normally suggesting that there is no clear relationship between CWP and free silica content of the coal. Some of these contradictions may be due to sampling problems and the difficulty of extracting conclusions from different types of analytical studies. For example, it is difficult to equate studies that deal with the free silica content in coal seams, in coal mine respirable dust, and in coal miners' lungs. As a result, it is not easy to come to firm conclusions on the role of free silica in the development of CWP.

The relationship that exists between silicosis and free silica that has been recognized in metal mining certainly leads one to believe that a similar relationship may exist in coal mining operations between free silica and pneumoconiosis if the other variables are similar. The pattern of conclusions in Table 1 does not strongly support such a relationship. However, Hamilton, et al. (14) and Hamilton (15) have provided a very plausible explanation for the manner in which free silica affects the occurrence of CWP. Hamilton's hypothesis, supported by many years of research on CWP in Great Britain, is that the free silica content does not affect the probability of developing pneumoconiosis until some threshold value (generally thought to be about 10%) is exceeded. This offers a great deal of hope in explaining the differences in the conclusions achieved by different researchers.

As far as other minerals are concerned, the only type of minerals that have been studied are the clay minerals, which normally account for much of the noncoal material within a coal seam. Leiteritz et al. (1) has studied the clay mineral content of coals in Britain and found that the clay mineral concentration is much higher in respirable dust and in the dust found in miners' lungs than in the total dust. This may be of consequence in the occurrence of CWP. However, the subject has not been studied widely enough to date to develop a valid conclusion.

Rank of Coal

The incidence and severity of CWP and its relationship with the rank of coal has been the subject of many research papers. These papers were produced mainly by investigators from Britain, the United States, and West Germany. A summary of the research results pertinent to the rank of coal is presented in Table 2. Most of the research indicates a higher prevalence and greater severity of CWP in miners subjected to the higher rank coals. The near unanimity of the results would lead one to conclude initially that the rank of coal is a causal factor in the occurrence of CWP. However, the more important knowledge to be gained is why this is so, and this is not readily apparent from the literature.

The rank of a coal is determined by the percentage of fixed carbon, the percentage of volatile matter, and the heat content of the coal. The fixed carbon is the most important of these variables and is defined as the portion of the carbon that remains when coal is heated in a closed vessel until the volatile matter is driven off. It is not clear from the literature sources whether the fixed carbon is the causative agent in CWP occurrences. There exists a number of other possible causal variables that are correlated with rank. Thakur (21), Dodgson et al. (22) and Jacobsen et al. (2) have pointed out the fact that the mass-number index (MNI) is related to the rank of coal with a high MNI being associated with high-rank coals. A second possibility that is evident from the conclusions stated by Nagelschmidt (19) is that the composition of airborne dusts generated is related to the rank of the coal. While Nagelschmidt performed his research in Great Britain, a similar possibility exists in U.S. coals, particularly when one realizes that our anthracite seams are dominated by quartzitic rocks. As a result, the respirable dust generated from roof and floor materials can conceivably be a major factor in the high incidence of CWP in high-rank coal seams.

One further complicating factor related to rank is the possibility that trace elements in the coal contribute in causing the pneumoconiosis (or, alternately, in protecting against it). This will be discussed in a subsequent section. As a result of these complicating factors, the authors conclude that the consideration of coal rank is important but those variables associated with rank should also be studied.

Mass of Respirable Dust

Most of the studies investigating the correlation between the mass of respirable dust in the mine environment and the prevalence of CWP have been performed since 1970. Some of the important findings of these studies are summarized in Table 3. The general consensus of all these research efforts has been to conclude that the greater the mass of dust in the working place, the greater the occurrence of CWP. The overwhelming nature of the evidence certainly points to the importance of the mass of dust in the overall picture. However, while the overall result is not easy to deny, the

Table 2. Studies Relating Rank of Coal and CWP.

Reference	Sites of study	Conclusions
Hart and Aslett (16)	16 South Wales Collieries in Britain	a. The order of prevalence of radiological abnormalities: 1. anthracite coal mines 2. steam coal mines 3. bituminous coal mines.
Hicks et al. (17)	20 collieries in Britain	a. The average period of work at the coal face required to produce a 20% prevalence of CWP: 8 years in the high rank coal 16 years in the medium rank coal 36 years in the low rank coal. b. The physical and chemical changes in evolving coal may underlie the differences in prevalence of CWP.
McBride et al. (18)	1,858 miners in Pennsylvania	a. The amount of fixed carbon in the coal may influence the production of CWP.
Nagelschmidt (19)	Britain	a. The composition of airborne dusts (coal dust, free silica) depends on the rank of coal. b. A positive association of the incidence of CWP with the rank of coal.
Leiteritz et al. (1)	Ruhr and Saar districts in West Germany	a. Rank is one of the determining factors for the size of airborne dusts developed during coal winning.
Morgan (20)	Pennsylvania and West Virginia	a. The prevalence of CWP is related to the rank of coal.
Thakur (21)	United States (20 coals from lignite to anthracite)	a. High rank coals produce larger masses of dust in the finer size range. b. Yield of respirable dust varies with coal properties and coal seams.
Dodgson et al. (22)	Britain	a. A clear correlation between the mass-number index (MNI: the mass in mg/m³ per 1000 particles/cm³ of dust in the respirable range) and coal rank. A high MNI occurs with high rank coal.
Jacobsen et al. (2)	Britain	a. A correlation of the index of progression of pneumoconiosis with mass of respirable dust which depends on the rank of coal.
Reisner (12)	West Germany	a. An association between high MNI and high rank of coal. b. Lower rank coal has finer particle size.
Morgan (5)	Not available	a. The silica content of coal mined seems to have little or no effect on the prevalence of CWP. b. There exists a relationship between the prevalence of CWP and the rank of coal.
Naeye et al. (4)	312 Appalachian miners	a. The association of CWP with the rank of coal in Appalachia is probably fortuitous. b. The level of exposure to free silica plays a more important role.
Reisner and Robock (23)	West Germany	a. The risk of simple pneumoconiosis increases with geological age and with higher rank of the seams.
Bennett et al. (24)	Britain	a. A close relationship between the prevalence of pneumoconiosis and the rank of coal. b. No correlation of mass concentration with rank. c. Mineralogical differences of coal may influence the dust-pneumoconiosis relationship.
Hurley et al. (13)	2,600 miners over a period of 20 years in Britain	a. Cumulative exposure to quartz is highly correlated (r=0.77) with exposure to mixed dust overall. b. A clear relationship between the cumulative dust exposure and the prevalence of pneumoconiosis. c. Among men with similar cumulative dust exposures, those who have worked longer hours in coal mining have a higher prevalence of CWP. d. Little evidence that exposure to quartz influenced the chance of developing CWP. e. No evidence of association of the prevalence of CWP with contents of ash and kaolin-plus-mica in respirable dust. f. Weak correlation between CWP prevalence and rank. the rank of coal.
Dessauer et al. (25)	Over 1,300 miners in Pennsylvania	a. The prevalence of category 3 of CWP and PMF (Progressive Massive Fibrosis) increases with the rank of coal.

Table 3. Studies Relating Mass of Dust and CWP.

Reference	Sites of study	Conclusions
Jacobsen et al. (26)	4,122 miners over a period of 10 years in Britain	a. A high correlation exists (r=0.80) between the prevalence of pneumoconiosis and the mean mass of respirable dust. b. A low correlation exists (r=0.44) between the prevalence of pneumoconiosis and the number of particles.
Jacobsen et al. (2)	Britain	a. A correlation of the index of progression of pneumoconiosis with mass of respirable dust which depends on the rank of coal.
Reisner (23)	West Germany	a. A correlation exists between MNI and the rank of coal. b. Lower-rank coal has finer particle size.
Dodgson et al. (22)	Britain	a. A clear correlation between MNI and rank of coal; high MNI with high-rank coal.
Morgan et al. (27)	10 states, 31 mines in the United States	a. A possible correlation with the physical and chemical composition of the coal mined (vs. the prevalence of CWP). b. It is doubtful that the quantity of respirable dust alone is responsible for the prevalence of CWP.
Walton et al. (11)	3,154 face-workers in Britain	a. The overall mass of respirable dust is the factor most closely related to the 10-year attack rate of pneumoconiosis.
Ogden and Rickmann (28)	Britain	a. Pneumoconiosis increases with increasing mass concentration of dust. b. Other properties of respirable dust (e.g., size distribution) may affect CWP. c. The size distribution of the respirable dust varies systematically with the type of coal and the mining method.

actual cause of the disease may still be questioned because of correlations between the mass of dust and the other hypothesized causative variables.

In particular, several correlations existing in the literature should be noted. Both Reisner (12) and Dodgson et al. (22) report a correlation between the MNI and the rank of a coal. This could be construed as an argument that the secondary variable, the rank of coal, is the causal factor in CWP incidence and not the mass of dust. This is not very likely but does pose some problems because other variables (such as some trace elements) are also positively correlated with rank. As a result, the single-mindedness of the previous conclusion on mass of dust should be noted with a certain amount of reservation.

Trace Elements

The possibility that certain trace elements in a coal seam contribute to CWP has been investigated by a limited number of researchers as shown in Table 4. A series of articles (6,7,8,9,10) published from 1967 to 1974 described the results of an extensive study in Raleigh County, West Virginia, relating trace elements found in lungs of coal miners and the severity of CWP. Several trace elements plus free silica, coal dust, and total dust were found to be correlated with lung damage. Thus it is possible to conclude that the trace elements may have some effect based on this study.

Further support for the hypothesis that trace elements may be responsible for CWP occurrence or severity is found in the reference by Sorenson et al. (29) that deals with two geographically dispersed bituminous coalfields. This reference outlines the trace element levels in a coal mine in Utah having a very low incidence of CWP with coal from a mine in Pennsylvania having a similar rank but associated with a very high CWP incidence. The results indicated higher levels of Cu, Fe, Ni, Pb, and Zn in the Pennsylvania coals. Elevated levels of these metals in lung tissue from coal miners may indicate some relationship with CWP. However, the study outlined here applies to only two coal mines, a situation that cannot lead to any broad conclusions. However, a general implication of the results is that the higher levels of Cu, Fe, Ni, Pb, and Zn may be contributing to the incidence of CWP.

A second line of thought is also possible when analyzing the effect of trace elements on CWP. Any study that is involved in measuring the contribution of trace elements to the development of CWP can possibly also measure the preventive or immunological effects of the trace elements. This possibility should be kept in mind during any investigation of the effects of trace elements on CWP incidence.

Table 4. Studies Relating Trace Elements and CWP.

Reference	Sites of study	Conclusions
Sweet et al. (6) Carlberg et al. (7) Keenan et al. (8) Crable et al. (9) Crable et al. (10)	Raleigh County, West Virginia	a. A monotonically increasing trend in means of Mg, Be, V, free silica, coal dust and total dust with increasing degrees of lung damage. b. No relationship between the severity of CWP and Cr, Cu, Fe, Mn, Ni, Ti, Zn and noncoal dust.
Sorenson et al. (29)	Pennsylvania and Utah bituminous coalfields	a. Higher incidence of CWP in Pennsylvania bituminous coal miners. b. Cd content of coal; no difference between Pennsylvania and Utah. c. Cu, Pb, Zn content of coal; 2-3 times higher in Pennsylvania. d. Fe, Ni content of coal; 5-10 times higher in Pennsylvania.

Pennsylvania-Based CWP Studies

The scrutiny of research results from Pennsylvania is important here for several reasons. First, the miners in the state were extensively X-rayed for evidence of pneumoconiosis during the 1960s by the Pennsylvania Department of Health. Second, our research effort at Penn State will be confined to Pennsylvania coal seams and any existing knowledge related to Pennsylvania should be of special importance to us.

The studies conducted by the Pennsylvania Department of Health have been summarized in Table 5. Several very interesting conclusions have been drawn based on this work. First, the studies were consistent in support of the idea that CWP incidence is greater as worker cumulative exposure is increased. Second, the studies by Baier and Diakun (31,33) showed the exposure to free silica content in the respirable mine dust was clearly a function of the job type with workers on haulage vehicles where sand was used for traction and rock drillers being subjected to significantly greater free silica content. Finally, it was firmly established in these studies that the incidence of CWP is positively correlated with the rank of coal in Pennsylvania, a conclusion that reinforces the results in studies performed elsewhere.

Implications of Past Research

The research performed to date on CWP has provided many insights into the disease, particularly its causes and the mechanisms by which the disease occurs. The studies seem to indicate a strong statistical case for greater incidence of CWP where the rank of coal is higher, where the mass of respirable dust is greater and where the free silica content

Table 5. Studies of CWP Variables in Pennsylvania Mines.

Reference	Sites of study	Conclusions
Lieben et al. (30)	5,072 miners in Central Pennsylvania	a. 25% of miners showed evidence of CWP. b. Weak correlation between years worked and CWP incidence. c. Low free silica content or high dust mass produce CWP.
Baier and Diakun (31)	24 anthracite mines in Pennsylvania	a. Free silica content high in haulage and drilling locations. b. Dust concentration similar on mechanized and nonmechanized sections.
McBride et al. (32)	10,869 miners in Western Pennsylvania	a. 11% of miners showed evidence of CWP. b. Positive correlation between years worked and CWP incidence.
Baier and Diakun (33)	24 anthracite mines in Pennsylvania	a. Higher dust levels in southern field. b. Free silica higher than in bituminous fields. c. Free silica content higher in haulage and drilling locations.
McBride et al. (34)	1,858 anthracite miners in Pennsylvania	a. 30% of miners showed evidence of CWP. b. Positive correlation between years worked and CWP incidence.
Tokuhata et al. (35)	954 anthracite miners in Pennsylvania	a. Incidence higher in large mines than in small mines. b. Smoking a factor.

of the respirable dust is higher. An interesting but less convincing case is made for the trace element levels in the coal seam. It is not absolutely clear, however, that these four major variables of coal are the actual causal variables. It may indeed be other variables that are more important. This is unlikely but possible and should be kept in mind in any research program.

A second observation based upon a study of past research is that most of the analyses have been performed in a univariate statistical fashion, i.e., the investigators have attempted to identify the relationship between CWP and the causal variables one-by-one. The evidence clearly points to more than one causal variable and to the possibility that multivariate statistical procedures will have distinct advantages.

Finally, the data collected on CWP has been of a variety of types with both medical and environmental data being collected. The possibility exists for better analysis of CWP problems if the dust samples taken in mines today were available in the past. This would have aided the medical personnel in evaluating worker exposure and the related development of CWP. Perhaps this is one of the things that will occur in the near future.

EXPERIMENTAL WORK

The review of the CWP literature led the authors to believe that some analysis of the trace elements in Pennsylvania coals might be of interest in the current study of CWP variables. To pursue this line of thought, the authors accessed the data of the Penn State Coal Sample Bank (36) managed by the Coal Research Section at Penn State. This data bank contains the chemical, physical, mineralogical, and petrographic data on over 1300 coal samples from 25 states. From this data bank, 250 coal samples from Pennsylvania were scanned for samples that contained values for ten trace elements (Ba, Be, Cr, Cu, Ni, Rb, Sr, V, Zn, Zr). A total of 97 samples that contained all the specified data were found. Only a few of these samples contained information on the mineralogical makeup of the coals.

The principal thrust of the statistical analysis of the 97 coal samples was to test the possible relationship between the trace element contents and the incidence of CWP in Pennsylvania coalfields. Accordingly, the samples were divided into three groups, each group being associated with a particular coalfield as follows:

(1) the eastern anthracite coalfield represented by 12 samples,
(2) the western middle bituminous coalfield (medium- and low-volatile bituminous coals) represented by 47 samples, and
(3) the western bituminous coalfield (high-volatile bituminous coals) represented by 38 samples.

The data set was then subjected to a group of statistical analyses using the SAS software package (37).

The first step in the statistical analysis was to test whether the mean values of the ten trace elements were significantly different in the three coalfields. To accomplish this, a stepwise discriminant analysis procedure was used. With the significance level set at 0.15, only five trace elements (Cr, Sr, Ni, Zn, and Zr) were found to be significant for discrimination among the three coalfields. Thus, these five elements were the only ones used in the discrimination process. Their mean values in ppm are given in Table 6.

Table 6. Mean Values (in ppm) for the Five Trace Elements Used in the Discriminant Function.

	Eastern Field (#1)	Central Field (#2)	Western Field (#3)
Cr	52.6	27.6	22.4
Ni	46.8	16.8	29.9
Sr	39.6	116.6	164.3
Zn	21.2	24.5	23.4
Zr	62.9	39.7	29.2

Using Hotelling's T^2 values, the F statistics for the three possible null hypotheses are as follows:

$F = 430.17$ with degrees of freedom = (5,53) for null hypothesis $\mu_1 = \mu_2$,

$F = 547.20$ with degrees of freedom = (5,44) for null hypothesis $\mu_1 = \mu_3$,

$F = 777.43$ with degrees of freedom = (5,79) for null hypothesis $\mu_2 = \mu_3$.

In all cases, the subscript on the μ values denotes the sample group number (or coalfield number). In all cases, the F statistics are significant at the 0.01 level of significance, resulting in rejection of all three null hypotheses. From this we can conclude that significant differences in the amount of the trace elements exist among the three coalfields.

To test the discriminant function, the ability of the function to classify the coal samples into their correct field of origin was used. The results of this process are shown in Table 7.

Table 7. Classifications Resulting from Use of the Five-Variable Discriminant Function.

Samples from \ Classified to	Field 1	Field 2	Field 3
Field 1	9	3	0
Field 2	2	38	7
Field 3	0	11	27

The discriminant function (which is quadratic) correctly classifies 74 of the 97 samples (based on a knowledge of only the Cr, Sr, Ni, Zn, and Zr values). This is a favorable result since it indicates the ability to discriminate. It is also noteworthy that none of the samples from the lowest rank field (field 3) were misclassified into the highest rank field (field 1) and vice versa. This indicates a strong systematic trend in the amount of trace elements in the three coalfields.

To further investigate the value of the five individual variables used in the discriminant analysis, an analysis of the canonical correlations was performed. The analysis showed that 54% of the variance in the criterion variables (the classification variables for coalfields 1, 2, and 3) was explained by the prediction variables, i.e., by the five trace elements used in the discriminant function. In addition, the standardized canonical coefficients were calculated with the results shown in Table 8. The absolute value of the canonical coefficients allows one to judge the relative importance of the variables in providing discriminatory power.

Table 8. Relative Importance of the Predictor Variables.

Trace Element	Canonical Coefficient
Cr	-1.7024
Ni	0.7946
Sr	0.6262
Zr	0.6127
Zn	0.0595

The data was then subjected to an exploratory factor analysis to investigate how many "factors" or variable clusters would be needed to explain the variation in the amount of trace elements. The SAS factor analysis program was used and the VARIMAX rotation method was specified to provide a more interpretable set of factors. Based on the eigenvalues generated, two factors were used to interpret the factor structure. The results from this two-factor analysis are provided in Table 9.

Table 9. Results of Factor Analysis and VARIMAX Rotation on the Ten-Variable Data Set.

	Factor 1 Loading	Factor 2 Loading	Communality
Ba	0.05701	0.37823*	0.15
Be	0.13436	0.56484*	0.34
Cr	0.98014*	0.08832	0.97
Cu	0.70769*	0.43172	0.69
Ni	0.58674*	-0.18352	0.38
Rb	0.60930*	0.36057	0.50
Sr	0.00834	0.48011*	0.23
V	0.77196*	0.55649*	0.91
Zn	0.19015	0.41766*	0.21
Zr	0.77147*	0.31600	0.70

In Table 9, those factor loadings marked by asterisks indicate that the variables (trace elements) are closely associated with that factor. For example, the elements Cr, Cu, Ni, Rb, V, and Zr are associated with Factor 1 while Ba, Be, Sr, V, and Zn are associated with Factor 2. The communalities indicate the percentage of the variation in each trace element explained by the two factors. It should also be noted here that Factor 1 is twice as important in explaining variation in the amount of trace elements than Factor 2. Based on the assumption that only two factors are statistically relevant, Factor 1 explains 67.7% of the variance while Factor 2 explains 32.3%.

The interpretation of these two factors is rather subjective; however, the data in Tables 6 and 9 and the sample factor scores are all of significance in this interpretation task. Both Cr and Zr have a positive correlation and a consistent trend based on rank while Sr has a consistent trend and a negative correlation with rank. Table 9 indicates that both Cr and Zr have a close association with Factor 1 while Sr has a close association with Factor 2. This result is interesting but takes on added significance when the individual sample factor scores are studied. The anthracite samples possess high scores for Factor 1 while the two groups of bituminous samples possess high scores for Factor 2. If we note further that the incidence of CWP has been correlated with rank, one can hypothesize the following:

(1) Cr and Zr (and Factor 1) are closely associated with the causes of CWP;

(2) Sr (and Factor 2) are closely associated with the prevention of CWP.

Readers should note that the data set used cannot provide proof of these hypotheses because incidence data was not also measured. They do provide some suggestion that these hypotheses may be true. Comparison of these results with conclusions provided by the authors listed in Table 4 are not very helpful.

Therefore, the hypotheses above are interesting but lacking for proof at present. As a result of these statistical correlations, however, the authors plan to give trace element analysis a prominent place in their subsequent work.

FUTURE RESEARCH

The authors have planned to perform all of their data collection in mines of the Allegheny Formation and above. The mines will probably all be located in Pennsylvania and, as much as possible, will be continuous miner operations. The anthracite mines are somewhat unique and thus may not have mining methods consistent with the other mines. The data to be collected and analyzed, the instrumentation, and the sampling plan have been planned to extract as much information as possible from each mine visit. Some of the details of the research are outlined in the following sections.

Dust Characteristics

The study of the literature and previous sampling strategies provides a good set of sampling goals. The characteristics of dust that are most desirable for measurement are those whose statistical association with CWP is known or those that have a good logical relationship with CWP. The previous research has established a strong correlation between CWP incidence and coal rank, the mass of respirable dust, and the free silica content of the respirable dust. A more tentative relationship between trace elements and CWP has been established. All of these variables will be measured for our coal samples and will be analyzed in the results. However, these variables are only a small part of the desired dust characteristics that are outlined in Table 10.

The relatively extensive list of characteristics are due primarily to two goals that we hoped to achieve in the data collection. First, it was hoped that the properties of the respirable dust can be related to the properties of the coal seam, the roof, and the floor. As a result, much of our work will be oriented toward channel sampling in order to provide this relationship. Second, the investigation of the variation of respirable coal dust properties with particle size has never been intensively undertaken. Thus, the respirable dust samples will all be segregated by the collection procedure. The properties can then be determined as a function of the size of the respirable dust particles.

The measurement of all the dust characteristics designated in Table 10 is a major effort. Thus it may not be feasible to determine all the properties specified. However, the sampling of the dust will proceed in the same manner regardless of how many of the sample properties can be obtained. The evaluation of the procedures for the analysis of the chemical elements in the coal dust has come to a tentative solution. After consideration of X-ray fluorescense techniques, the problems of utilizing the procedure seemed to be extreme. As a result, the proton-induced X-ray emission (PIXE) procedure (38) was

Table 10. Desired Dust Characteristics.

Physical Characteristics:
- Respirable dust concentration
  - Variation with location
  - Variation with time
  - Fraction of respirable dust in the total dust
- Respirable dust size distribution
  - Number vs. size distribution
  - Size vs. surface area
  - Size vs. mass or volume
  - Size distribution on each substrate
  - Shape factor
  - Variation of size distribution at various sampling locations
- Hardness of coal
  - Variation in coal bands
- Specific gravity of coal
  - Variation in coal bands
- Broken coal size distribution
  - Variation in coal bands

Chemical Characteristics:
- Chemical element concentrations
- Chemical elements as a function of size distribution
- Free silica content
- Respirable dust characteristics vs. coal seam characteristics
- Coal seam characteristics vs. roof and floor characteristics
- Variation of chemical characteristics by location
- Rank of the coal

Mineralogical Characteristics:
- Mineral content
  - Clay minerals (kaolinite, illite, mixed layer illite/montmorillonite)
  - Sulfide and sulfate minerals (pyrite, marcasite, gypsum)
  - Carbonates (calcite, dolomite, siderite)
  - Quartz
- Composition as a function of size
- Comparison between respirable and total dust
- Comparison between coal and total dust
- Comparison between respirable dust and host rock
- Variation of mineralogy at different locations

considered as a solution to providing the chemical element concentration for the dust samples. The advantages of this procedure are:

(1) the analysis can be performed on a mylar substrate from a multi-stage impactor,
(2) the analysis is non-destructive,
(3) the chemical element analysis can be performed on all elements simultaneously,
(4) the cost of the analysis is relatively inexpensive, and
(5) the analysis can be performed on rather minute sample sizes.

Because no disadvantages are presently known, the analysis of the chemical elements will most likely be performed by PIXE.

The analysis of the physical and mineralogical characteristics of the respirable dust samples collected will be directed by other personnel associated with the Generic Mineral Technology Center for Respirable Dust. Some of the procedures, particularly those associated with the physical characteristics of the dust, will utilize well-established techniques. Others will require more research before they can adequately handle the specified job. The biggest remaining problem appears to be the mineralogical analysis of the dust samples. A general procedure is available in the literature (39). However, the procedure has several disadvantages, and project personnel are not equally convinced of the merit of the method.

Sampling Plan

The sampling plan has been designed for use in a continuous miner section. The basic plan will utilize about eight sampling stations with the stations located in the section as shown in Figure 1. The prime objectives of this sampling plan are to:

(1) determine the characteristics of the respirable coal dust at numerous points in the mine layout,
(2) relate the characteristics of the coal seam, the roof, and the floor to the characteristics observed in the respirable coal dust,
(3) identify the source of the dust by mass and characteristics in the section,
(4) provide a mass balance for the dust in the working section, and
(5) establish a data set to be used in the identification of dust behavior underground that can be used in further laboratory work.

Within the layout all stations will be equipped with Sierra Model 298 eight-stage impactors powered by Dupont Model P2500A pumps. All of the stations except stations 2, 3, and 6 will be stationary. Stations 1, 2, 3, and 6 will be used primarily to detect the sources of the dust in the section while stations 4, 5, 7, and 8 will be used to determine the settling characteristics of the dust and to complete the mass balance on the section dust.

Because of the objective of relating the coal dust properties with the geologic materials, the data acquisition plan calls for channel sampling of the entire coal seam plus the taking of samples from the floor and roof. The present plan calls for three channel samples to be taken from the face previous to dust sampling. The samples will be divided into benches where visual inspection can identify different layers within the seam. This will allow analysis of the geologic materials as they occur in the sedimentary sequence so that the geologic materials can be related statistically to the respirable dust characteristics. The channel samples will also enable other investigators to relate physical characteristics of the coal to the dustiness of the mine atmosphere.

It should be noted that a variation of the sampling plan will be required for work performed in the anthracite coalfield. The mines in that region are located in steeply dipping coal seams, a condition that changes the mining layout and methods considerably. The sampling plan for anthracite operations must therefore be somewhat different than for bituminous coal mines. The same prime objectives of the sampling plan will be utilized. However, the arrangement of the sampling stations in the intake and return airways will be altered to suit the mining system.

Instrumentation

The Generic Mineral Technology Center for Respirable Dust was allocated space in September of this year for use as a respirable dust lab. Thus, the project personnel have been busy equipping the lab and testing their field equipment. The lab has recently been equipped with an aerosol test chamber by Elpram Systems, Inc. and auxiliary equipment consisting of a TSI Model 3400 fluidized bed aerosol generator, a TSI Model 3012 aerosol neutralizer, and a TSI Model 3074 air supply system. The equipment has been put through two stages of testing and is now ready for lab use. A Mettler Model M-3 microbalance has been chosen for dust mass determination and will be added to the lab equipment soon.

The field equipment for underground use consists of eight sets of Sierra Model 298 eight-stage impactors with accompanying Dupont Model P2500A constant-flow pumps. These sets of instruments have been tested in our mine

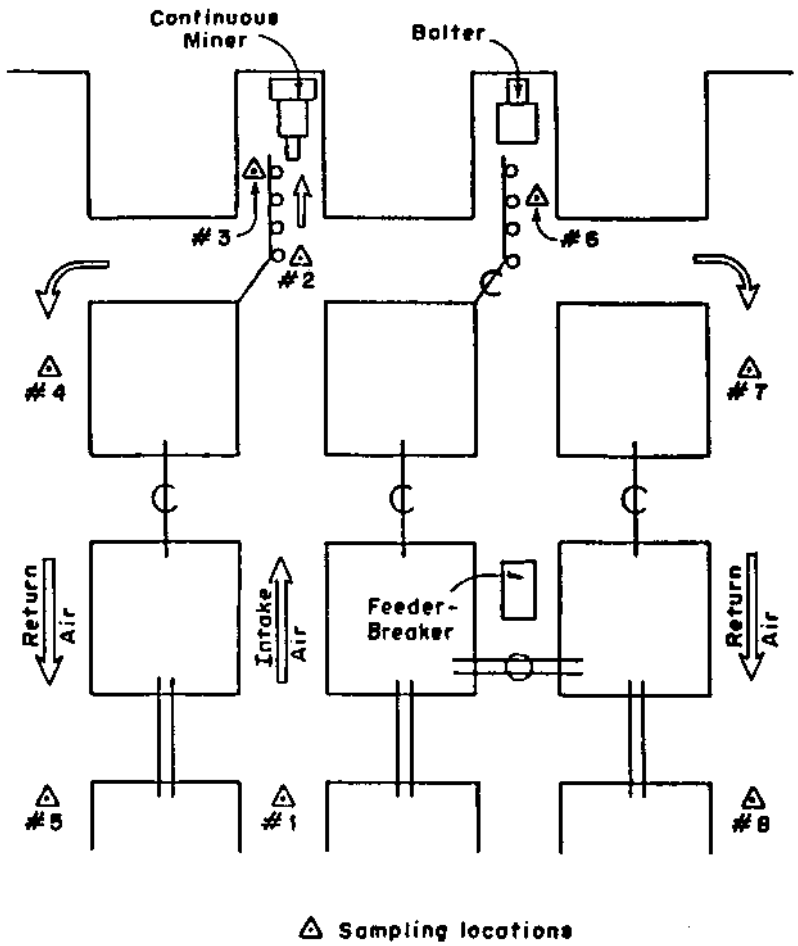

Figure 1. Generalized layout of sampling locations.

ventilation lab using mylar substrates coated with grease. Several types of grease were tested. However, a coating of petroleum jelly sprayed on the substrate with an air brush was used on the recommendation of the PIXE experts. To provide for proper consistency of grease, the grease is dissolved in toluene to achieve a 20% mixture by weight. Subsequent tests have been very successful with uniform grease and dust coatings and absence of apparent problems. Advice rendered by personnel at NIOSH in Morgantown, West Virginia, and at the University of Minnesota has been very helpful in avoiding the pitfalls of using impactors for the first time.

The final piece of instrumentation of note here is a GCA Corporation Mini-Ram real-time aerosol monitor (Model PDM-1). This equipment will be supplemented with a compatible printer and a cyclone filter. The Mini-Ram will be used for a variety of purposes including monitoring of laboratory runs and determination of proper sampling times for the field tests.

Projected Analysis of Dust Data

The major thrust of the analysis portion of this project will be an attempt to apply multivariate statistical analysis to the CWP problem. The nature of the data we are seeking may make that possible. However, several problems still must be solved before a comprehensive multivariate analysis is possible. First, the ability of obtaining good mineralogical analyses on our dust samples, which was alluded to in a previous section, must be achieved. Second, the connection between the dust characteristics in various seams and the incidence of CWP must be completed. Because the authors are not medical personnel, other data sources may be necessary. The authors are presently working on this problem.

The authors are confident that multivariate statistical analysis is the proper method to attack this problem and will yield more meaningful results than comparable univariate statistical procedures. The problem has all the attributes of a multivariate problem but only a major effort to collect the necessary data will determine the validity of this hypothesis.

CONCLUSIONS

The paper presented here represents an initial exploration of certain aspects of the respirable dust problem and its relationship to CWP. It is therefore difficult to make any broad or revolutionary conclusions at this point. However, the authors can state the following as preliminary conclusions:

(1) The literature on CWP has established a strong relationship between the incidence of CWP and the following: (a) free silica content of the respirable dust, (b) rank of the coal, and (c) mass of the respirable dust.

(2) The hypothesis that trace elements affect the incidence of CWP is an interesting possibility. However, there is no compelling reason to believe that a relationship exists at present.

(3) The relationship between the properties of the geologic materials and the characteristics of respirable dust has not been investigated to any extent and should be studied further.

(4) The properties of respirable dust as a function of the particle size have not been extensively researched. Additional research in this area would also be helpful.

(5) The previous research has established that the incidence of CWP is a multivariate problem and points the way to multivariate analysis of the problem.

All of the conclusions stated above will be considered in the future research to be conducted in the authors' project. Attempting to implement all of these conclusions will present some practical problems. However, the research philosophy appears to be sound and the attempt at a more comprehensive multivariate analysis may be very productive.

ACKNOWLEDGMENTS

The authors gratefully acknowledge that the Generic Mineral Technology Center for Respirable Dust supported this project. The Center is funded by the U.S. Bureau of Mines through the Pennsylvania Mining and Mineral Resources Research Institute at The Pennsylvania State University. The authors appreciate the support of these organizations.
Grant Number G1135142

DISCLAIMER

The opinions and conclusions expressed in this paper are those of the authors alone and do not represent the opinions of the Generic Mineral Technology Center for Respirable Dust, the Pennsylvania Mining and Mineral Resources Research Institute, or the U.S. Bureau of Mines. Citation of manufacturers' names in the paper were made for general information purposes, and do not imply endorsement of the products by the authors.

REFERENCES

1. Leiteritz, H., H. J. Einbrandt, and W. Klosterkotter, "Grain Size and Mineral Content of Lung Dust of Coal Miners Compared with Mine Dust," Inhaled Particles and Vapours II, C. N. Davies, Ed., Pergamon Press, London, 1967, pp. 381-392.

2. Jacobsen, M., S. Rae, W. H. Walton, and J. M. Rogan, "The Relation between Pneumoconiosis and Dust Exposure in British Coal Miners," Inhaled Particles III, W. H. Walton, Ed., Old Woking (Surrey): Unwin Bros., 1971, pp. 903-919.

3. McLintock, J. S., S. Rae, and M. Jacobsen, "The Attack Rate of Progressive Massive Fibrosis in British Coalminers," Inhaled Particles III, W. H. Walton, Ed., Old Woking (Surrey): Unwin Bros., 1971, pp. 933-952.

4. Naeye, R. L., J. K. Mahon, and W. S. Dellinger, "Rank of Coal and Coal Workers Pneumoconiosis," American Review of Respiratory Diseases, Vol. 103, 1971, pp. 350-355.

5. Morgan, W. K. C., "Coal Workers' Pneumoconiosis," American Industrial Hygiene Association J., Vol. 32, No. 1, January 1971, pp. 29-34.

6. Sweet, D. V., W. E. Crouse, J. V. Crable, J. R. Carlberg, and W. S. Lainhart, "The Relationship of Total Dust, Free Silica, and Trace Metal Concentrations to the Occupational Respiratory Disease of Bituminous Coal Miners," American Industrial Hygiene Association J., Vol. 35, No. 8, August 1974, pp. 479-489.

7. Carlberg, J. R., J. V. Crable, L. P. Limhaco, H. B. Norris, J. L. Holtz, P. A. Mauer, and F. R. Wolowicz, "Total Dust, Coal, Free Silica, and Trace Metal Concentrations in Bituminous Coal Miners' Lungs," American Industrial Hygiene Association J., Vol. 32, No. 7, July 1971, pp. 432-440.

8. Keenan, R. G., J. V. Crable, A. W. Smallwood, and J. R. Carlberg, "Chemical Composition of the Coal Miner's Lung," American Industrial Hygiene Association J., Vol. 32, No. 6, June 1971, pp. 392-297.

9. Crable, J. V., R. G. Keenan, R. E. Kinser, A. W. Smallwood and P. A. Mauer, "Metal and Mineral Concentrations in Lungs of Bituminous Coal Miners," American Industrial Hygiene Association J., Vol. 29, No. 2, March-April 1968, pp. 106-110.

10. Crable, J. V., R. G. Keenan, F. R. Wolowicz, M. J. Knott, J. L. Holtz, and C. H. Gorski, "The Mineral Content of Bituminous Coal Miners' Lung," American Industrial Hygiene Association J., Vol. 28, No. 1, January-February 1967, pp. 8-12.

11. Walton, W. H., J. Dodgson, G. G. Hadden, and M. Jacobsen, "The Effect of Quartz and Other Non-Coal Dusts in Coal Workers' Pneumoconiosis," Inhaled Particles IV, W. H. Walton, Ed., Oxford: Pergamon Press, 1977, pp. 669-690.

12. Reisner, M. T. R., "Results of Epidemiological Studies of Pneumoconiosis in West German Coal Mines," Inhaled Particles III, W. H. Walton, Ed., Old Woking (Surrey): Unwin Bros., 1971, pp. 921-929.

13. Hurley, J. F., J. Burns, L. Copland, J. Dodgson and M. Jacobsen, "Coal Workers' Simple Pneumoconiosis and Exposure to Dust at 10 British Coalmines," British Journal of Industrial Medicine, Vol. 39, 1982, pp. 120-127.

14. Hamilton, R. J., T. L. Ogden and J. H. Vincent, "Status of Work-Environment Aerosols in Great Britain," Ch. 1 in Aerosols in the Mining and Industrial Work Environments, Vol. 2, B. Y. H. Lin and V. A. Marple, Eds., Ann Arbor Science Publishers, Ann Arbor, Michigan, 1983, pp. 3-20.

15. Hamilton, R. J., Personal Communication, 1984.

16. Hart, P. D. A. and E. A. Aslett, "Chronic Pulmonary Disease in South Wales Coal Miners," Medical Research Council Special Report Series, No. 243, HMSO, London, 1942.

17. Hicks, D., J. W. T. Fay, J. R. Ashford, and S. Rae, The Relation between Pneumoconiosis and Environmental Conditions, National Coal Board (Pneumoconiosis Field Research), London, 1961.

18. McBride, W. W., E. Pendergrass, and J. Lieben, "Pneumoconiosis Study of Western Pennsylvania Bituminous Coal Miners," J. of Occupational Medicine, Vol. 5, No. 8, August 1963, pp. 376-388.

19. Nagelschmidt, G., "The Study of Lung Dust in Pneumoconiosis," American Industrial Hygiene Association J., Vol. 26, No. 1, January-February 1965, pp. 1-7.

20. Morgan, W. K. C., "The Prevalence of Coal Workers' Pneumoconiosis," American Review of Respiratory Diseases, Vol. 98, 1968, pp. 306-310.

21. Thakur, P. C., "Mass Distribution, Percent Yield, Non-settling Size, and Aerodynamic Shape Factor of Respirable Coal Dust Particles," Unpublished M.S. Thesis, The Pennsylvania State University, University Park, Pennsylvania, 1971.

22. Dodgson, J., G. G. Hadden, C. O. Jones, and W. H. Walton, "Characteristics of Airborne Dust in British Coal Mines," Inhaled Particles III, W. H. Walton, Ed., Old Woking (Surrey): Unwin Bros., 1971, pp. 757-782.

23. Reisner, M. T. R. and K. Robock, "Results of Epidemiological, Mineralogical and Cytotoxicological Studies on the Pathogenicity of Coal Mine Dusts," Inhaled Particles IV, W. H. Walton, Ed., Oxford, Pergamon Press, 1977, pp. 703-716.

24. Bennett, J. G., J. A. Dick, Y. S. Kaplan, P. A. Shand, D. H. Shennan, D. J. Thomas, and J. S. Washington, "The Relationship between Coal Rank and the Prevalence of Pneumoconiosis," British J. of Industrial Medicine, Vol. 36, 1979, pp. 206-210.

25. Dessauer, P., E. J. Baier, G. M. Crawford, and J. A. Beatty, "Development of Patterns of Coal Workers' Pneumoconiosis in Pennsylvania and its Association with Respiratory Impairment," Annals of the New York Academy of Science, 1972, pp. 220-251.

26. Jacobsen, M., S. Rae, W. H. Walton, and J. M. Rogan, "New Dust Standards for British Coal Mines," Nature, Vol. 227, No. 5257, August 1970, pp. 445-447.

27. Morgan, W. K. C., D. B. Burgess, G. Jacobson, R. J. O'Brien, E. Pendergrass, R. B. Reger and E. P. Schoub, "The Prevalence of Coal Workers' Pneumoconiosis in U.S. Coal Miners," Archives of Environmental Health, Vol. 27, No. 4, October 1973, pp. 221-226.

28. Ogden, T. L., and A. M. Rickmann, "Characterization of the Volume Size Distribution of Respirable Coal-Mine Dust Samples by Coulter Counter," Annals of Occupational Hygiene, Vol. 20, 1977, pp. 257-270.

29. Sorenson, J. J., T. E. Kober and H. G. Petering, "The Concentration of Cd, Cu, Fe, Ni, Pb, and Zn in Bituminous Coals from Mines with Differing Incidences of Coal Workers' Pneumoconiosis," American Industrial Hygiene Association J., Vol. 35, No. 2, February 1974, pp. 93-98.

30. Lieben, J., E. Pendergrass, and W. W. McBride, "Pneumoconiosis Study in Central Pennsylvania Coal Mines, Medical Phase," J. of Occupational Medicine, Vol. 3, No. 11, November 1961, pp. 493-506.

31. Baier, E. J. and R. Diakun, "Environmental Dust Study of Anthracite Coal Mines of Eastern Pennsylvania," J. of Occupational Medicine, Vol. 5, No. 8, August 1963, pp. 396-403.

32. McBride, W. W., E. Pendergrass, and J. Lieben, "Pneumoconiosis Study of Western Pennsylvania Bituminous Coal Miners," Journal of Occupational Medicine, Vol. 5, No. 8, August 1963, pp. 376-388.

33. Baier, E. J. and R. Diakun, "Pneumoconiosis Study in Central Pennsylvania Coal Mines, Environmental Phase," J. of Occupational Medicine, Vol. 3, No. 11, November 1961, pp. 507-521.

34. McBride, W. W., E. Pendergrass, and J. Lieben, "Pneumoconiosis of Pennsylvania Anthracite Miners," J. of Occupational Medicine, Vol. 8, No. 7, July 1966, pp. 365-376.

35. Tokuhata, G. K., P. Dessauer, E. Pendergrass, T. Hartman, E. Digon, and W. Miller, "Pneumoconiosis among Anthracite Coal Miners in Pennsylvania," American J. of Public Health, Vol. 60, No. 3, March 1970, pp. 441-451.

36. Anonymous, "The Penn State Coal Sample Bank," Coal Research Section, The Pennsylvania State University, University Park, Pennsylvania.

37. Anonymous, SAS User's Guide, SAS Institute Inc., Cary, North Carolina, 1982.

38. Johansson, S. A. E. and T. B. Johansson, "Analytical Application of Proton-Induced X-Ray Emission," Nuclear Instruments and Methods, North-Holland Publishing Co., 1976, pp. 473-516.

39. Lee, R. J., "Electron Optical Identification of Particulates," Chap. 16 in Electron Microscopy and X-ray Applications (Russel and Hutchings, Eds.), Ann Arbor Science Publishers, Ann Arbor, Michigan, 1978, pp. 175-188.

THE RELATIONSHIP BETWEEN THE HARDGROVE GRINDABILITY INDEX AND THE POTENTIAL FOR RESPIRABLE DUST GENERATION

Michael P. Moore
Graduate Assistant
and
Christopher J. Bise
Assistant Professor of Mining Engineering

Department of Mineral Engineering
The Pennsylvania State University
University Park, PA 16802

INTRODUCTION

Over the past twenty years, there have been numerous studies which have attempted to correlate the prevalence of Coal Workers' Pneumoconiosis (CWP) with different characteristics of the coal seam. Some investigators have tried to find a relationship, or the lack of a relationship, between the rank of coal seams and the incidence of CWP. Others have attempted to show that there is a positive correlation between the mean mass of respirable dust in the mine atmosphere and the prevalence of CWP. Still others have tried to determine the influence of the quartz content of respirable dust on the incidence of CWP. Unfortunately, many of these different investigations have conflicting conclusions.

PREVIOUS AREAS OF RESEARCH

One area of research with conflicting conclusions deals with the relationship between the rank of the coal and the incidence of CWP. For example, an investigation conducted in Pennsylvania and West Virginia coal mines concluded that the prevalence of CWP increases with an increase in coal rank (1). A study in Great Britain also observed a close relationship between the rank of coal and the prevalence of CWP (2). However, another study involving 312 Appalachian coal miners concluded that the association between coal rank and CWP might be fortuitous and that other factors may be more important (3). In addition, an investigation involving 2,600 miners during a period of twenty years in Great Britain established that there is only a weak correlation between the prevalence of CWP and the rank of the coal (4). Consequently, it appears that there is still uncertainty as to whether or not the rank of the coal seam has an influence on the development of CWP.

Another area of investigation concerns the relationship between the mean mass of respirable dust present in the mine atmosphere and the prevalence of CWP. A study involving 4,122 miners over a period of ten years in Great Britain noted a high correlation between the mean mass of respirable dust and the incidence of CWP (5). Another investigation involving 3,154 British face workers concluded that the overall mass of respirable dust is the factor most closely related to the ten-year attack rate of CWP (6). However, a study conducted in thirty-one mines in the United States concluded that it is doubtful that the quantity of respirable dust alone is responsible for the difference in the prevalence of CWP (7). Even though there are conflicting conclusions, there are many more investigators who confirm, rather than deny, the relationship between the mean mass of respirable dust and the development of CWP.

The third subject of investigation is the role of quartz in the incidence of CWP. For example, two studies in Great Britain concluded that the quartz content in coal mine dust has no relationship to the prevalence of CWP (8,9). But a study involving 312 Appalachian coal miners revealed that the level of exposure to free silica plays an important role in the development of CWP (10). Once again, the conclusions reached by different researchers are conflicting.

Probably the most important factor in the discrepancy among the studies is the variability among different coal mines. A mine operating in an inherently "dusty" seam may have a low concentration of respirable dust while a mine operating in a less dusty seam may have a high concentration of respirable dust. This discrepancy is a result of variables such as the effectiveness of ventilation or the efficiency of the water sprays. Consequently, it is very difficult to compare the dustiness of different coal seams by in-mine measurements of the respirable dust concentration. A laboratory test would more accurately characterize a coal seam according to its respirable dust production.

BASIS OF LABORATORY PROCEDURE

One way to quantify the respirable dust generation potential of a coal seam is to pulverize a sample of the coal and then to determine the amount of respirable dust that is produced. In this manner, each coal seam can be ranked according to its respirable dust

Presented at the Proc. Coal Mine Dust Conference, Morgantown, W. Va., October 8-10, 1984.

generation. Furthermore, this test would determine if the coals in one geographic region are dustier than the coals in another region.

The aforementioned procedure for determining respirable dust potential is very similar to the procedure for determining a coal's Hardgrove Grindability Index (HGI).

DESCRIPTION OF HGI

The Hardgrove Grindability Method is used to determine the relative grindability or ease of pulverization of a coal in comparison with a coal chosen as the standard; the standard coal is 100 on the HGI scale (11). Briefly, the procedure consists of grinding a prepared sample in a miniature pulverizer for three minutes and then determining the change in size consist by sieving.

The HGI was chosen as the basis of the testing procedure to determine respirable dust potential for several reasons. The grindability of coal is a function of such properties as fracture, tenacity, strength and hardness. These properties may also influence the amount of respirable dust that a coal will produce when cut. Consequently, it was felt that the HGI may be a good starting point for this investigation. Furthermore, the HGI is used to estimate the capacity of mills used to grind coals to the fineness required for pulverized-coal furnaces; it is a technique that is already known and accepted in industry (12). Finally, since it is not known whether or not rank influences CWP, it was felt that the HGI test could establish some trends in the relationship between coal rank and respirable dust potential.

In the HGI procedure, a quantity of Number 4 sieve-size (4.75 mm) coal is riffled to about 1000-gram portions and air-dried from twelve to forty-eight hours. The coal is then stage crushed in a plate mill and sieved in 200-gram lots for two minutes on a mechanical sieving machine. The sieves consist of a Number-16 sieve on top of a Number-30 sieve. The +16-mesh material is returned to the plate mill, while the -30-mesh material is discarded. After all the coal has been crushed, the 16x30-mesh fraction is divided into 120-gram lots by riffling. As the final step in preparation, the 120 grams of 16x30-mesh coal is sieved on a Number-30 sieve for five minutes to remove any -30-mesh material that may be adhering to the larger particles. Following this step, 50 ± 0.01 grams of the 16x30-mesh coal are placed in the ball-and-race mill. The machine is operated for 60 ± 0.25 revolutions (13). After the mill has stopped, the crushed sample is removed and placed on a set of nested sieves on top of a catch pan; the top sieve is 200 mesh and the bottom sieve is 400 mesh. The addition of a 400-mesh screen is the only way that this laboratory procedure deviates from the Hardgrove Grindability Test. A cover is placed on top of the 200-mesh screen and the sample is shaken for ten minutes on the mechanical shaker. After ten minutes, the undersides of the screens are swept with a soft-bristled brush; this prevents the particles from lodging in the screens. This process is repeated three more times but with five rather than ten-minute shaking periods.

Upon the completion of sieving, the coal retained on the 200-mesh screen, the 400-mesh screen, and the catch pan is weighed to the nearest 0.01 gram. The weight of material retained on the 200-mesh sieve determines the HGI. The weight of the -400 mesh material is needed to calculate the quantity of respirable dust. The weight of the 200x400 material, along with the weight of the +200 and the -400 mesh material, is used to determine the amount of coal that was lost from the original 50 ± 0.01 grams. The HGI is determined by subtracting the weight of the coal remaining on the 200-mesh screen from the test sample weight (50 ± 0.01 grams) then multiplying this number by 6.93 and adding 13.6 (14).

SOURCE OF COAL SAMPLES

To date, a total of twenty-five samples have been subjected to the HGI Test. The source of the coal seam samples is The Penn State Coal Data Base, which contains over 1300 coal samples representing every known seam in the United States. The coal is handled according to prescribed procedures from the time it is first collected to the time it is sealed in airtight containers. Consequently, a coal sample can be stored almost indefinitely with no oxidation effects.

In addition to the raw coal samples, the data base possesses a computerized compilation of a broad spectrum of various analytical data. Included in this data is information about the coal's geologic and geographic location, seam strata, petrographic analysis, physical properties, and elemental analysis, as well as other information. The data are stored in a computer at the University Computation Center (15).

PARTICLE SIZE ANALYSIS

A Microtrac Particle Size Analyzer is used to determine the size distribution of the pulverized samples. The Microtrac utilizes low-angle, forward-scattering light from a laser beam. The laser beam is projected through a transparent cell containing a stream of moving particles suspended in water. The light, upon striking the moving particles, is scattered in a definite direction depending upon the particle's size. Small particles cause the light to scatter at large angles while large particles cause the light to scatter at small angles. A rotating optical filter contains thirteen windows which are located at different radial distances from the center of the filter. The amount of light passing through each window is measured by a photodetector. Since each window receives light from a narrow size range of particles, the amount of light measured through a window indicates the volume of particles of that size range in the sample.

The size of particles passing through one window compared to the size of particles passing through the next smaller window is in a square-root-of-two ratio. The measurement range is from 1.9 to 176 microns.

The printed output displays a "percent less than" graph, a relative volume graph, and a histogram of "percent between the listed and the next smaller size."

A subsample, weighing approximately 1.5 grams, is taken from each -400 mesh sample and thoroughly mixed in a dispersant before being analyzed in the Microtrac. The sample weight of 1.5 grams is used in accordance with the Microtrac operator's manual which recommends a sample weight in grams equal to the specific gravity of the material (16). The purpose of the dispersant is to prevent the crushed material from agglomerating in the analyzer. Each subsample is run through the Microtrac at least two times. The results of the two runs are then compared to determine the consistency of the size distributions.

QUANTITY OF RESPIRABLE DUST PRODUCED

The Microtrac data printout, as mentioned earlier, contains a graph of cumulative percent finer versus size. Since the weight of the -400 mesh sample is already known, the actual quantity of respirable dust can be calculated by multiplying the percentage less than 5.5 microns by the weight of the -400 mesh sample.

In addition to the amount of material less than 5.5 microns, the amount of material less than 7.8 and 11 microns is also calculated. The reason for doing this is to minimize the inherent error in the indicated size distribution caused by the -1.9 micron material. Since the Microtrac cannot detect particles smaller than 1.9 microns, it will indicate that two samples with different size distributions contain the same quantity of -2.8 micron material. By including the -7.8 and the -11 micron material, a better estimate of the true amount of respirable dust is given.

After determining the amount of material less than 5.5, 7.8, and 11 microns for each sample, the coal seams can be ranked according to the amount of respirable dust found in each of the three sizes. The accompanying charts indicate the relative order of the various coal seams that were tested.

RESULTS TO DATE

Figure 1 is a plot of respirable dust (< 5.5 microns) versus HGI for seven Pennsylvania coal seams. Although twenty-five seams were tested, only seven are shown for the sake of clarity. These seams were chosen since they represent a wide range of Hardgrove values. The Wharton seam is at the low end of the scale. It is an anthracite which has an HGI of 31.5 and produces 0.14 grams of respirable dust from the original 50.0 grams. At the high end of the scale is the Upper Freeport coal seam. It is a medium volatile bituminous coal which has an HGI of 115.0 and produces 1.10 grams of respirable dust. The other seams, the Lower Kittanning, the Clarion, the Bloss, the Pittsburgh, and the Lower Freeport fall between these values.

The next two charts, coal dust (< 7.8 microns) versus HGI and coal dust (< 11 microns) versus HGI, show the same trend (see Figures 2 and 3). The only difference is that as the cutoff point increases the quantity produced also increases.

A linear regression was applied to quantify the relationship between HGI and the amount of respirable dust produced by the plate mill. The following equation was developed by the method of least squares:

$$D_{5.5} = 0.012(HGI) - 0.287$$

where: D = the amount of -5.5 micron dust in grams.

The correlation coefficient, r, for this linear equation is 0.86. This indicates that there is a close relationship between a coal's HGI and the amount of -5.5 micron material it will generate when pulverized in a plate mill.

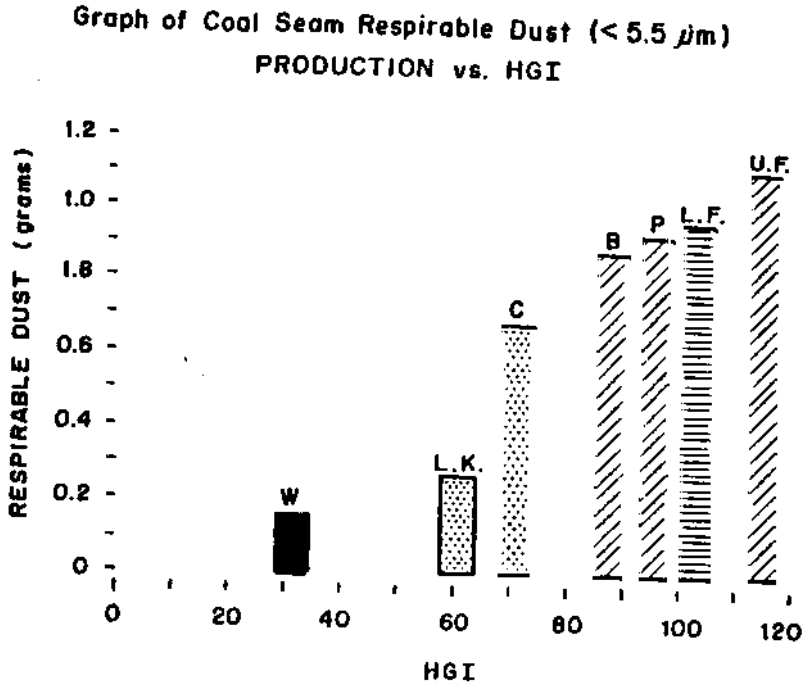

Figure 1

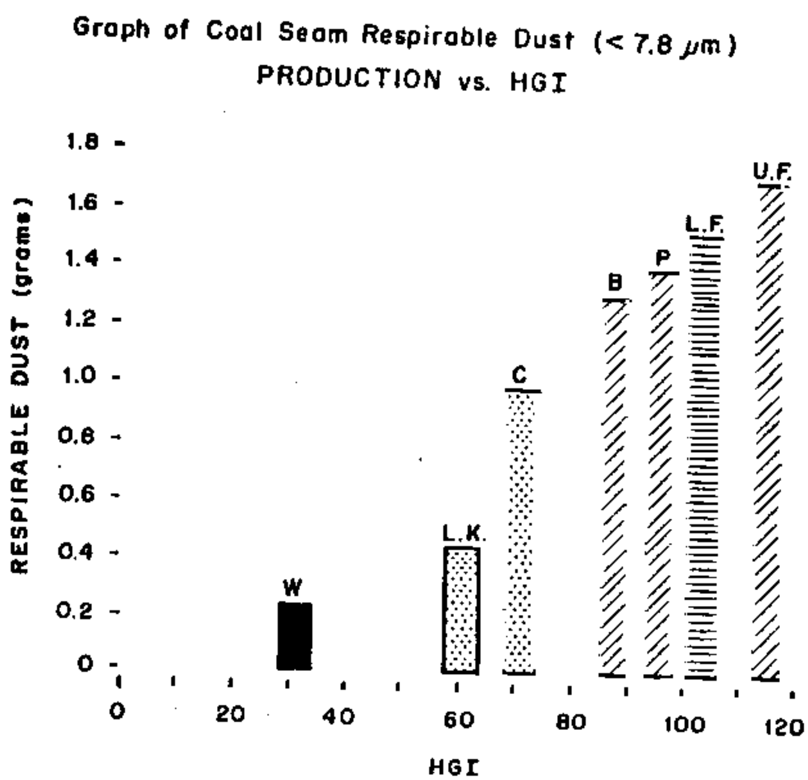

Figure 2

Graph of Coal Seam Respirable Dust (< 11 μm)
PRODUCTION vs. HGI

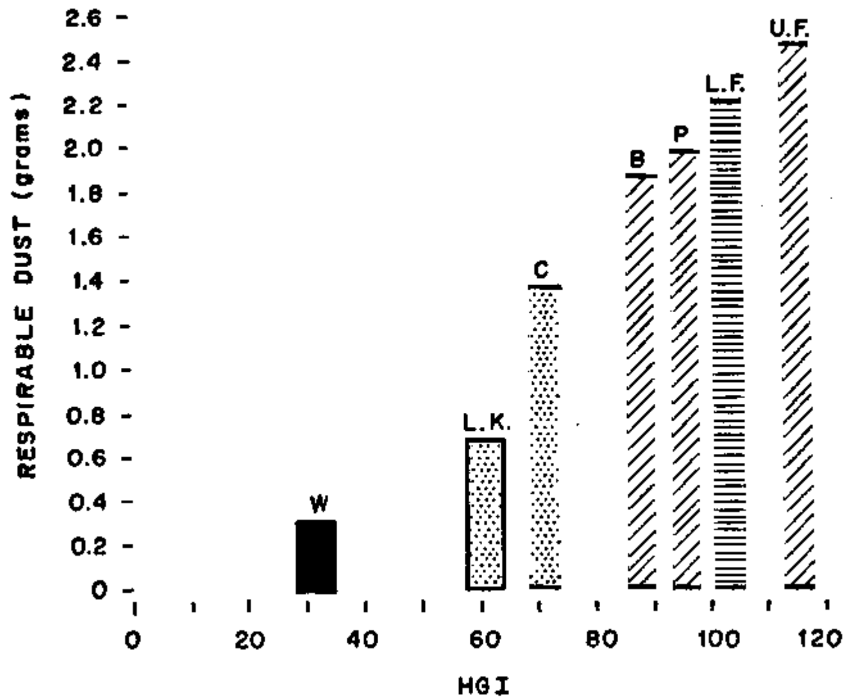

Figure 3

Similarly, a linear regression was applied to determine the relationship between HGI and the quantity of -7.8 and -11 micron dust produced, respectively.

$$D_{7.8} = 0.020(HGI) - 0.594$$

where: D = the amount of -7.8 micron material in grams.
The correlation coefficient, r, is 0.90.

$$D_{11} = 0.028(HGI) - 0.808$$

where: D = the amount of -11 micron material in grams.
The correlation coefficient, r, is 0.92.

SUMMARY

Based on the coal samples that have been tested thus far, HGI is a good predictor of the quantity of respirable dust that will be generated in a plate mill. The Wharton seam, an anthracite, produced the least amount of respirable dust while the Upper Freeport, a medium volatile bituminous, produced the most. It, however, cannot be generalized that a mine in an anthracite seam will be less dusty than a mine in a bituminous seam since there are many other variables to consider. Thus, the fact that anthracite mines appear to be more conducive to black lung development than bituminous mines may be attributed more to the methods of mining than to the dustiness of the seams.

ACKNOWLEDGMENTS

The authors gratefully acknowledge that the Generic Mineral Technology Center for Respirable Dust supported this project. The Center is funded by the U.S. Bureau of Mines through the Pennsylvania Mining and Mineral Resources Research Institute at The Pennsylvania State University. The authors appreciate the support of these organizations.
Grant Number G1135142

DISCLAIMER

The opinions and conclusions expressed in this paper are those of the authors alone and do not represent the opinions of the Generic Mineral Technology Center for Respirable Dust, the Pennsylvania

Mining and Mineral Resources Research Institute, or the U.S. Bureau of Mines. Citation of manufacturers' names in the paper were made for general information purposes and do not imply endorsement of the products by the authors.

REFERENCES

1. W. K. C. Morgan, "The Prevalence of Coal Workers' Pneumoconiosis," American Review of Respiratory Diseases, 1968, pp. 306-310.
2. J. G. Bennett, et al., "The Relationship Between Coal Rank and the Prevalence of Pneumoconiosis," British Journal of Industrial Medicine, 1979, pp. 206-210.
3. R. L. Naeye, et al., "Rank of Coal and Coal Workers' Pneumoconiosis," American Review of Respiratory Diseases, 1971, pp. 350-355.
4. J. F. Hurley, et al., "Coal Workers' Simple Pneumoconiosis and Exposure to Dust at 10 British Coal Mines," British Journal of Industrial Medicine, 1982, pp. 120-127.
5. M. Jacobson, et al., "New Dust Standards for British Coal Mines," Nature, Vol. 227, 1970, pp. 445-447.
6. W. H. Walton, et al., "The Effect of Quartz and Other Non-coal Dusts in Coal Workers' Pneumoconiosis," Inhaled Particles IV, 1977, pp. 669-690.
7. W. K. C. Morgan, et al., "The Prevalence of Coal Workers' Pneumoconiosis in U.S. Coal Miners," Archives of Environmental Health, October 1973, pp. 221-226.
8. M. Jacobson, et al., "The Relationship Between Pneumoconiosis and Dust Exposure in British Coal Mines," Inhaled Particles III, 1971, pp. 903-919.
9. J. S. McLintock, et al., "The Attack Rate of Progressive Massive Fibrosis in British Coal Mines," Inhaled Particles III, 1971, pp. 933-952.
10. Naeye, pp. 350-355.
11. James D. McClung and M. R. Geer, "Properties of Coal Impurities," Coal Preparation, Ed. J. W. Leonard, The American Institute of Mining, Metallurgical and Petroleum Engineers, Inc., 1979, pp. 1-34.
12. M. P. Corriveau and Norman Schapiro, "Projecting Data from Samples," Coal Preparation, Ed. J. W. Leonard, The American Institute of Mining, Metallurgical and Petroleum Engineers, Inc., 1979, pp. 1-46.
13. Annual Book of ASTM Standards, Part 26, Grindability of Coal by the Hardgrove Machine Method, ASTM-D409, 1978.
14. L. G. Austin and J. D. McClung, "Size Reduction of Coal," Coal Preparation, Ed. J. W. Leonard, The American Institute of Mining, Metallurgical and Petroleum Engineers, Inc., 1979, pp. 7-26.
15. The Penn State Coal Data Base: Management, Operations, and Content, pp. 2-10.
16. Operator's Manual: Microtrac Particle Size Analyzer, pp. 5-8.

CORRELATION OF RESPIRABLE DUST MASS CONCENTRATION WITH WORKER POSITIONS

R. L. Grayson and S. S. Peng
Department of Mining Engineering
College of Mineral and Energy Resources
West Virginia University
Morgantown, WV 26506

INTRODUCTION

Research has been conducted during the past year on a study to correlate respirable coal mine dust characteristics with worker positions and coal seams. The first characteristic of respirable coal mine dust which has been addressed in the correlation study is respirable dust mass concentration. In fulfillment of this objective, two mines operating in different coal seams have been selected for respirable dust mass sampling on both longwall panels and continuous mining sections. At present, sampling has been completed on the longwall panel operating in the first mine, and one half of the planned sampling has been accomplished on the continuous mining section.

The first mine sampled is operating in the Pittsburgh coal seam. The average mining height is approximately 78" with an average of 8" of bottom shale being mined. The mine is primarily a longwall mine, and continuous mining machines are used to support the longwall.

DESCRIPTION OF THE LONGWALL PANEL

Figure 1 shows the layout of the longwall panel which was sampled. Intake air is coursed via the track heading up to the headgate area. The air splits at the headgate. Approximately 20,000-30,000 cubic feet of air per minute (CFM) is used to ventilate the longwall face and about 5,000-10,000 CFM is routed down the belt entry. Substantial leakage across the gob was noted during the sampling period. An average of 1800 CFM per 100 feet of face leaked through the shields into the gob from #1 shield to #112 shield. A substantial amount of leakage also occurred between the #1 shield and the solid rib of the headgate development panel. The path of the air used to ventilate the panel is shown with arrows in Figure 1. Direction of air flow was opposite to the coal moving direction on the armored face conveyor.

A double-drum ranging shearer is used on the face to cut a 30-inch web of coal. Normal practice is to cut from the tailgate to headgate with the leading drum raised and the tail drum lowered for cutting bottom. After reaching the headgate, the shearer is reversed and both drums are lowered for a clean-up pass. The last 40 feet of face on the tailgate is cut on the clean-up pass.

The shearer is equipped with 2 banks of 4 water sprays each and 2 large sprays on the headgate end and 1 bank of 4 sprays on the tailgate end. Additionally, sprays are located above bits on the cutting drums. Actual cutting speed was approximately 14-18 feet per minute, depending on conditions.

The cross sectional area for air flow on the face was approximately 60 square feet before a pass was mined and 80 square feet after a pass was mined but before the shields were advanced. The cross sectional area at the shearer was about 35 square feet.

The condition of both the tailgate and headgate of the panel was good with no signs of significant roof problems. The roof conditions along the face during the sampling period were variable. At times, as much as 3 feet of drawslate fell from the roof for a span of as much as 40 shields. Generally, however, relatively local areas of falling roof were encountered, usually limited to a 10-20 shield span when appearing.

SAMPLING PROCEDURES ON THE LONGWALL PANEL

Ten days were spent gathering respirable dust samples on the longwall panel. Mine Safety Appliance (MSA) sampling units equipped with 10-mm nylon cyclones, preweighed MSA PVC filters, and constant-flow DuPont pumps were used to obtain the samples. The pumps were calibrated at a 2 liters-per-minute flow rate. The 10-mm cyclone was selected for classifying total dust into the desired respirable fraction in order to obtain "legally defined" respirable dust samples for detailed physical characterization.

Each day, nearly a full shift was used to gather samples, thereby emulating the average shift mass concentrations required for compliance sampling by operators. The mass concentrations determined by recording the sampling time and net weight of the dust collected were then multiplied by 1.38 to obtain their equivalent MRE mass

Presented at the Proc. Coal Mine Dust Conference, Morgantown, W. Va., October 8-10, 1984.

concentrations which are used by MSHA for enforcement of dust standards.

Sampling locations on the longwall panel are numbered 1 through 9 on Figure 1. Sampling locations 1 through 8 were at fixed points on the panel. Sampling location 1 was in the intake air, number 2 was at #1 shield in the headgate entry, number 3 was at #55 shield, number 4 was at #75 shield, and number 5 was located at #112 shield at the tailgate.

Sampling locations 6 through 8 were on the shearer with number 6 fixed on the headgate end of the shearer by the lead operator, number 7 fixed at mid-shearer, and number 8 fixed on the tailgate end of the shearer by the tail operator. Sampling location number 9 was on one of the shield movers, located in his breathing zone.

Sampling pumps which were located in fixed positions were oriented such that the cyclone inlet flow direction was perpendicular to the panel air flow direction. This orientation was maintained throughout the sampling period. Sampling units were located at a height of approximately 5.5 feet from the ground at shields and at a height of approximately 5 feet from the ground at the shearer.

During the sampling period, observations and/or measurements regarding water sprays, cutting speed, air-dust flow patterns, roof conditions, mean air velocity and shift cutting time were recorded. Water sprays were maintained consistently throughout the sampling period. It should be noted, however, that the two large sprays and one bank of 4 sprays on the headgate end of the shearer were oriented such that water flow from the sprays was directed opposite to air flow on the panel. This caused a zone where dust was pushed over toward the shearer operator. Bits on the shearer were changed regularly.

RESPIRABLE DUST MASS CONCENTRATION RESULTS ON THE LONGWALL PANEL

Average, MRE-equivalent, respirable-dust, mass concentrations in milligrams/cubic meter obtained for sampling locations are also shown in Figure 1. At fixed sampling locations on shields, it is seen that compliance with the 2 mg/cubic meter general dust standard is maintained until some point between #75 shield and the tailgate. It is apparent that a person who would spend a full shift at the tailgate would receive a dose of respirable dust in excess of 2 mg/cubic meter.

A person who would spend a full shift working at any location at the shearer would be sampled as "out of compliance" regularly. However, the work practice at this mine was to alternate workers at the shearer. A particular lead shearer operator was personally sampled on one occasion and a 0.68 mg/cubic meter mass concentration was obtained for a full shift. He was relieved throughout the shift. Similarly, shield movers were found to average only 0.87 mg/cubic meter per shift sampled, but they were not on the panel during the cutting cycle, generally. Whenever the shearer approached the headgate during the cutting cycle, the shield movers were summoned from the dinner area to begin moving shields on the clean-up pass.

The very high mass concentrations obtained at the shearer sampling locations were due primarily to the reduced cross sectional area for air flow and to the effect of the "boiling" over of dust caused by misdirected water sprays.

PREDICTION OF RESPIRABLE DUST CONCENTRATIONS FOR SPECIFIC LOCATIONS ON THE LONGWALL PANEL

A linear regression analysis was performed on the sampling data for the longwall panel to explore the possibility of predicting the respirable dust mass concentration at specific locations. Using "location on face" as a single independent variable (V1), respirable dust mass concentration (C_m) in mg/m^3 can be predicted as

$$C_m = -0.2835 + 0.8106\ V1$$

where

Coefficient of determination, $r^2 = 0.6486$
Coefficient of correlation, $r = 0.8054$
Standard error of estimate, SE = 1.2650.

Only data for locations ranging from the headgate to the tailgate were used for building the model. The lowest average value for C_m would then be 0.53 mg/m^3 for V1 = 1 (headgate location). This matches exactly with actual results as seen in Figure 1.

The ranking of variable V1 (location on face) is:

1 = headgate
2 = #55 shield
3 = #75 shield
4 = tailgate
5 = tail shearer operator
6 = mid-shearer
7 = lead shearer operator.

Good correlation was achieved using the simple, single variable model. A large amount (65%) of the total variation of mass concentrations could be explained by the fitted model. However, an attempt to include some other cause system variables was made, hopefully to improve the model's predictive capability.

Since water spray performance, drum rotation speed, and cutting speed appeared consistent throughout the sampling period, the independent variables selected to be used in the model were:

- V1 - sampling location on face (ranked 1-7)
- V2 - condition of roof on panel (ranked 1-10)
- V3 - method of cutting (ranked 1-5)
- V4 - cutting time during shift (minutes)
- V5 - cross-sectional area at sampling location (square feet)
- V6 - air velocity at sampling location (fpm).

A multiple, linear regression analysis of the data resulted in the model:

$$C_m = 1.0047 + 1.0263V1 + 0.1757V2 - 0.2234V3 - 0.0037V4 + 0.0059V5 - 0.0074V6$$

with

$r^2 = 0.7801$
$r = 0.8832$
$SE = 1.0515$
$f(6,48) = 28.38 >> F_{0.01}(6,48) = 3.22$

This is an adequate model for predicting the respirable mass concentration for a worker location, assuming he spends the entire shift at that location. Scaling of values for variables is out of line somewhat and the relative significance of different coefficients of variables to each other is somewhat obscured. Table 1 shows the results of using the model to predict mass concentrations for various locations under average conditions. An average percentage difference of 9.1% is observed. However, the standard error of the estimate is closer to 35% of the average panel value (2.97 mg/m^3). It is seen that the model does a better job predicting the higher mass concentrations than the lower ones.

Further regression analysis, stepwise, does not yield a better model. The standard error of estimate remains high (above 1.0) and the coefficient of multiple correlation remains high (> 0.85). Thus, some variables of significance may be missing or, more likely, the variability of the data itself is high. (Personal sampling under similar conditions has been reported to introduce about 20% error).

DESCRIPTION OF THE CONTINUOUS MINING SECTION

Figure 2 shows the layout of the continuous mining section which has been partially sampled. Intake air is supplied to the right side of the section. The air is then split with about 5000 CFM sent down the belt heading and the remaining 25,000 to 30,000 CFM directed across the faces to the return heading on the left side. A check in the second heading from the right is normally removed during a production shift to provide a second tram route for a shuttle car.

A continuous miner with a 13.5-foot wide drum is used to extract coal from the face in a single pass. The cut is five feet deep and 6.5 feet high. The continuous miner dumps the coal on the floor and a loading machine loads it into alternating shuttle cars. The shuttle cars tram an average distance of 400 feet to a feeder where their payload is discharged to the conveyor belt system. After a 5-foot pass is mined, 2 bolts are installed at the face with the bolting mechanism provided on the continuous miner. An auxiliary fan with tubing is used to ventilate the face. One hundred feet are driven in a heading before a move is made to the next face. The continuous miner and the fan are moved to the next heading to the right. After all four headings are driven up 100 feet, then the crosscut is connected from right to left across the section.

Mining conditions throughout the section were good. The places were dry and well rock dusted at all times. No problems with methane gas emission were realized.

SAMPLING PROCEDURES ON THE CONTINUOUS MINING SECTION

It is intended to spend ten days gathering respirable dust samples on this section. At present, only five days have been completed. Sampling procedures were the same as on the longwall panel except for locations at which samples were taken.

Figure 2 shows the locations where samples were taken over a nearly full shift, numbered 1 through 7. Sampling locations 1 through 3, 6 and 7 were at fixed points. Each MSA sampling unit was oriented perpendicular to the direction of air flow and hung at a point approximately 6 inches from the roof. Thus, the height of each apparatus was about 6 feet from the floor. The sampling units at locations 4 and 5 were hung on the continuous mining machine and loading machine, respectively. The unit on the continuous miner was at a height of 4.5 feet from the floor, and it was maintained on the outby side of the ventilation tubing at all times. The unit on the loading machine was at a height of 5.5 feet from the floor.

RESPIRABLE MASS CONCENTRATION RESULTS ON THE CONTINUOUS SECTION

Average, MRE-equivalent, respirable-dust, mass concentrations in mg/cubic meter obtained for sampling locations are also shown in Figure 2. It is apparent that compliance with the 2.0 mg/cubic meter dust standard is maintained throughout the areas of the section where men would normally work. The samples obtained at the auxiliary fan and in the return 150 feet outby the fan were obtained to see the potential hazard for a person exposed at that location (say, plastering a stopping on the back side).

The results obtained on the continuous mining section are not surprising. In fact, the industry is aware of the good success for controlling respirable dust mass concentrations on continuous mining sections. The problems of noncompliance which now result are primarily due to reduced standards imposed whenever high levels of quartz are found in samples. The results in Figure 2 indicate that if the level of quartz reaches 6.25% on this section, then the continuous miner operator/roof bolter locations would be out of compliance. Going one step farther, the next location out of compliance would be the loading machine operator if the level of quartz were to reach 10.10% (very unlikely).

ACKNOWLEDGEMENTS

This research has been supported by the Department of the Interior's Mineral Institute program administered by the Bureau of Mines through the Generic Mineral Technology Center for Respirable Dust under grant number G1135142.

Table 1. Predicted vs. Average Mass Concentration for Various Locations

Variable \ Location	Head Gate	#75 Shield	Tail Gate	Tail Shearer Oper.	Mid-Shearer	Lead Shearer Oper.
V1 (Rank)	1	3	4	5	6	7
V2 (Rank)	5	5	5	5	5	5
V3 (Rank)	3	3	3	3	3	3
V4 (Min.)	160	160	160	160	160	160
V5 (ft^2)	100	70	70	35	35	35
V6 (fpm)	220	260	240	375	375	375
Predicted C_m	0.61	2.19	3.36	3.18	4.21	5.24
Average C_m	0.53	1.75	3.73	3.54	4.55	5.42
% Difference from Avg. C_m	15%	25%	9.9%	10.2%	7.5%	3.3%

RESPIRABLE DUST MASS CONCENTRATION

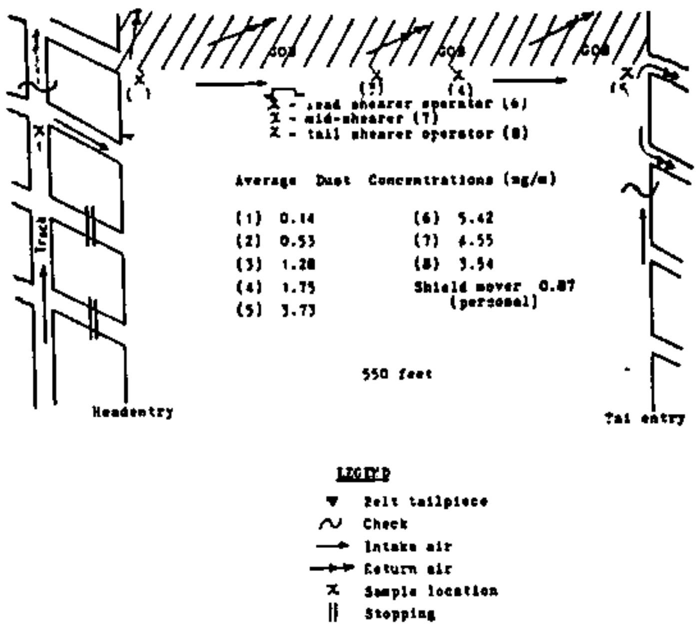

Figure 1. Sample locations and results on the longwall panel.

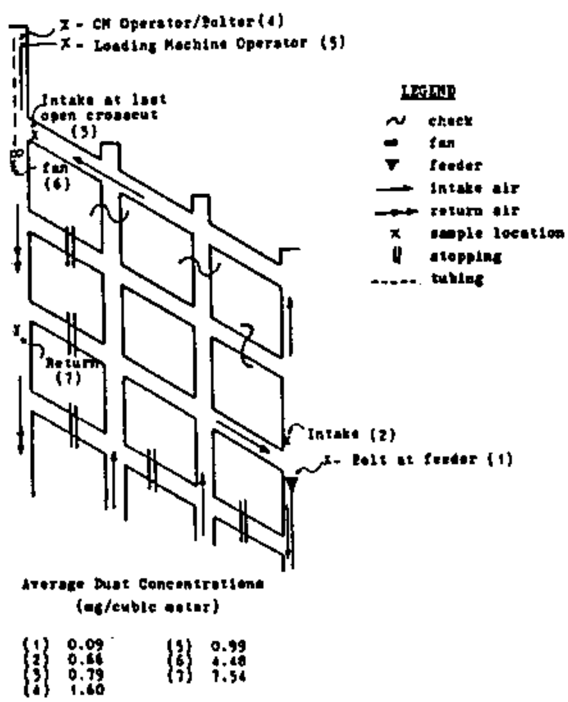

Figure 2. Sample locations and results on a continuous mining section.

INDEX

THE CUMULATIVE AUTHOR INDEX

Authors are sorted alphabetically. Papers by the same author are sorted in decreasing chronological order which puts the more recent papers first.

Authors' names appear in standardized form, that is, last names and initials. This is not necessarily the way the name appears on the paper.

THE CUMULATIVE SUBJECT INDEX

Every entry in the CUMULATIVE SUBJECT INDEX contains the following information:

1) Last name of the first listed author with the number of authors in parenthesis if the article had multiple authors.

2) A short descriptive phrase, generally the title of the paper.

3) The year in which the paper was published or presented.

4) The location of the paper in The Respirable Dust Center publication volume.

GENERIC MINERAL TECHNOLOGY CENTER FOR RESPIRABLE DUST

CUMULATIVE AUTHOR INDEX
1984

Bhaskar, R. Vol. 3, 25-31
Bise, C. J. Vol. 3, 85-90

Castranova, V. Vol. 3, 53-60
Chiang, H. S. Vol. 3, 32-34
Cilento, E. V. Vol. 3, 63-67

DiGregorio, K. A. Vol. 3, 63-67

Grayson, R. L. Vol. 3, 35-42; Vol. 3, 91-94

Keane, M. J. Vol. 3, 53-60
Khair, A. W. Vol. 3, 3-10; Vol. 3, 11-22

Lantz, R. C. Vol. 3, 63-67
Lee, C. Vol. 3, 71-84

Marple, V. A. Vol. 3, 45-52
Moore, M. P. Vol. 3, 85-90
Mutmansky, J. M. Vol. 3, 71-84

Ong, T. M. Vol. 3, 53-60

Peng, S. S. Vol. 3, 32-34; Vol. 3, 35-42; Vol. 3, 91-94

Ramani, R. V. Vol. 3, 25-31
Rubow, K. L. Vol. 3, 45-52

Sun, G. C. Vol. 3, 32-34

Vallyathan, V. Vol. 3, 53-60

Wallace, W. E. Vol. 3, 53-60

Zhao, Y. F. Vol. 3, 32-34

GENERIC MINERAL TECHNOLOGY CENTER FOR RESPIRABLE DUST

CUMULATIVE SUBJECT INDEX
1984

CONTROL OF DUST GENERATION

Khair, A. Wahab Design and fabrication of a rotary cutting simulator, 1984, Vol. **3**, 3-10.

Khair, A. Wahab Study of fracture mechanisms in coal subjected to various types of surface tractions using holographic interferometry, 1984, Vol. **3**, 11-22.

DILUTION, DISPERSION, AND COLLECTION OF DUST

Chiang, H. S. (4) Some factors influencing the airborne dust distribution in longwall face area, 1984, Vol. **3**, 32-34.

Grayson, Robert L. (2) Analysis of an airborne dust study made for a southwestern Pennsylvania underground bituminous coal mine, 1984, Vol. **3**, 35-42.

Ramani, R. V. (2) Dust transport in mine airways, 1984, Vol. **3**, 25-31.

DUST CHARACTERIZATION

Marple, Virgil A. (2) Instrumentation for the measurement of respirable coal mine dust, 1984, Vol. **3**, 45-52.

Wallace, W. F. (5) Pulmonary surfactant interaction with respirable dust, 1984, Vol. **3**, 53-60.

DUST LUNG INTERACTION

DiGregorio, Kevin A. (3) The development of an electro-optical techique to measure superoxide release from pulmonary alveolar macrophages exposed to coal dusts, 1984, Vol. **3**, 63-67

RELATIONSHIP OF MINE ENVIRONMENT, GEOLOGY AND SEAM CHARACTERISTICS TO DUST GENERATION AND MOBILITY

Grayson, R. L. (2) Correlation of respirable dust mass concentration with worker positions, 1984, Vol. **3**, 91-94.

Moore, Michael P. (2) The relationship between the hardgrove grindability index and the potential for respirable dust generation, 1984, Vol. **3**, 85-90.

Mutmansky, Jan M. An analysis of coal and geologic variables related to coal workers' pneumoconiosis, 1984, Vol. **3**, 71-84.